2019

Novel Hybrid Analogs of Estrone Origin Exhibits Cytotoxic Effects against EGFR-dependent Cancers

Felix Acheampong
South Dakota State University

NOVEL HYBRID ANALOGS OF ESTRONE ORIGIN EXHIBITS CYTOTOXIC

EFFECTS AGAINST EGFR-DEPENDENT CANCERS

BY

FELIX ACHEAMPONG

A dissertation submitted in partial fulfillment of the requirement for the

Doctor of Philosophy

Major in Biochemistry

South Dakota State University

2019

NOVEL HYBRID ANALOGS OF ESTRONE ORIGIN EXHIBITS CYTOTOXIC

EFFECTS AGAINST EGFR-DEPENDENT CANCERS

FELIX ACHEAMPONG

This dissertation is approved as a credible and independent investigation by a candidate for Doctor

of Philosophy in Biochemistry degree and is acceptable for meeting the dissertation requirements

for this degree. Acceptance of this does not imply that the conclusions reached by the candidate are

necessarily the conclusions of the major department.

Fathi T. Halaweish, Ph.D.   Date
Dissertation Advisor

Douglas Raynie, Ph.D.   Date
Head, Department of Chemistry and Biochemistry

Kinchel C. Doerner, Ph.D.   Date
Dean, Graduate School

DEDICATION

I dedicate this dissertation first to God Almighty through His son Jesus Christ with thanksgiving for his protection and guidance throughout my education and my entire life. I thank Him and give glory to His name: "But you, LORD, are a shield around me, my glory, the One who lifts my head high". You deserve all the praise and adoration.

To my father, Mr Edward Acheampong and in memory of my late mother, Mrs Christiana Acheampong.

ACKNOWLEDGEMENTS

CONTENTS

ABBREVIATIONS

(p70) S6Kα   (p70) S6 kinase alpha

ADME   Absorption, Distribution, Metabolism and Excretion

AKT   AKR mouse thymoma kinase

ALK   Anaplastic lymphoma kinase

AP-1   Activator protein 1

APAF-1   Apoptotic protease activating factor 1

ARAF   V-Raf murine sarcoma 3611 viral oncogene homolog

BAK   Bcl-2 antagonist killer 1

BAX   Bcl-2 associated X protein

BCL2   B-cell lymphoma gene 2

BRAF   V-Raf murine sarcoma viral oncogene homolog B1

BRCA1   Breast cancer 1, early onset

CDK4/6   Cyclin-dependent kinase 4 and 6

CDKI   Cyclin-dependent kinase inhibitor

DYRK1B   Dual-specificity tyrosine-(Y)-phosphorylation regulated kinase 1B

E2F   Transcription factor activating adenovirus E2 gene

EGF   Epidermal growth factor

EGFR	Epidermal Growth Factor Receptor (ERBB1)
ERK	Extracellular Signal-Related Kinase
FDA	U.S. Food and Drug Administration
G_1	Gap 1 phase (of the cell cycle)
G_2	Gap 2 phase (of the cell cycle)
HTS	High Throughput Screening
IC_{50}	Concentration required to obtain 50% inhibition
ICW	In-Cell Western
mAb	Monoclonal antibodies
MAPK	Mitogen-activated protein kinase
MEK	MAPK/ERK kinase
mTOR	Mammalian target of rapamycin
mTORC1	Mammalian target of rapamycin complex 1
mTORC2	Mammalian target of rapamycin complex 2
MTT	3-(4,5-dimethylthiazol-2-yl)-2,5-diphenyltetrazolium bromide
NMR	Nuclear Magnetic resonance
NSCLC	Non-small cell lung cancer
PI3K	Phosphatidylinositol-3 kinase

PIP$_2$ Phosphatidylinositol (4,5) bisphosphate

PIP$_3$ Phosphatidylinositol (3,4,5) trisphosphate

PS   Phosphatidyl serine

RAF   V-Raf-1 murine leukemia viral oncogene homolog

TKIs   Tyrosine Kinase Inhibitors

TNBC   Triple negative breast carcinoma

LIST OF FIGURES

LIST OF TABLES

LIST OF SCHEMES

ABSTRACT

NOVEL HYBRID ANALOGS OF ESTRONE ORIGIN EXHIBITS CYTOTOXIC

EFFECTS AGAINST EGFR-DEPENDENT CANCERS

FELIX ACHEAMPONG

2019

Cancer is second only to cardiovascular illnesses as the deadliest human disease globally. Currently, non-small cell lung cancer (NSCLC) and triple negative breast carcinoma (TNBC) are the most frequent types of cancer and have the highest mortalities. Epidermal growth factor receptor (EGFR), a central regulator of tumor progression, is frequently overexpressed in both cancers and is a key clinical target for therapeutic intervention. Natural products and their synthetic analogs have been utilized as EGFR tyrosine kinase inhibitors (TKIs) with potent antitumor effects. However, acquired resistance limits the long-term efficacy of these drugs. Estrone has been used as a scaffold in some studies where pharmacophores with antitumor properties were introduced to generate lead candidates with improved efficacy and safety. In our research group, estrone is employed as a starting material to synthesize novel hybrid analogs. Many of our estrone analogs, especially those bearing cucurbitacin pharmacophores have been documented to exhibit

potent cytotoxic effects against distinct cancers. However, these hybrid analogs have never been explored as potential agents targeting EGFR-dependent cancers. Here, we describe the cytotoxic effects of novel estrone analogs: a hybrid of estrone base-scaffold and modified cucurbitacin (**MMA series**) or triazole (**Fz series**) pharmacophores as potent agents against EGFR-dependent cancers, viz. NSCLC (NCIH226) and TNBC (MDA-MB-231, MDA-MB-468) tumor models. Molecular docking studies were carried out with OpenEye software. The MTT cell viability and trypan blue stain assays were used to perform cytotoxicity studies. Morphological changes and cell cycle arrest were carried out by microscopy and flow cytometric techniques, respectively. Annexin V assay was utilized to evaluate initial apoptosis induction in all cells and In-cell western assay was used to detect protein expression levels associated with mitochondrial apoptosis, cell cycle, EGFR and its downstream AKT and ERK1/2 pathways. Molecular docking studies revealed that most estrone analogs exhibited improved potency and binding compared to the positive controls, erlotinib and sorafenib when docked against the EGFR kinase-domain (pdb codes: 2ITW, 1M17). Subsequently, several estrone analogs exhibited significant cytotoxic effects against the different cancer cell lines *in vitro*. Notably, **MMA307** and **MM320** recorded lower IC_{50} molarities of 2.88 ± 0.21 and 9.68 ± 0.24 µM compared to the positive control, sorafenib, IC_{50} value of 20.62 ± 1.32 µM in NCIH226 cells. Similarly, administration of **MMA307** and **MMA321** to MDA-MB-468 cells yielded potent IC_{50} concentrations of 0.85 ± 0.00 and 0.56 µM ± 0.01 µM, respectively, when compared to sorafenib, IC_{50} value of 10.09 ± 0.68 µM. Furthermore, **Fz25** recorded IC_{50} dose of 8.13 ± 0.15 µM in MDA-MB-231 cell lines when compared to sorafenib, 12.21 ± 0.96 µM. Treatment with the **MMA307** and **MMA320** resulted in downregulation of Dyrk1B (dual-

specificity tyrosine phosphorylation-regulated kinase B), cyclin D1 and concomitant upregulation of phospho-cyclin D1 and $p21^{waf1/cip1}$ contributing to cell cycle arrest in the G_1 phase. Also, downregulation of EGFR and phospho-EGFR levels as well as suppression of activated MAP kinase signaling proteins-phospho-B-Raf, phospho-MEK1/2 and phospho-ERK1/2 were observed after NCIH226 cells were exposed to estrone analogs. Similarly, **MMA307** and **MMA321** downregulated cyclin D1 expression levels resulting in G_1 phase cell cycle arrest in MDA-MB-468 cells. Also, these compounds halted the MAPK and AKT signaling pathways due to their ability to downregulate EGFR and activated EGFR expressions. Moreover, mitochondrial apoptosis was induced in the TNBC model, MDA-MB-468, upon **MMA307** and **MMA321** exposures. In a different study, treatment of MDA-MB-231 cells with **Fz25** induced mitochondrial apoptosis and contributed to the G_1 phase of cell cycle arrest due to decreased expressions of cyclin D1 and Dyrk1B. Interestingly, this compound impacted the MAPK and AKT signaling pathways due to its ability to decrease EGFR and activated EGFR expressions. To conclude, the present study is the first to report on the cytotoxic potential of novel estrone analogs and provide evidence that **MMA307**, **MMA320**, **MMA321** and **Fz25** are promising novel lead compounds. Further investigations are needed to develop these potent compounds as the next generation anti-EGFR therapies for treating serious EGFR-dependent lung and breast cancers.

Chapter 1

1.1   Introduction and Background

Cancer is a complex genetic disease or group of diseases characterized by the uncontrolled growth and spread of nonhealthy cells. The spread of malignant cells (a phenomenon called metastasis) is responsible for patient's death. The disease incidence and mortality are rapidly growing globally; ageing, unhealthy lifestyle, family history, chemical and environmental factors, and genetic susceptibility are the major risk factors proposed for developing cancer. In the past cancers were classified based on histology and primary site (location in the body), therefore, six major categories, namely carcinoma, sarcoma, myeloma, leukemia, lymphoma, and mixed types have been established based on histology alone. According to primary site lung, breast, prostate, liver, stomach, head and neck, etc. cancers have all been identified (Figure 1.1).
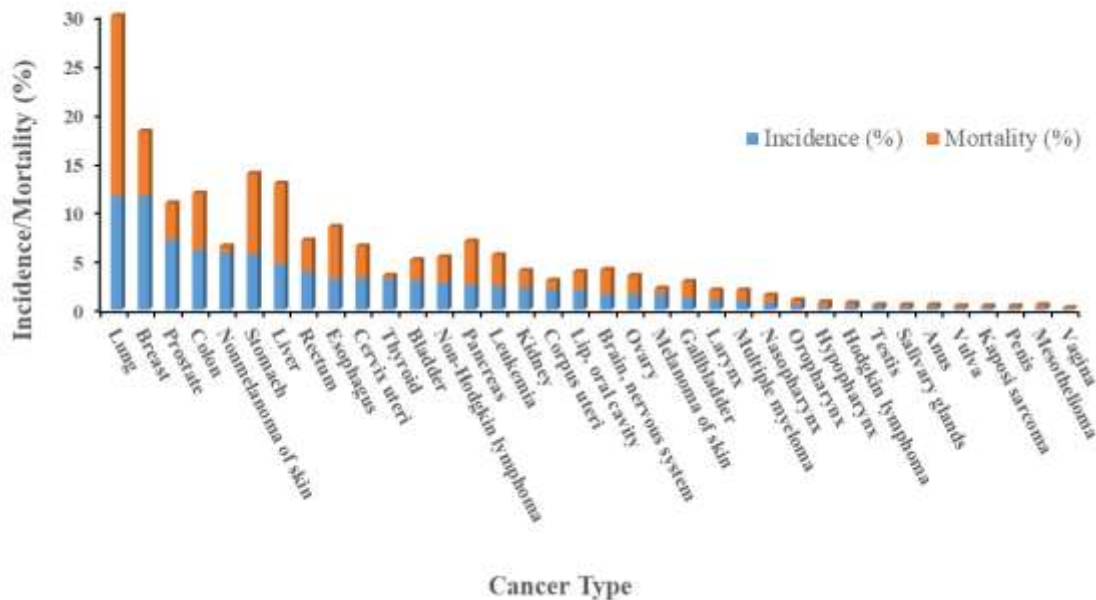
Figure 0.1. Cancer incidence and mortality. Lung and breast cancers have the highest incidence in both males and females. Lung cancer has the highest mortality rate followed by stomach, liver and breast cancers in both sexes. However, in females, breast cancer has the highest mortality. Data adapted from Bray *et al*., 2018.

1.2 Lung and Breast cancers as serious illnesses worldwide

Lung cancer is the most common cause of cancer mortality worldwide with an estimated 1.8 million deaths yearly (Bray *et al*., 2018). Also, it accounts for more than a quarter of all cancer-related deaths (Siegel *et al*., 2017). Usually, lung cancer is classified into small cell lung cancer (SCLC) and non-small cell lung cancer (NSCLC). "Small cell or non-small cell" refers to the type of cell within the lung where the cancer originated. About 85% of lung cancer cases are NSCLC (the most frequent type), of which lung adenocarcinoma and lung squamous cell carcinoma are the most common subtypes (Herbst *et al*., 2018). Large cell carcinoma is the less common type. The remaining 15% represent SCLC cases, four subtypes have been identified: oat cell carcinoma, small cell carcinoma of the intermediate cell type, combined oat cell carcinoma, and undifferentiated carcinoma of the small cell type (Nomori *et al*., 1986). Many lung cancer patients have locally advanced disease at the time of initial diagnosis and about 7-10% of patients present with brain metastases (Ali *et al*., 2013). The key cause of lung cancer is attributed to tobacco smoking, accounting for more than 80% of the cases in countries where smoking is common (Alberg *et al*., 2013). However, nonsmokers also develop lung cancer when exposed to conditions like second-hand smoking, pollution and occupational carcinogens, and with inherited genetic susceptibility (Herbst *et al*., 2018).

Breast cancer has the second highest incidence rate globally after lung cancer and accounts for the fourth highest mortality after lung, stomach and liver cancers. In

females, breast cancer records the most deaths every year (Bray *et al*., 2018). This disease is usually classified into four subtypes, luminal A-like (ER-positive (ER+) and/or PR-positive (PR+), HER2-negative (HER2–)), luminal B-like (ER+ and/or PR+, HER2-positive (HER2+)) HER2-enriched (ER-negative (ER–)/PR-negative (PR–)/HER2+), and triple-negative breast cancer (TNBC; ER–/PR–/HER2–) based on immunohistochemistry studies on estrogen receptor (ER), progesterone receptor (PR), and human epidermal growth factor receptor-2 (HER2) (Ma *et al*., 2017). The luminal A-like subtype is the most frequently occurring subtype and accounts for 62–67% of invasive cases; TNBC is the second most common subtype and accounts for 10–25% of invasive cases and is more aggressive with poor prognosis (Dai *et al*., 2015; Uscanga-Perales *et al*., 2016; Lee and Djamgoz, 2018). In comparison to non-TNBC (luminal A-like, luminal B-like and HER2-enriched) tumors, TNBC tumors are frequently larger and less differentiated and are almost 2.5-fold more likely to metastasize within five years of diagnosis (Uscanga-Perales *et al*., 2016). Moreover, TNBC metastasizes preferentially to the viscera and nervous system in contrast to non-TNBC which spreads mostly to the bone. Also, it is more often associated with breast cancer type 1 (BRCA1) mutation and to a less extent, BRCA2 mutations (Podo *et al*., 2016). In the past, TNBC was subclassified into six types based on gene expression profiling (Lehmann *et al*., 2011), however, currently, these have been narrowed down or refined into four subclasses: basal-like 1 (BL1), basal-like 2 (BL2), luminal androgen receptor (LAR) and mesenchymal (M) (Lehmann *et al*., 2016). These TNBC subtypes are known to activate different signaling pathways. BL1 shows elevated expression of Ki67, BL2 presents with elevated expression of TP63, MET and activate

glycolysis and gluconeogenetic pathways. On the other hand, LAR increases the expression of androgen receptors and M activates mTOR and angiogenesis signaling (Uscanga-Perales *et al*., 2016). It must be noted that racial ancestry, gestation, lack of lactation, high body mass index, metabolic syndrome, type 2 diabetes, obesity and/or insulin resistance are all risk factors to developing the TNBC phenotype (Ma *et al*., 2017; Kim *et al*., 2015).

Recent breakthroughs in molecular and cellular biology have allowed the use of biomarkers or genetic markers to classify cancers into distinct phenotypes and to identify druggable targets. In the past 30 years, important molecular markers associated with several mechanisms including proliferation, growth, survival, angiogenesis, cell death, metastasis, etc. pathways have all been reported for both NSCLC and TNBC. The most reported and targeted biomarker is the epidermal growth factor receptor (EGFR), a central regulator of tumor progression.

1.3   Key molecular drivers associated with NSCLC and TNBC progression

NSCLC and TNBC are molecularly heterogeneous disease and understanding their biology is crucial for the development of effective therapies. Molecular profiling studies have led to the identification of driver mutations in more than 50% of patients with NSCLC (Baumgart, 2015) and an almost equal number in TNBC cases (Annunziato *et al*., 2019). From variant mutation analyses, alterations in the Kirsten rat sarcoma (KRAS), BRAF and EGFR genes have been associated with NSCLC initiation and represent attractive targets for therapeutic intervention. In TNBC, mutations in BRCA1/2 (germLine), TP53, MYC and driver-genes associated with growth pathways like EGFR, MEK have been reported (Santoro *et al*., 2019; Sabatier *et al*., 2019). KRAS is frequently mutated in NSCLC and is found in approximately 32.2% of patient cases (Ha *et al*., 2015; Anguera and Majem, 2018). The RAS genes encode for membrane-bound GTP binding proteins, which are part of the RAS/MAPK signaling pathway linking EGFR activation to cell proliferation and survival. Mutations in the KRAS gene tend to be mutually exclusive from EGFR mutations and ALK translocations and are believed to be a negative prognostic factor for survival (Baumgart, 2015). Also, BRAF, a downstream mediator of KRAS, activates the MAP kinase pathway involved in cell proliferation. Mutations in BRAF are found in about 4%

of patients with NSCLC adenocarcinoma; specifically, BRAFV600E represents about 56.7% of the identified mutations within the gene (Anguera and Majem, 2018).

On the other hand, TNBC tumors show different mutation characteristics compared to NSCLC tumors. Loss of BRCA1/2, because of either germLine or somatic mutations or due to promoter hypermethylation, has been suggested in about 50% of patient cases (Garrido-Castro *et al*., 2019). BRCA1/2 genes are crucial for error-free repair of DNA double-strand breaks via homologous recombination, and loss of or reduced expression of these genes results in elevated levels of chromosomal instability and a specific mutator phenotype. Also, mutations in TP53 tumor suppressor gene, occur in more than 80% of TNBC cases (Bae *et al*., 2018). This gene is frequently mutated in basal-like TNBC, with nonsense and frameshift mutations enriched. TP53 regulates several genes and is involved in DNA-damage response and cell-cycle regulation mechanisms. In addition, next-generation sequencing (NGS) data shows that MYC amplification was noted in about 26% of TNBC group (Shi *et al*., 2018). MYC (an oncogenic transcription factor) regulates the transcriptional activity of multiple genes involved in cell proliferation, metabolism, and survival. It is suggested that MYC conjoins with RAS–MAPK to drive tumor progression in TNBC cell lines, and MEK inhibition potently inhibits tumor growth in MYC-overexpressed breast cancer (Balko *et al*., 2014).

EGFR is expressed on the cell surface of a substantial percentage of NSCLC and TNBC cells. This member of the receptor tyrosine kinase class of receptors is important in

transducing extracellular signals from the cell surface to the cell interior, mediating crucial processes such as cell proliferation, differentiation, migration, and apoptosis. Dysregulated expression of these receptors can lead to the aberration of homeostatic cellular processes, resulting in malignant transformation of cells. Activating EGFR mutations have been reported in cancers such as NSCLC, TNBC and head and neck cancers. These EGFR mutations are predictive of response to anti-EGFR therapy (Teng *et al*., 2011). These mutations often are associated with poor prognosis. In NSCLC, EGFR overexpression or alterations in the kinase domain have been observed in 40-80% of primary cases and around 88% in patients with metastatic disease (Sim *et al*., 2018). When compared to KRAS, EGFR mutations in smokers and non-smokers varies irrespective of racial background. Non-smokers tend to have higher expression of somatic EGFR mutations compared to smokers. It is noteworthy to mention that, among the identified EGFR kinase domain mutations, over 90% appear as short in-frame deletions in exon 19 or as point mutations in exon 18-21, the latter resulting in arginine replacing leucine at codon 858 (L858R) (Jorge *et al*., 2014). Thus, patients with NSCLC are classified as either being EGFR mutants (having mutations within the kinase domain) or EGFR wild-type (exhibiting EGFR overexpression or amplification). Based on this, different treatments are recommended for the unique NSCLC patient population.

Though TNBC lacks the expressions of ER, PR, and HER2, studies have revealed that EGFR is highly expressed or amplified in TNBC (50-75% of cases), especially in the advanced state (Dent *et al*., 2007). According to Teng *et al*., 2011, TNBC cells harbor

EGFR mutations, including exon 19 deletions, inversions and exon 21 missense substitutions. However, TNBC patients have not been well classified based on EGFR status as found in the case of NSCLC. The same study predicted that these EGFR mutations may sensitize TNBC towards tyrosine kinase inhibitors (TKIs) and may enhance the potential use of anti-EGFR therapy.

1.3.1   Role of EGFR and its downstream pathways in tumor progression

EGFR is a receptor tyrosine kinase (RTK) and a member of the HER family of receptors composed of EGFR/HER1/ERB1, HER2/ERB2, HER3/ERB3, and HER4/ERB4. There are 11 different growth factors associated with the receptors which can be broadly divided into those that specifically bind with EGFR (EGF, TGF-α, Amphiregulin), those that bind with EGFR and HER4 (BTC, HB-EGF, Epidermal regulators), and those that bind with HER3 and HER4 (Neuregulin). EGFR structurally consists of a C-terminus intracellular region that possesses the kinase activity, an N-terminus extracellular ligand-binding site, and a hydrophobic transmembrane domain (Liu *et al*., 2017). Downstream signaling from these receptors proceeds via tyrosine phosphorylation which activates multiple downstream signaling pathways including RAS/MAPK and PI3K/Akt cascades that lead to transcriptional regulation of genes involved in cell proliferation, motility, and survival (Figure 1.2). Phosphorylation on serine and threonine residues within the kinase domain leads to its sequestering and degradation (Liu *et al*., 2017).

1.3.1.1 Mitogen-activated protein (MAPK) kinase signaling

The mitogen-activated protein kinases (MAPK) pathway, often known as a cascade of protein kinases, composed of RAS, RAF, mitogen-activated protein/extracellular signal-regulated kinase (MEK) and the extracellular signal-regulated kinase (ERK), is a highly conserved signal transduction pathway in all eukaryotic cells. The MAPK pathway is one of the best-characterized signaling cascades that regulates a variety of normal cellular functions, such as cell proliferation, differentiation, survival and apoptosis, by transmitting signals from upstream extracellular growth factors to diverse downstream effectors located in the nucleus (Molina and Adjei, 2006). The RAS/MAPK pathway is initiated through the promotion of Ras binding to guanosine triphosphate (GTP), which in turn activates RAF kinases MAPK/extracellular signal-regulated kinases (MEK), and ERK. Activated ERK is thought to translocate into the nucleus, where it phosphorylates and activates numerous targets such as elk-1, c-jun, fos, etc. involved in cell cycle progression and proliferation (MacCorkle and Tan, 2005). Moreover, activated ERK phosphorylates multiple substrates ranging from kinases to transcription factors and is positioned as a key kinase that controls multiple cellular processes due to its rather broad nature of substrate recognition.

1.3.1.2 Phosphatidylinositol-3 kinase (PI3K) signaling

Upon EGFR autophosphorylation on tyrosine residues, PI3K is recruited to the membrane by directly binding to phosphotyrosine consensus residues of EGF receptors or by binding

to adaptors through p85 regulatory subunit. PI3K activation leads to the production of the second messenger phosphatidylinositol-3,4,5-triphosphate (PIP3) from the substrate phosphatidylinositol-4,4-bisphosphate. PIP3 then recruits a subset of signaling proteins with pleckstrin homology (PH) domains to the membrane, including protein serine/threonine kinase-3′-phosphoinositide-dependent kinase 1 (PDK1) and Akt/protein kinase B (PKB) (Portia *et al*., 2014). The constitutively active PDK1 then induces the phosphorylation of AKT kinase domain at Thr308 and Ser473 at the carboxyl-terminal position to initiate the complete activation of AKT. Subsequently, AKT can indirectly inhibit (phosphorylate) tuberous sclerosis complex 1/2 (TSC1/2 - hamartin and tuberin), thereby activating the mammalian target of rapamycin (mTOR) signaling. mTOR activity is carried out by two distinct complexes: mTORC1 and mTORC2 that act downstream and upstream of AKT, respectively. As a key signaling node, the mTORC1 complex contains the regulatory protein, raptor which regulates the phosphorylation of p70S6 kinase and 4E-binding protein 1 (4EBP1), and controls their downstream functions in protein translation, cell growth, and cell proliferation (Fruman *et al*., 2017). Also, mTORC2 is known to activate AKT, thereby promoting cell proliferation and survival. Previous research suggested that malfunctioning of the EGFR-RAS-MAPK and EGFR-Akt-mTOR signaling axes play important roles in NSCLC and TNBC progression. Particularly, overexpression of EGFR and phosphorylated EGFR as well as overexpression of phosphorylated MAPK, AKT and mTOR is documented in the advanced stages both cancers (Ignacio *et al*., 2018; Chen and Costa, 2018; Foidart *et al*., 2019; Liu *et al*., 2017; Sato *et al*., 2018). It is also reported that increased expression of phosphorylated mTOR and MAPK leads to G_1 to S-

phase cell cycle entry by modulating cyclin and cyclin-dependent kinases expression (Foidart *et al*., 2019; Nagata *et al*., 2010; Gridelli *et al*., 2008).

1.3.1.3   G$_1$ phase cell cycle progression

The increased expression of cyclins, particularly cyclin D, activates cyclin-dependent kinase (CDK) 4/6 activity and inactivates retinoblastoma tumor suppressor (Rb) activity, resulting in the activation of the transcription factor E2F and the upregulation of target genes that are essential for progressing from the G$_1$ to S phase of the cell cycle. On the other hand, the expression levels of the cyclin-dependent kinase inhibitors, p^{21cip1} and p^{27kip1}, are decreased when the RAS/MAPK and PI3K/AKT pathways are activated (Nagata *et al*., 2010). Dyrk1B-(dual-specificity tyrosine phosphorylation-regulated kinase B), a G$_1$-S phase checkpoint kinase, is amplified or overexpressed in certain human cancers signifying that it may be an oncogene (Ashford *et al*., 2014; Gao *et al*., 2013). It is thought to arrest damage tumors in the G$_0$/G$_1$ phase to allow their repair in the quiescent state while maintaining the clonogenicity of tumors via mediating cyclin D1 turnover and stabilizing p^{21cip1}. Gao *et al*., 2013, suggested that increased expression of activated MAPK positively correlated with Dyrk1B expression in NSCLC and ovarian cancers.
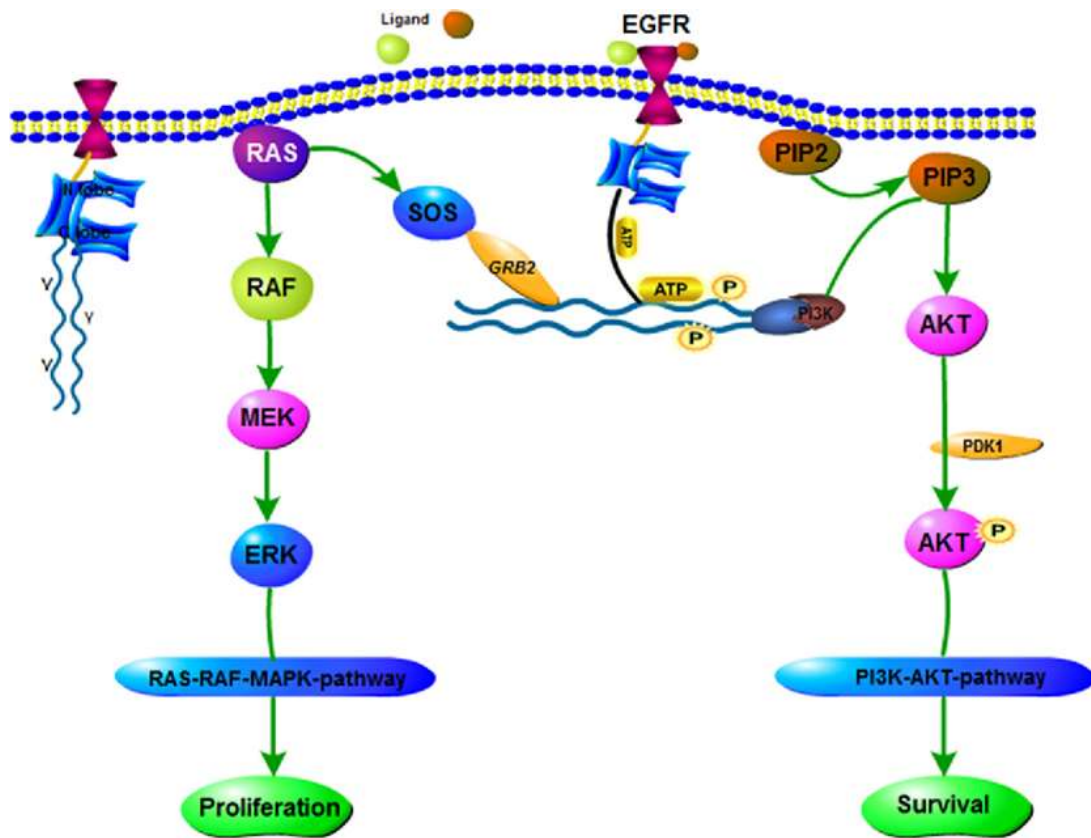
Figure 0.2. EGFR signaling pathway. EGFR is a receptor protein that spans the cell membrane. Binding of EGF to the receptor leads to the formation of an asymmetric dimer. Autophosphorylation of tyrosine residues activates the RAS-RAF-MAPK and PI3K-AKT pathways. Figure adapted from Liu *et al*, 2017.

1.3.1.4   Apoptosis pathways

Activation of RAS/MAPK and PI3K/AKT/mTOR pathways in NSCLC and TNBC tumors is suggested to override apoptosis by activating antiapoptotic proteins and suppressing proapoptotic proteins. Apoptosis occurs through two distinct molecular pathways, which are regulated by caspases. The intrinsic or mitochondrial pathway is activated by intracellular events and depends on the release of pro-apoptotic and anti-apoptotic factors from the mitochondria, such as the B-cell lymphoma 2 (Bcl-2) family proteins, cytochrome c and APAF-1, among others. The released cytochrome c from the mitochondrial to the cytoplasm binds and activate apoptotic protease activating factor 1 (APAF-1). Activated APAF-1 apoptosome then activates caspase-9 which subsequently activates caspase-3 (Winter *et al.*, 2014). The extrinsic pathway is initiated by the binding of an extracellular death ligand to its cell-surface death receptor. This leads to the activation of caspase 8, which also activates the effector caspase 3 (Winter *et al.*, 2014). The extrinsic pathway can crosstalk with the intrinsic pathway through caspase-8-mediated cleavage of BID (a member of the Bcl2 family of proteins) (Billen *et al.*, 2008). Finally, caspase-3 cleaves and inactivates PARP-poly (ADP-ribose) polymerase-which is important for damaged DNA repair, thereby inducing apoptosis (Figure 1.3) (Soldani and Scovassi, 2002).

EGFR and its downstream pathways represent attractive therapeutic targets, and the inhibition of multiple pathways is likely to prevent the compensatory effect of the feedback loop which is a major issue for molecular targeted therapy in many types of cancer.
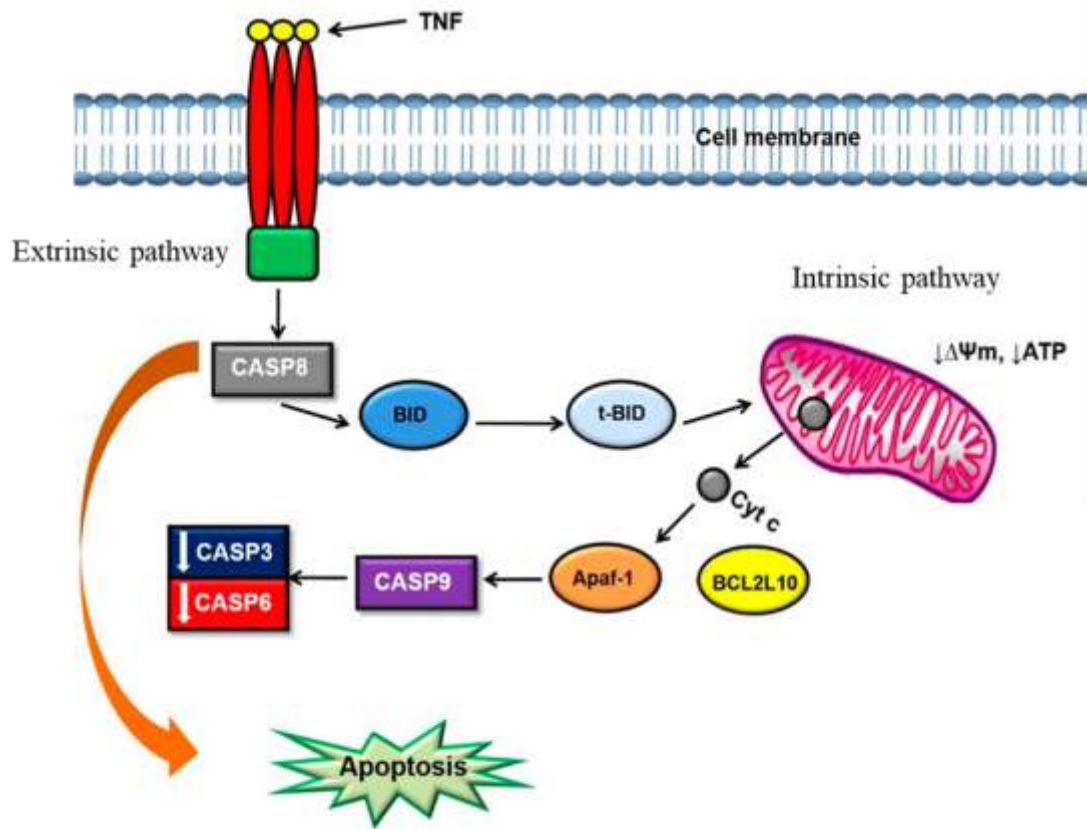
Figure 0.3 Apoptosis pathways. Apoptosis can occur through the intrinsic (mitochondrial) pathway or extrinsic pathway. Intrinsic apoptosis is characterized by cytochrome c release, apoptosome formation by APAF1 and activation of caspase 9. Extrinsic mechanism occurs via ligands binding to the death receptor and activating caspase 8. Both mechanisms crosstalk through truncation of the protein called BID. Figure adapted from Manoto *et al*, 2017.

1.4   Therapies for NSCLC and TNBC

Most patients with NSCLC or TNBC are diagnosed with metastatic disease. In NSCLC, the five-year overall survival in the advanced stage of the disease is 5% (Baxevanos and Mountzios, 2018) whereas in TNBC the 5-year survival in advanced stage tends to be about 22% (American Cancer Society, 2019). Chemotherapy has been the mainstay of treatment in patients with metastatic NSCLC or TNBC for a long time and since no cure can be achieved, it is given with palliative intent. It must be mentioned that treatments such as surgery, radiation, immunotherapy, among others are also recommended for NSCLC and TNBC patients.

1.4.1   Chemotherapy as a treatment modality for TNBC and NSCLC-success and challenges

1.4.1.1   Chemotherapy as a superior treatment for wild-type NSCLC

Chemotherapy is the application of chemicals or drugs to kill cancer cells, and its effects are systemic. In NSCLC, chemotherapy is the recommended first line treatment for patients with overexpressed (wild-type) EFGR whereas targeted agents such as EGFR-TKIs are used as second- or third-line agents. However, the treatment order is reversed for NSCLC patients carrying mutant EGFR. Platinum-based doublet therapy (for example, cisplatin in combination with another cytotoxic therapy) has been the standard therapy for patients with

advanced stage NSCLC and shows a superior performance status (Herbst *et al*., 2018). Particularly, adjuvant cytotoxic therapy with a cisplatin-based doublet administrated to patients in stages II and IIIA NSCLC yielded improved survival with complete resection. Also, Hotta *et al*., 2004, analyzed eight clinical trials and reported a higher response rate for cisplatin compared with carboplatin treatment with no survival difference. In the same study, subgroup analyses revealed that patients treated with cisplatin alone had longer survival than those receiving a third generation TKI in conjunction with carboplatin. Moreover, from the FLEX and BMS099 studies, it was revealed that cetuximab (anti-EGFR monoclonal antibody) used as monotherapy after prior administration of TKIs yielded no response (Wang *et al*., 2013). However, cetuximab addition to platinum doublet cisplatin/vinorelbine demonstrated a significant improvement in overall survival benefit of 1.2 months in NSCLC patients with EGFR-positive tumors (Wang *et al*., 2013). Overall, the above reports have demonstrated that cytotoxic chemotherapy regimens or their combinations administered to patients with EGFR-wild-type NSCLC produced a better response. Nonetheless, it must be mentioned that the median overall survival for EGFR-wild-type NSCLC patients after chemotherapy treatment remains less than 1 year and the progression-free survival is 6 months at the most (Lin *et al*., 2016). This indicates that newer therapies with improved outcomes are needed for this unique NSCLC patient's population.

1.4.1.2   Chemotherapy as a successful treatment for TNBC

The standard of systemic treatment for TNBC follows the same general principle with other types of breast cancer. Therefore, neoadjuvant or adjuvant chemotherapy remains a key component of systemic treatment in early and advanced TNBC, which is determined primarily by its clinical or pathologic stage (Park *et al*., 2018). In previous pivotal neoadjuvant trials, patients with TNBC showed significantly higher response rates to anthracycline and taxane-based chemotherapy than those of other subtypes, achieving pathologic complete response (pCR) rates of approximately 40% (Cortazar *et al*., 2014). Subsequent clinical trials of metastatic TNBC showed a modest efficacy of platinum-based monotherapy, consistently suggesting a greater benefit in BRCA1/2 mutation carriers. In early TNBC, patients with stage II–III treated with neoadjuvant cisplatin alone showed a 22% pCR rate in a small retrospective study, in which only 7% of patients carried germLine BRCA mutations (Byrski *et al*., 2014). Further phase II studies exclusively for patients with BRCA1 mutation demonstrated markedly higher pCR rates from 61-90% after neoadjuvant cisplatin monotherapy, which validated the significance of BRCA gene in predicting platinum sensitivity in TNBC (Silver *et al*., 2010). Despite, the effectiveness of single-agent chemotherapy, some TNBC non-responders were identified and that called for the use of combinatorial chemotherapy. Masuda *et al*., 2017 report that the CREATE-X trial demonstrated a potential survival benefit of adding capecitabine to the standard adjuvant chemotherapy regimen in early TNBC with a residual tumor burden after neoadjuvant treatment. Also, a meta-analysis by Natori and colleagues, 2017, provided some justification for combining capecitabine with either neoadjuvant or adjuvant standard chemotherapy in patients with TNBC. In a different phase II clinical trial, BRCA1/2-mutant TNBC patients achieved the highest pCR rate of about 56% after neoadjuvant

combination chemotherapy with gemcitabine, carboplatin, and the PARP inhibitor iniparib (Telli *et al*., 2015). Despite the effectiveness of these treatment modalities, patients who do not respond to chemotherapy develop resistance, and a more aggressive recurrent disease results which then becomes virtually incurable (Székely *et al*., 2017; Wahba and El-Hadaad, 2015).

Over the past three decades, targeted agents have been developed as a replacement therapy to treat cancer patients with the idea of achieving selectivity, specificity, efficacy and safety, as well as preventing adverse side effects. Some of these agents have already been approved by the Food and Drugs Administration (FDA) for treating different cancers. Targeted agents against EGFR are the most abundant in clinical use (Imai and Takaoka, 2006). Examples include monoclonal antibodies - (cetuximab and panitumumab) and tyrosine kinase inhibitors - (erlotinib and gefitinib).

1.4.2 EGFR targeted therapy for TNBC and NSCLC patients-success and challenges

1.4.2.1 EGFR targeted therapy as a successful treatment for NSCLC

In NSCLC, EGFR has been exploited as a molecular target for two distinct kinds of molecules, monoclonal antibodies (mAbs) and tyrosine kinase inhibitors (TKI). mAbs, which are thought to be efficacious in EGFR wild-type NSCLC patients and target the

extracellular domain of EGFR. On the other hand, TKIs which are effective in NSCLC patients with mutations in the EGFR kinase domain, target the intracellular domain of EGFR (Figure 1.4) (Imai and Takaoka, 2006). Usually, EGFR wild-type NSCLC patients with advanced disease receive chemotherapy as a first-line of treatment, while TKIs (gefitinib, erlotinib, afatinib) or mAbs (cetuximab, panitumumab and necitumumab) serve as second line (Zhang *et al*., 2014) of treatment. EGFR wild-type NSCLC patients have responded better to a chemotherapy regimen compared to anti-EGFRs. Notably, the TAILOR trial (Tarceva Italian Lung Optimization Trial), which compared the efficacy of erlotinib in patients with wild-type EGFR to that of docetaxel as a second-line therapy, showed that the progression-free survival (PFS) was significantly better with docetaxel than with erlotinib: median PFS was 2.9 months with docetaxel versus 2.4 months with erlotinib (Morales-Espinosa and Rosell, 2015). In a similar Chinese trial, which compared pemetrexed to gefitinib in wild-type EGFR non-squamous NSCLC patients, it was observed that progression-free survival was significantly better with pemetrexed than gefitinib and there was a trend for an improvement in overall survival in favor of docetaxel (Sculier *et al*., 2015). Other studies have also reported that the combination of chemotherapy and anti-EGFRs administered to EGFR wild-type NSCLC patients leads to a superior overall response. Particularly, the FLEX trial demonstrated improved overall survival for chemotherapy plus cetuximab in patients who harbored overexpressed (wild-type) EGFR in their tumors (Pirker, 2012). Similarly, the Sculier *et al*., 2015 study reported that the addition of cetuximab to chemotherapy significantly improved the overall survival and progression-free survival compared with chemotherapy alone. However, anti-EGFR administered alone to this patient population is deemed ineffective by these same reports.

Therefore, in terms of evidence-based medicine, these studies are strongly against the use of TKIs in wild-type EGFR NSCLC. In EGFR mutant NSCLC, two common mutations observed are the L858R mutation in exon 21 and the exon 19 deletions. Both are found within the tyrosine kinase domain and are drug-sensitizing mutations. These mutations activate the kinase action increasingly and sustain the activated receptor in a gain-of-function manner through ligand binding. Therefore, it has been observed that del 19 and L585R are gain-of-function mutations because they cause activation of the EGFR signaling pathway in the mutant EGFR-positive oncogenic cells, and some of these mutations also lead to greater sensitivity to EGFR TKIs compared to cases with wild-type EGFR (Pirker, 2012). TKIs are mainly recommended as either first- or second-line therapies for advanced stage NSCLC patients with EGFR-mutations. TKIs are suggested to covalently bond to the ATP binding sites of the tyrosine kinases, causing permanent inhibition to this site, whilst also inhibiting the HER2 receptor. Many reports suggest that anti-EGFRs are highly recommended for treating EGFR-mutant NSCLC patients due to improve overall response rate and the significant increase in progression-free survival when compared to chemotherapy. In support of this, the IPASS clinical study reported that tumor response rate in patients with EGFR activating mutations was about 71.2% in the gefitinib group which was statistically significant compared to 47.3% in the chemotherapy arm. The primary endpoint of progression-free survival (PFS) was significantly prolonged in the gefitinib treatment group (9.8 vs 6.4 months) (Yi-Long *et al*., 2012). In a similar study, researchers randomized 173 NSCLC patients with EGFR mutations to erlotinib and chemotherapy; The median PFS was 9·7 months in erlotinib set which was significantly longer than 5·2 months in chemotherapy set (Nan *et al*., 2017). Despite the huge success

reported for anti-EGFR targeted therapies for NSCLC patients, the overall survival after anti-EGFR therapy, especially after TKIs administration, is less than 15% (Lin *et al*., 2016), probably due acquired resistance, and a more aggressive disease phenotype develop after a patient's remission to treatment (Lin *et al*., 2016).

1.4.2.2 EGFR targeted therapy as a clinical need for TNBC

In cancers like NSCLC and colorectal cancer, anti-EGFR agents, small molecule tyrosine kinase inhibitors and monoclonal antibodies, have been developed and are currently being used to treat these diseases. Cetuximab and panitumumab are two mAbs that are approved for the treatment of EGFR-expressing metastatic colorectal cancer with KRAS wild-type phenotype. Osimertinib, gefitinib, afatinib, and erlotinib are few selective EGFR-TKIs used as therapy for patients with metastatic NSCLC who carry activating EGFR mutations (Rosa *et al*., 2015; Bartholomew *et al*., 2017). In TNBC, there is no classification for patients based on their EGFR status, thus patients are not represented as harboring wild-type EGFR or mutant EGFR phenotypes. As reported above, chemotherapy is the preferred treatment for TNBC patients. Nonetheless, several clinical trials report the use of already discovered anti-EGFR agents, either alone or in combination with chemotherapy, as a treatment option for TNBC patients (Baselga *et al*., 2005; Dickler *et al*., 2009; Nakai *et al*., 2016). The use of anti-EGFRs mostly yielded partial responses. Juggling through previous reports, in a phase II clinical trial, gefitinib and erlotinib used as monotherapies in metastatic and recurrent TNBC patients returned only a partial response of about 3%

(Baselga *et al*., 2005; Dickler *et al*., 2009). In another phase II clinical trial with second-generation irreversible EGFR TKI, afatinib, no objective responses were produced in patients with metastatic TNBC (Nakai *et al*., 2016). However, the combination of anti-EGFR TKI and chemotherapy generated improved responses as suggested by some recent studies. Noticeably, in a phase II clinical study, the combination of cetuximab plus carboplatin or irinotecan or ixabepilone or docetaxel showed an improved response rate compared to the single agents alone (Carey *et al*., 2012; Trédan *et al*., 2015; Crozier *et al.*, 2016; Nabholtz *et al*., 2016). In the same phase 2 trial, gefitinib, an EGFR TKI, was reported to have minimal activity in patients' with advanced TNBC, and modest activity when combined with standard chemotherapy in the patients population (Bernsdorf *et al*., 2011). From all the above reports, it is evident that no anti-EGFR agents are currently approved for TNBC treatment, as results from clinical trials are disappointing. This is often attributed to the existence of compensatory pathways that confer resistance to EGFR inhibition, thus allowing continued cancer cell growth and survival (Diluvio *et al*., 2018). Therefore, the need for a more effective treatment modality is imminent and natural products have proven to be the main source for the discovery of anticancer therapies.
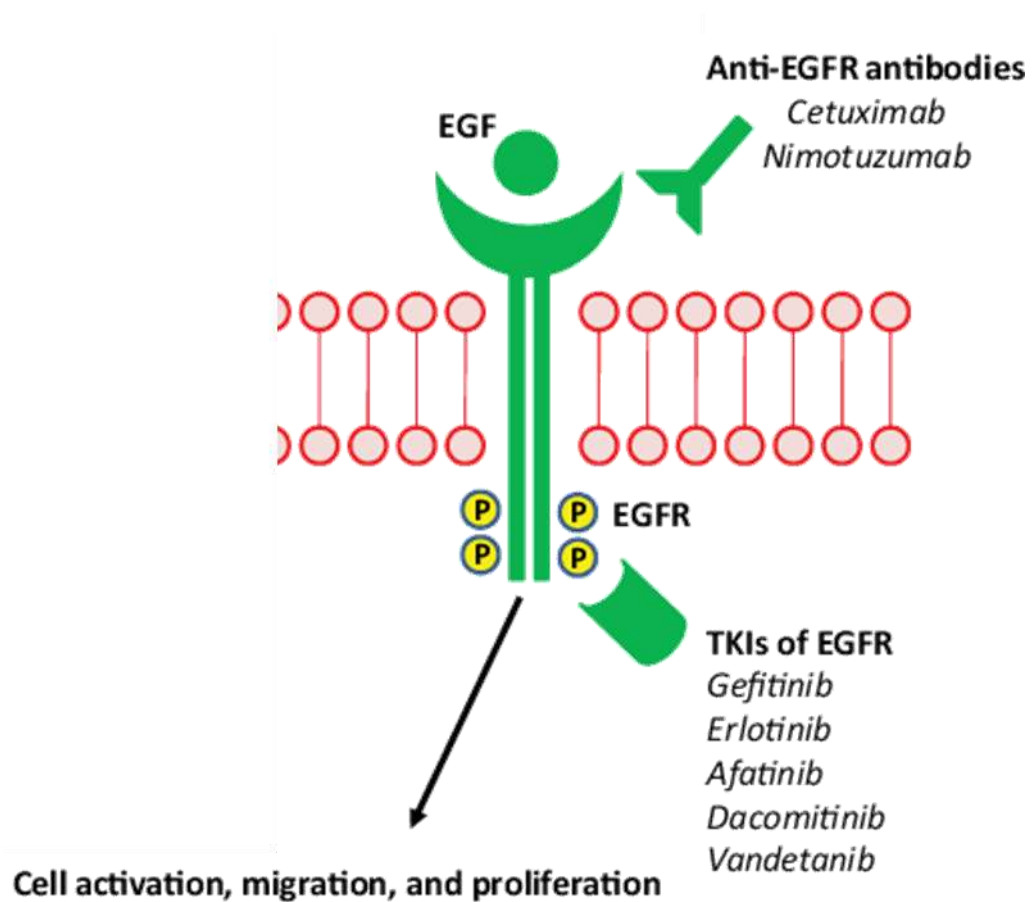
Figure 0.4 Anti-EGFR targets in NSCLC. Monoclonal antibodies target the extracellular domain of EGFR. TKIs, small molecules, target the kinase domain of EGFR. Figure adapted from Farhat and Houhou, 2013.

1.5   Natural products as a rich source of discovering novel anticancer therapies

Natural products are often regarded as sources of phytochemicals or drug leads for the discovery of novel drugs. Phytochemicals are naturally occurring secondary metabolites, i.e. biologically active compounds found in plants, animals, microorganisms, and marine organisms, that are able to inhibit various diseases including cancer. Notable examples include the vinca alkaloids (vincristine and vinblastine) isolated from *Catharanthus roseus,* as well as taxol isolated from *Taxus brevifolia* for the treatment of various cancers (Acheampong *et al*, 2017; Larbie *et al*, 2015; Acheampong *et al*, 2015). In the face of worldwide disease challenges, natural products research and development potentially play a key function in innovative drug discovery. About 33% of FDA-approved drugs over the past two decades are based on natural products or their derivatives and these have transformed medicine (Thomford *et al*, 2018).

1.5.1   Cucurbitacins as important antitumor agents

Numerous successful anticancer drugs in clinical use are either natural products or their synthetic analogs. For this reason, cucurbitacins (cucs) and their analogs have become a focus of research because of their ability to significantly inhibit the growth of distinct cancers. Cucs belong to a large family of triterpenoids present in Cucurbitaceae plants, and possess many biological activities, with the most relevant a without doubt being anticancer properties toward different cancers (Sikander *et al*., 2016; Hall *et al*., 2015). There are about 18 members in this family. Notably, cucurbitacin B, its derivative and semisynthetic

analogs are documented to induce apoptosis by suppressing Akt and MAPK signaling as well as inhibiting metastasis and invasion in A549 lung cells (Silva *et al*., 2016). Moreover, Wang *et al*., 2016 reported that cucurbitacin A inhibited the growth of A549 lung cells via arresting the G_2/M phase of the cell cycle and modulating Akt signaling. Furthermore, the outcome of the studies by Shukla *et al*., 2016 revealed that Cuc B demonstrated strong anti-migratory and anti-invasive capabilities against metastatic NSCLC at nanomolar concentrations; This inhibition of metastasis and angiogenesis was attributed to the downregulation of the Wnt/β-catenin signaling axis. In TNBC, findings by Kong *et al*., 2014, showed that Cuc E significantly inhibited the growth of the MDA-MB-468 and SW527 cell models by inducing cell cycle arrest within the G_2/M phase, inducing apoptosis, and inhibiting ERK and AKT expressions. Also, Sinha *et al*., 2016, demonstrated that treatment with Cuc B significantly inhibited the migratory and invasive potential of MDA-MB-231 and 4T1 cells; Cuc B significantly inhibited the vascular endothelial growth factor (VEGF)-induced phosphorylation of focal adhesion kinase and MMP-9 signaling. The important anticancer activity of the Cuc compounds is as a result of unique pharmacophores present on each member. Despite the promising anticancer activities of Cucs, some challenges have been identified that limits their usefulness. These compounds are secreted in minute quantities in plants and isolating substantial amount remains a challenge. Also, low doses of Cucs administered to mammals elicit adverse toxicity effects. Moreover, the total synthesis of Cucs is challenging due to the complexity of their structure. Interestingly, Cucs possess a similar base-scaffold to estrone with a minor difference. To overcome the challenges identified, a simple solution would be to use

estrone as a starting material and then introducing the anticancer pharmacophores of Cucs to synthesize novel hybrid.

1.5.2   Estrone analogs as effective anticancer small molecules

Estrone, a major mammalian estrogen, is naturally converted from androstenedione or from testosterone via estradiol and estrone sulfate. Estrone is in high demands nowadays as most synthetic or medicinal chemists use it as a starting material to synthesize novel derivatives. Some studies suggest that derivatives of estradiol, an isomer of estrone, exert significant antimitotic effects against various cancers including breast cancer. In particular, Stander *et al.*, 2011 report that 2-methoxyestradiol (2ME), an endogenous metabolite of 17β-estradiol, possess both antiangiogenic and anti-breast cancer effects *in vitro* and *in vivo*. This compound exerts its cytotoxic effect independently of the cellular estrogen receptors and has no significant systemic hormonal effects (Leese *et al.*, 2006). Estradiol, however, promotes the proliferation of various cancers (Verwey *et al.*, 2016). The above studies also report on the limited bioavailability of 2ME (Panzem®) due to its fast-metabolic breakdown during phase II clinical studies. Recently, a sulfamate derivative of 2ME has been found to possess potent antitumor activity against breast cancer cells due to its increased bioavailability by avoiding hepatic first-pass metabolism (Visagie *et al.*, 2013; Verwey *et al.*, 2016). A similar study reports the induction of mitochondrial apoptosis as the underlying mechanism for the observed cytotoxicity of 2ME sulfamate derivative against the NSCLC model, A549 (Nolte *et al.*, 2018). This suggests that estrone maybe a

privileged scaffold upon which modifications can be added to generate lead candidates with improved potency, pharmacokinetic properties and reduced toxicities. Discovering new drugs through research and development in the pharmaceutical industry is traditionally a tedious process which involves high cost. Novel approaches are always needed to reduce time and cost. Molecular docking is one means to provide a fast prediction of the proposed compounds' behavior against a biological target with a low cost (Csermely *et al*, 2013).

1.5.3 Molecular docking studies as first steps toward drug discovery

Molecular docking is a process where small organic compounds or large macromolecules like antibodies are fitted into the active site of target molecules, usually proteins to predict the molecules desirable properties. The main goal of this process is to find the most stable (lowest energy) conformer that interacts with the active site of the molecular target. Thus, molecular modeling is a powerful technique that can predict the characteristics of a set of compounds with specific pharmacophores based on their interaction with the targeted protein. This has often led to the identification of promising hits and novel lead candidates. The entire molecular docking process begins with building a library of compounds, then generating the appropriate conformation of the receptor of interest and finally performing the docking simulations to identify the hit compounds with better binding affinity and potency. Afterward, the large compound library is narrowed down into predicted active compounds, enabling optimization of lead compounds by improving the biological

properties, like affinity and absorption, distribution, metabolism, excretion, and toxicity (ADMET) (Osakwe and Rizvi, 2016).

It is noteworthy to mention that the drug discovery process has improved since computational approaches emerged over three decades ago (Osakwe and Rizvi, 2016). Several computational methods have been used in the drug discovery process. These include but are not limited to computer-aided drug design (CADD) and fragment-based drug discovery (FBDD). CADD entails a vast number of computational methodologies including virtual screening. Virtual screening technique can be divided into ligand- and structure-based drug design techniques (LBDD and SBDD). LBDD usually takes advantage of information from known bioactive compounds (ligand) and are essential tools when structural information of a biological target is missing or when the molecular design is not directed toward a target-centric approach but intended to modulate cellular pathways or phenotypic traits without a precise knowledge of the mechanism of action (Del Rio and Varchi, 2016). SBDD usually exploits the three-dimensional (3D) structure of the biological target (protein) to identify putative modulators of the protein activity. The compounds that show high binding affinity to the target protein, called "hits", are screened in a high-throughput bioassay screening (HTS) to identify the lead compound (Wolber and Sippl, 2015).

1.6   Research strategy and objectives

In our research group, estrone analogs are designed *in silico* for superior pharmacokinetics and virtually screened against different receptors including the EGFR kinase domain. The virtual hit compounds are subsequently synthesized using estrone as a starting material (Figure 1.5) and further tested for their cytotoxic effects before elucidating their mechanism of action. Many of our estrone derivatives, especially those bearing cucurbitacin pharmacophores have previously demonstrated potent cytotoxic effects against distinct cancers *in vitro* (Kopel *et al.,* 2013; Ahmed *et al.,* 2017; Ahmed *et al.*, 2014). Recently, a new series of estrone analogs (bearing either a modified cucurbitacin (MMA series) or triazole (Fz series) pharmacophores) have been synthesized and found to be potent against EGFR's kinase domain *in silico* and cytotoxic against EGFR dependent cancers, viz models of NSCLC and TNBC *in vitro* compared to the TKIs, erlotinib and sorafenib. This raises the question, "could these novel estrone analogs be more effective in the treatment of EGFR-dependent cancers than the current EGFR TKIs? We, therefore, hypothesized that the lead candidates will have a superior set of qualities for preclinical and clinical development compared to the current EGFR TKIs.
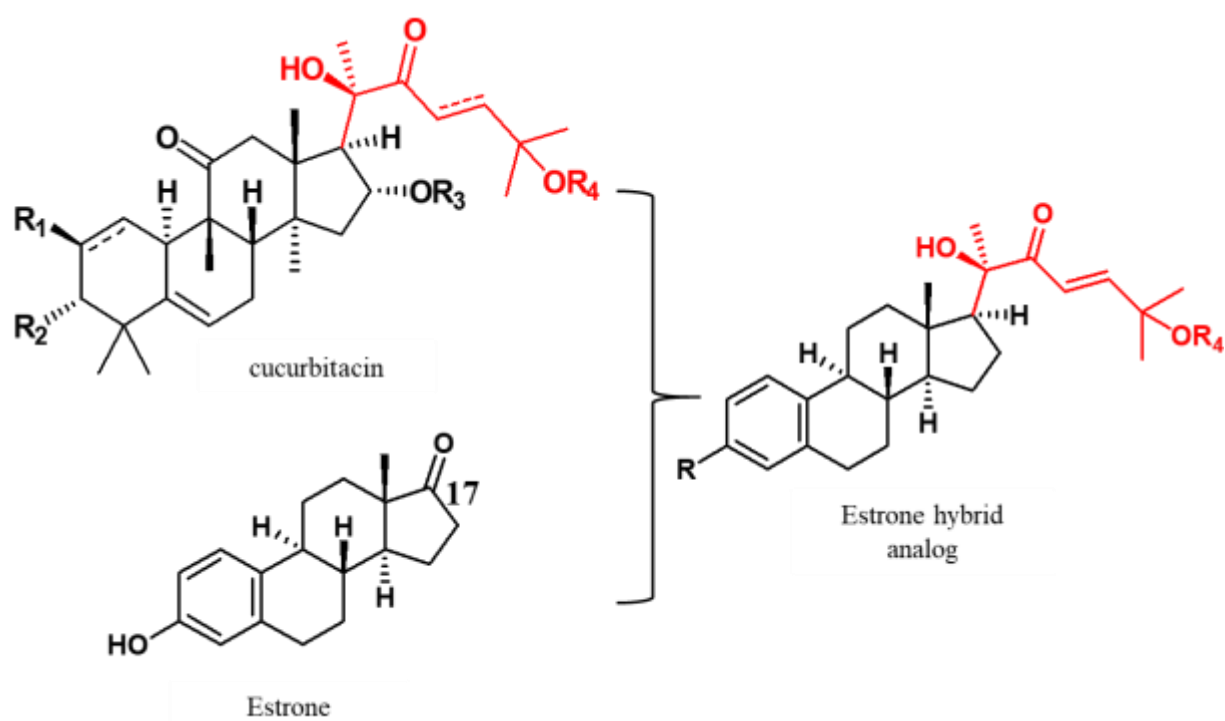
Figure 0.5 Design strategy for hybrid estrone derivatives. Estrone is used as a scaffold upon which modifications are made to obtain MMA or Fz series of compounds.

Objective 1: Screen a library of estrone analogs against EGF receptor in silico using a computer-aided molecular modeling (CAMM) to identify potential virtual hits.

To address the goal of our study, we first performed molecular docking studies to identify hits from our drug libraries. The co-crystallized structure of the EGFR kinase domain (PDB code: 2ITW, 1M17) was prepared and the three-dimensional structures of the estrone analogs constructed using Chem. 3D ultra 12.0 software. Virtual screening was carried out using the FRED application (version 2.2.5) of OpenEye® software. A lower consensus score indicated better potency and binding affinity of the ligands toward the receptor. For objective 1, the following research questions were investigated: I. Do the estrone analogs show better potency and binding compared to the co-crystallized compounds? II. What are the key molecular interactions utilized by estrone analogs to achieve drug potency?

Objective 2: Investigate the cytotoxic effects of estrone analogs against cancer cell lines using cell viability assays in vitro.

During the research and development process, to predict the therapeutic use of a new compound, one must know its biological activity and corresponding toxicity. Cell-based assays in the form of monolayer cell culture screens are usually the first approach used to confirm a compounds biological activity and cytotoxicity. In this objective, cell viability assays, including MTT and trypan blue cell counting, were employed to establish the cytotoxicity of the compounds. This allowed us to answer the question, are our hit compounds were more potent against NSCLC and TNBC cell lines compared to known TKIs *in vitro*?

Objective 3: Elucidate the estrone analogs molecular mechanism of action in cancer cells using cell-based and immuno assays in vitro.

When elucidating the mechanism of action of antitumor drugs, the extent of the compound's ability to inhibit cell proliferation, induce the death of a cell, or both are considered. There are diverse ways of determining inhibition of cell proliferation, but usually, inhibition of cell cycle progression depicted by an accumulation of DNA within distinct phases of the cell cycle is widely exploited by scientists. Also, programmed cell death (apoptosis) investigation is the most popular cell death mechanism studied by many researchers. In the third objective, both cell-based assays and immuno-assays were adopted to characterize the compound's mechanism of action that underlies their observed cytotoxicity. For this objective, we asked, "do estrone analogs inhibit NSCLC and TNBC cells proliferation or induce apoptotic cell death or both?"

1.7   Research relevance and innovation

Chemotherapy and anti-EGFRs are the current treatment modalities recommended for TNBC and NSCLC patients, respectively. Chemotherapy is effective and non-selective in its action whereas anti-EGFRs either irreversibly bind to the ATP binding site of EGFR kinase domain or EGFR extracellular domain in their mode of action. Despite the significant success of these therapeutic interventions over the years, acquired resistance and aggressive recurrent disease have been reported. Therefore, the search for potent and

safe next generation anti-EGFRs is imperative. Estrone analogs have shown great promise in various preclinical and clinical studies. These compounds exert their cytotoxic effect either dependently or independently of the cellular estrogen receptors. Particularly, Visagie *et al*., 2013; Verwey *et al*., 2016 report on a sulfamate derivative of 2ME that has been found to possess potent antitumor activity against breast cancer cells due to its increased bioavailability by avoiding hepatic first-pass metabolism. Also, a similar study reports induction of mitochondrial apoptosis as the underlying mechanism for the observed cytotoxicity of 2ME sulfamate derivative against the NSCLC model, A549 (Nolte *et al*., 2018). The above studies made modifications to the C-2 (ethyl group), C-3 (sulfamoyl or methoxy moieties) and C-17 (ketone or hydroxy functionalities) positions of the estrone skeleton. Amr *et al.*, 2019 reports on the synthesis of estrone derivatives using estrone aryl methylenes as a starting material. This study reports that the most effective compounds showed better binding towards EGFR, VEGFR-2 and induced p53 ubiquitination in MCF-7 cells. Amr and colleagues, 2019 in their design strategy made modifications (attached a heterocyclic ring) to C-16 and C-17 of the estrone scaffold.

It is interesting to note that during the pathogenesis of lung cancer, a type of non-hormonal cancer, estrogen receptor and aromatase enzyme which are important for estradiol biosynthesis and modulation are overexpressed. These proteins together with EGFR helps lung cancer cells to use estradiol for their growth and survival through the non-genomic pathway. Even though hormone receptors under expression have been observed in TNBC, EGFR overexpression persists especially in the advanced stage of the disease. Therefore, targeting EGFR, a central regulator of cell proliferation, is a promising strategy to inhibiting various downstream signaling pathways and ultimately inhibiting the growth of

cancer. We have designed a different series of estrone analogs against EGFR by installing

unique potent pharmacophores onto the estrone base scaffold yielding the MMA and Fz

series of compounds. The positions on the estrone skeleton targeted by our research group

are C-3 (various functionalities including methoxy, sulfamoyl, hydroxy, phenyl, etc.) and

C-17 (cucurbitacin pharmacophores or their modifications, triazole pharmacophore or its

modifications, etc.). The pharmacophores we introduced onto the estrone scaffold make

our design and synthesis approach very novel. We suggest that our new analogs may hold

the key to treating serious EGFR-specific cancers like NSCLC and TNBC. The current

research is novel and innovative because for the first time these estrone analogs have been

synthesized and their cytotoxic effects evaluated against EGFR-dependent cancers, viz.

NSCLC and TNBC monolayer models.

1.8   References

Acheampong, F., Reilly, J., Larbie, C., Spencer, M., Gunderson, K., Appiah-Opong, R., and Voytek, S. (2017). Methoxy-flavones identified from Ageratum conyzoides induce caspase-3 and-7 activations in Jurkat cells. *Journal of Medicinal Plants Research*, 11(38), 583-590.

Acheampong, F., Larbie, C., and Fareed, K. N. A. (2015). Antioxidants and anticancer study of Ageratum conyzoides aqueous extracts. *Journal of Global Biosciences*. 4(1), 1804-1815.

Ahmed, M. S., El-Senduny, F., Taylor, J., and Halaweish, F. T. (2017). Biological screening of cucurbitacin inspired estrone analogs targeting mitogen-activated protein kinase (MAPK) pathway. *Chemical Biology and Drug Design*, 90(3), 478-484.

Ahmed, M. S., Kopel, L. C., and Halaweish, F. T. (2014). Structural optimization and biological screening of a steroidal scaffold possessing cucurbitacin-like functionalities as B-raf inhibitors. *ChemMedChem*, 9(7), 1361-1367.

Alberg, A. J., Brock, M. V., Ford, J. G., Samet, J. M., and Spivack, S. D. (2013). Epidemiology of lung cancer: Diagnosis and management of lung cancer: American College of Chest Physicians evidence-based clinical practice guidelines. *Chest*, 143(5), e1S-e29S.

American Cancer Society. Cancer Facts and Figures 2019. Atlanta, Ga: *American Cancer Society*; 2019.

Anguera, G., and Majem, M. (2018). BRAF inhibitors in metastatic non-small cell lung cancer. *Journal of Thoracic Disease*, 10(2), 589.

Annunziato, S., de Ruiter, J. R., Henneman, L., Brambillasca, C. S., Lutz, C., Vaillant, F., and van Gerwen, B. (2019). Comparative oncogenomics identifies combinations of driver genes and drug targets in BRCA1-mutated breast cancer. *Nature Communications*, 10.

Ashford, A. L., Oxley, D., Kettle, J., Hudson, K., Guichard, S., Cook, S. J., and Lochhead, P. A. (2014). A novel DYRK1B inhibitor AZ191 demonstrates that DYRK1B acts independently of GSK3β to phosphorylate cyclin D1 at Thr286, not Thr288. *Biochemical Journal*, 457(1), 43-56.

Bae, S. Y., Nam, S. J., Jung, Y., Lee, S. B., Park, B. W., Lim, W., and Jung, S. P. (2018). Differences in prognosis and efficacy of chemotherapy by p53 expression in triple-negative breast cancer. *Breast Cancer Research and Treatment*, 172(2), 437-444.

Balko, J. M., Giltnane, J. M., Wang, K., Schwarz, L. J., Young, C. D., Cook, R. S., and Kurupi, R. (2014). Molecular profiling of the residual disease of triple-negative breast cancers after neoadjuvant chemotherapy identifies actionable therapeutic targets. *Cancer Discovery*, 4(2), 232-245.

Bartholomew, C., Eastlake, L., Dunn, P., and Yiannakis, D. (2017). EGFR targeted therapy in lung cancer; an evolving story. *Respiratory Medicine Case Reports*, 20, 137-140.

Baselga, J., Albanell, J., Ruiz, A., Lluch, A., Gascón, P., Guillém, V., and Koehler, M. T. (2005). Phase II and tumor pharmacodynamic study of gefitinib in patients with advanced breast cancer. *Journal of Clinical Oncology*, 23(23), 5323-5333.

Baumgart, M. (2015). New Molecular Targets on the Horizon in NSCLC| GoToPER. com. *American Journal of Hematology/Oncology®*, 11(6).

Baxevanos, P., and Mountzios, G. (2018). Novel chemotherapy regimens for advanced lung cancer: have we reached a plateau?. *Annals of Translational Medicine*, 6(8).

Bernsdorf, M., Ingvar, C., Jörgensen, L., Tuxen, M. K., Jakobsen, E. H., Saetersdal, A., and Ejlertsen, B. (2011). Effect of adding gefitinib to neoadjuvant chemotherapy in estrogen receptor negative early breast cancer in a randomized phase II trial. *Breast Cancer Research and Treatment*, *126*(2), 463-470.

Billen, L. P., Shamas-Din, A., and Andrews, D. W. (2009). Bid: a Bax-like BH3 protein. Oncogene, 27(S1), S93.

Byrski, T., Huzarski, T., Dent, R., Marczyk, E., Jasiówka, M., Gronwald, J., and Lubinski, J. (2014). Pathologic complete response to neoadjuvant cisplatin in BRCA1-positive breast cancer patients. *Breast Cancer Research and Treatment*, 147(2), 401-405.

Caiazza, F., Murray, A., Madden, S. F., Synnott, N. C., Ryan, E. J., O'Donovan, N., and Duffy, M. J. (2016). Preclinical evaluation of the AR inhibitor enzalutamide in triple-negative breast cancer cells. *Endocrine-Related Cancer*, 23(4), 323-334.

Carey, L. A., Rugo, H. S., Marcom, P. K., Mayer, E. L., Esteva, F. J., Ma, C. X., and Wolff, A. C. (2012). TBCRC 001: randomized phase II study of cetuximab in combination with carboplatin in stage IV triple-negative breast cancer. *Journal of Clinical Oncology*, *30*(21), 2615.

Chen, Q. Y., and Costa, M. (2018). PI3K/Akt/mTOR signaling pathway and the biphasic effect of arsenic in carcinogenesis. *Molecular Pharmacology*, 94(1), 784-792.

Choy, C., Raytis, J. L., Smith, D. D., Duenas, M., Neman, J., Jandial, R., and Lew, M. W. (2016). Inhibition of β2-adrenergic receptor reduces triple-negative breast cancer brain metastases: the potential benefit of perioperative β-blockade. *Oncology Reports*, 35(6), 3135-3142.

Cortazar, P., Zhang, L., Untch, M., Mehta, K., Costantino, J. P., Wolmark, N., and Swain, S. M. (2014). Pathological complete response and long-term clinical benefit in breast cancer: the CTNeoBC pooled analysis. *The Lancet*, 384(9938), 164-172.

Crozier, J. A., Advani, P. P., LaPlant, B., Hobday, T., Jaslowski, A. J., Moreno-Aspitia, A., and Perez, E. A. (2016). N0436 (Alliance): a phase II trial of irinotecan with cetuximab in patients with metastatic breast cancer previously exposed to anthracycline and/or taxane-containing therapy. *Clinical Breast Cancer*, *16*(1), 23-30.

Csermely, P., Korcsmáros, T., Kiss, H. J., London, G., and Nussinov, R. (2013). Structure and dynamics of molecular networks: a novel paradigm of drug discovery: a comprehensive review. *Pharmacology and Therapeutics*, 138(3), 333-408.

Dai, X., Li, Y., Bai, Z., and Tang, X. Q. (2015). Molecular portraits revealing the heterogeneity of breast tumor subtypes defined using immunohistochemistry markers. *Scientific Reports*, 5, 14499.

Del Rio, A., and Varchi, G. (2016). Molecular Design of Compounds Targeting Histone Methyltransferases. In Epi-Informatics (pp. 257-272). Academic Press.

Dent, R., Trudeau, M., Pritchard, K. I., Hanna, W. M., Kahn, H. K., Sawka, C. A., and Narod, S. A. (2007). Triple-negative breast cancer: clinical features and patterns of recurrence. *Clinical Cancer Research*, 13(15), 4429-4434.

Dickler, M. N., Cobleigh, M. A., Miller, K. D., Klein, P. M., and Winer, E. P. (2009). Efficacy and safety of erlotinib in patients with locally advanced or metastatic breast cancer. *Breast Cancer Research and Treatment*, 115(1), 115-121.

Diluvio, G., Del Gaudio, F., Giuli, M. V., Franciosa, G., Giuliani, E., Palermo, R., and Maroder, M. (2018). NOTCH3 inactivation increases triple negative breast cancer sensitivity to gefitinib by promoting EGFR tyrosine dephosphorylation and its intracellular arrest. *Oncogenesis*, 7(5), 42.

Farhat, F. S., and Houhou, W. (2013). Targeted therapies in non-small cell lung carcinoma: what have we achieved so far?. *Therapeutic Advances in Medical Oncology*, 5(4), 249-270.

Foidart, P., Yip, C., Radermacher, J., Blacher, S., Lienard, M., Montero-Ruiz, L., and Coibion, M. (2019). Expression of MT4-MMP, EGFR, and RB in Triple-Negative

Breast Cancer Strongly Sensitizes Tumors to Erlotinib and Palbociclib Combination Therapy. *Clinical Cancer Research*, 25(6), 1838-1850.

Fruman, D., A, Chiu, H., Hopkins, B., D, Bagrodia, S., Cantley, L., C, and Abraham R., T. (2017) The PI3K pathway in human disease. *Cell* 170:605–635.

Gao, J., Zhao, Y., Lv, Y., Chen, Y., Wei, B., Tian, J., and Shi, H. (2013). Mirk/Dyrk1B mediates G0/G1 to S phase cell cycle progression and cell survival involving MAPK/ERK signaling in human cancer cells. *Cancer Cell International*, 13(1), 2.

Garmpis, N., Damaskos, C., Garmpi, A., Kalampokas, E., Kalampokas, T., Spartalis, E., and Kontzoglou, K. (2017). Histone deacetylases as new therapeutic targets in triple-negative breast Cancer: Progress and promises. *Cancer Genomics-Proteomics*, 14(5), 299-313.

Garrido-Castro, A. C., Lin, N. U., and Polyak, K. (2019). Insights into Molecular Classifications of Triple-Negative Breast Cancer: Improving Patient Selection for Treatment. *Cancer Discovery*, 9(2), 176-198.

Gridelli, C., Maione, P., and Rossi, A. (2008). The potential role of mTOR inhibitors in non-small cell lung cancer. *The Oncologist*, 13(2), 139-147.

Ha, S. Y., Choi, S. J., Cho, J. H., Choi, H. J., Lee, J., Jung, K., and Kim, H. K. (2015). Lung cancer in never-smoker Asian females is driven by oncogenic mutations, most often involving EGFR. *Oncotarget,* 6(7), 5465.

Hall, J. A., Seedarala, S., Rice, N., Kopel, L., Halaweish, F., and Blagg, B. S. (2015). Cucurbitacin D is a disruptor of the HSP90 chaperone machinery. *Journal of Natural Products*, 78(4), 873-879.

Herbst, R. S., Morgensztern, D., and Boshoff, C. (2018). The biology and management of non-small cell lung cancer. *Nature*, 553(7689), 446.

Hotta, K., Matsuo, K., Ueoka, H., Kiura, K., Tabata, M., and Tanimoto, M. (2004). Meta-analysis of randomized clinical trials comparing cisplatin to carboplatin in patients with advanced non-small-cell lung cancer. *Journal of Clinical Oncology*, 22(19), 3852-3859.

Ignacio, R. M. C., Gibbs, C. R., Lee, E. S., and Son, D. S. (2018). The TGFα-EGFR-Akt signaling axis plays a role in enhancing proinflammatory chemokines in triple-negative breast cancer cells. *Oncotarget*, 9(50), 29286.

Imai, K., and Takaoka, A. (2006). Comparing antibody and small-molecule therapies for cancer. *Nature Reviews Cancer*, 6(9), 714.

Jorge, S. E. D. C., Kobayashi, S. S., and Costa, D. B. (2014). Epidermal growth factor receptor (EGFR) mutations in lung cancer: preclinical and clinical data. *Brazilian Journal of Medical and Biological Research*, 47(11), 929-939.

Kim, B. K., Chang, Y., Ahn, J., Jung, H. S., Kim, C. W., Yun, K. E., and Ryu, S. (2015). Metabolic syndrome, insulin resistance, and mammographic density in pre-and postmenopausal women. *Breast Cancer Research and Treatment*, 153(2), 425-434.

Kong, Y., Chen, J., Zhou, Z., Xia, H., Qiu, M. H., and Chen, C. (2014). Cucurbitacin E induces cell cycle G2/M phase arrest and apoptosis in triple negative breast cancer. *PloS One*, 9(7), e103760.

Kopel, L. C., Ahmed, M. S., and Halaweish, F. T. (2013). Synthesis of novel estrone analogs by incorporation of thiophenols via conjugate addition to an enone side chain. *Steroids*, 78(11), 1119-1125.

Larbie, C., Inkabi, S. E., Appiah-Opong, R., Acheampong, F., Tuffour, I., Uto, T., and Tagoe, D. N. (2015). Anti-proliferative effect of Ficus pumila Linn. on human leukemic cell lines. *International Journal of Basic and Clinical Pharmacology,* 4(2), 330-336.

Lee, A., and Djamgoz, M. B. (2018). Triple negative breast cancer: emerging therapeutic modalities and novel combination therapies. *Cancer Treatment Reviews*, 62, 110-122.

Leese, M. P., Leblond, B., Smith, A., Newman, S. P., Di Fiore, A., De Simone, G., and Potter, B. V. (2006). 2-substituted estradiol bis-sulfamates, multitargeted antitumor agents: synthesis, in vitro SAR, protein crystallography, and in vivo activity. *Journal of Medicinal Chemistry*, 49(26), 7683-7696.

Lehmann, B. D., Bauer, J. A., Chen, X., Sanders, M. E., Chakravarthy, A. B., Shyr, Y., and Pietenpol, J. A. (2011). Identification of human triple-negative breast cancer subtypes and preclinical models for selection of targeted therapies. *The Journal of Clinical Investigation*, 121(7), 2750-2767.

Lehmann, B. D., Jovanović, B., Chen, X., Estrada, M. V., Johnson, K. N., Shyr, Y., and Pietenpol, J. A. (2016). Refinement of triple-negative breast cancer molecular subtypes: implications for neoadjuvant chemotherapy selection. *PloS One*, 11(6), e0157368.

Lin, J. J., Cardarella, S., Lydon, C. A., Dahlberg, S. E., Jackman, D. M., Jänne, P. A., and Johnson, B. E. (2016). Five-year survival in EGFR-mutant metastatic lung adenocarcinoma treated with EGFR-TKIs. *Journal of Thoracic Oncology*, *11*(4), 556-565.

Liu, X., Wang, P., Zhang, C., and Ma, Z. (2017). Epidermal growth factor receptor (EGFR): A rising star in the era of precision medicine of lung cancer. *Oncotarget*, 8(30), 50209.

Ma, H., Ursin, G., Xu, X., Lee, E., Togawa, K., Duan, L., and Simon, M. S. (2017). Reproductive factors and the risk of triple-negative breast cancer in white women and African-American women: a pooled analysis. *Breast Cancer Research*, 19(1), 6.

MacCorkle, R. A., and Tan, T. H. (2005). Mitogen-activated protein kinases in cell-cycle control. *Cell Biochemistry and Biophysics*, 43(3), 451-461.

Manoto, S., Houreld, N., Hodgkinson, N., and Abrahamse, H. (2017). Modes of cell death induced by photodynamic therapy using zinc phthalocyanine in lung cancer cells grown as a monolayer and three-dimensional multicellular spheroids. *Molecules*, 22(5), 791.

Masuda, N., Lee, S. J., Ohtani, S., Im, Y. H., Lee, E. S., Yokota, I., and Yanagita, Y. (2017). Adjuvant capecitabine for breast cancer after preoperative chemotherapy. *New England Journal of Medicine*, 376(22), 2147-2159.

Molina, J. R., and Adjei, A. A. (2006). The Ras/Raf/MAPK pathway. *Journal of Thoracic Oncology*, *1*(1), 7-9.

Morales-Espinosa, D., and Rosell, R. (2015). Second-line treatment in EGFR-unselected patients: is it time to close one arm of this river's DELTA?. *Journal of Thoracic Disease*, 7(3), 227.

Nabholtz, J. M., Chalabi, N., Radosevic-Robin, N., Dauplat, M. M., Mouret-Reynier, M. A., Van Praagh, I., ... and Bahadoor, M. R. K. (2016). Multicentric neoadjuvant pilot Phase II study of cetuximab combined with docetaxel in operable triple negative breast cancer. *International Journal of Cancer*, *138*(9), 2274-2280.

Nagata, Y., Takahashi, A., Ohnishi, K., Ota, I., Ohnishi, T., Tojo, T., and Taniguchi, S. (2010). Effect of rapamycin, an mTOR inhibitor, on radiation sensitivity of lung cancer cells having different p53 gene status. *International Journal of Oncology*, 37(4), 1001-1010.

Nan, X., Xie, C., Yu, X., and Liu, J. (2017). EGFR TKI as first-line treatment for patients with advanced EGFR mutation-positive non-small-cell lung cancer. *Oncotarget*, 8(43), 75712.

Natori, A., Ethier, J. L., Amir, E., and Cescon, D. W. (2017). Capecitabine in early breast cancer: a meta-analysis of randomised controlled trials. *European Journal of Cancer*, 77, 40-47.

Nolte, E., Joubert, A., Lakier, R., Van Rensburg, A., and Mercier, A. (2018). Exposure of Breast and Lung Cancer Cells to a Novel Estrone Analog Prior to Radiation Enhances Bcl-2-Mediated Cell Death. *International Journal of Molecular Sciences*, 19(10), 2887.

Nomori, H., Shimosato, Y., Kodama, T., Morinaga, S., Nakajima, T., and Watanabe, S. (1986). Subtypes of small cell carcinoma of the lung: morphometric, ultrastructural, and immunohistochemical analyses. *Human Pathology*, 17(6), 604-613.

Osakwe, O., and Rizvi, S. A. A. (2016). The significance of discovery screening and structure optimization studies. Social Aspects of Drug Discovery, Development and Commercialization *(Elsevier;)*, 109-128.

Papadimitriou, M., Mountzios, G., and Papadimitriou, C. A. (2018). The role of PARP inhibition in triple-negative breast cancer: unraveling the wide spectrum of synthetic lethality. *Cancer Treatment Reviews*. 67, 34-44.

Park, J. H., Ahn, J. H., and Kim, S. B. (2018). How shall we treat early triple-negative breast cancer (TNBC): From the current standard to upcoming immuno-molecular strategies. *ESMO Open*, 3(Suppl 1), e000357.

Pirker, R. (2012). EGFR-directed monoclonal antibodies in non-small cell lung cancer: how to predict efficacy?. *Translational Lung Cancer Research*, 1(4), 269.

Podo, F., Santoro, F., Di Leo, G., Manoukian, S., De Giacomi, C., Corcione, S., and Preda, L. (2016). Triple-Negative versus Non–Triple-Negative Breast Cancers in High-Risk Women: Phenotype Features and Survival from the HIBCRIT-1 MRI-Including Screening Study. *Clinical Cancer Research*, 22(4), 895-904.

Porta, C., Paglino, C., and Mosca, A. (2014). Targeting PI3K/Akt/mTOR signaling in cancer. *Frontiers in Oncology*, 4, 64.

Rosa, B., de Jesus, J. P., de Mello, E. L., Cesar, D., and Correia, M. M. (2015). Effectiveness and safety of monoclonal antibodies for metastatic colorectal cancer treatment: systematic review and meta-analysis. *Ecancermedicalscience*, 9.

Sabatier, R., Lopez, M., Guille, A., Billon, E., Carbuccia, N., Garnier, S., and Pakradouni, J. (2019). High Response to Cetuximab in a Patient With EGFR-Amplified Heavily Pretreated Metastatic Triple-Negative Breast Cancer. *JCO Precision Oncology*, *3*, 1-8.

Santoro, A., Vlachou, T., Luzi, L., Melloni, G., Mazzarella, L., D'Elia, E., and Punzi, S. (2019). p53 Loss in Breast Cancer Leads to Myc Activation, Increased Cell Plasticity, and Expression of a Mitotic Signature with Prognostic Value. *Cell Reports*, *26*(3), 624-638.

Sato, H., Yamamoto, H., Sakaguchi, M., Shien, K., Tomida, S., Shien, T., and Yoshioka, T. (2018). Combined inhibition of MEK and PI3K pathways overcomes acquired resistance to EGFR-TKIs in non-small cell lung cancer. *Cancer Science*, 109(10), 3183.

Shukla, S., Sinha, S., Khan, S., Kumar, S., Singh, K., Mitra, K., and Meeran, S. M. (2016). Cucurbitacin B inhibits the stemness and metastatic abilities of NSCLC via downregulation of canonical Wnt/β-catenin signaling axis. *Scientific Reports*, 6, 21860.

Sikander, M., Hafeez, B. B., Malik, S., Alsayari, A., Halaweish, F. T., Yallapu, M. M., and Jaggi, M. (2016). Cucurbitacin D exhibits potent anti-cancer activity in cervical cancer. *Scientific Reports*, 6, 36594.

Silva, I. T., Geller, F. C., Persich, L., Dudek, S. E., Lang, K. L., Caro, M. S. B., and Simões, C. M. O. (2016). Cytotoxic effects of natural and semisynthetic cucurbitacins on lung cancer cell line A549. *Investigational New Drugs*, 34(2), 139-148.

Silver, D. P., Richardson, A. L., Eklund, A. C., Wang, Z. C., Szallasi, Z., Li, Q., and Fatima, A. (2010). Efficacy of neoadjuvant Cisplatin in triple-negative breast cancer. *Journal of Clinical Oncology*, 28(7), 1145.

Sim, E. H., Yang, I. A., Wood-Baker, R., Bowman, R. V., and Fong, K. M. (2018). Gefitinib for advanced non-small cell lung cancer. *Cochrane Database of Systematic Reviews*, (1).

Sinha, S., Khan, S., Shukla, S., Lakra, A. D., Kumar, S., Das, G., and Meeran, S. M. (2016). Cucurbitacin B inhibits breast cancer metastasis and angiogenesis through VEGF-mediated suppression of FAK/MMP-9 signaling axis. *The International Journal of Biochemistry and Cell Biology*, 77, 41-56.

Soldani, C., and Scovassi, A. I. (2002). Poly (ADP-ribose) polymerase-1 cleavage during apoptosis: an update. *Apoptosis*, 7(4), 321-328.

Stander, A., Joubert, F., and Joubert, A. (2011). Docking, synthesis, and in vitro evaluation of antimitotic estrone analogs. *Chemical Biology and Drug Design*, 77(3), 173-181.

Székely, B., Silber, A. L., and Pusztai, L. (2017). New Therapeutic Strategies for Triple-Negative Breast Cancer: Page 2 of 2. *Oncology*, 31(2).

Telli, M. L., Jensen, K. C., Vinayak, S., Kurian, A. W., Lipson, J. A., Flaherty, P. J., and Carlson, R. W. (2015). Phase II study of gemcitabine, carboplatin, and iniparib as neoadjuvant therapy for triple-negative and BRCA1/2 mutation–associated breast cancer with assessment of a tumor-based measure of genomic instability: PrECOG 0105. *Journal of Clinical Oncology*, *33*(17), 1895.

Teng, Y. H. F., Tan, W. J., Thike, A. A., Cheok, P. Y., Tse, G. M. K., Wong, N. S., and Tan, P. H. (2011). Mutations in the epidermal growth factor receptor (EGFR) gene in triple negative breast cancer: possible implications for targeted therapy. *Breast Cancer Research*, 13(2), R35.

Thomford, N., Senthebane, D., Rowe, A., Munro, D., Seele, P., Maroyi, A., and Dzobo, K. (2018). Natural products for drug discovery in the 21st century: Innovations for novel drug discovery. *International Journal of Molecular Sciences*, 19(6), 1578.

Trédan, O., Campone, M., Jassem, J., Vyzula, R., Coudert, B., Pacilio, C. and Aloe, A. (2015). Ixabepilone alone or with cetuximab as first-line treatment for advanced/metastatic triple-negative breast cancer. *Clinical Breast Cancer*, *15*(1), 8-15.

Uscanga-Perales, G. I., Santuario-Facio, S. K., and Ortiz-López, R. (2016). Triple negative breast cancer: Deciphering the biology and heterogeneity. *Medicina Universitaria*, 18(71), 105-114.

Verwey, M., Nolte, E. M., Joubert, A. M., and Theron, A. E. (2016). Autophagy induced by a sulphamoylated estrone analogue contributes to its cytotoxic effect on breast cancer cells. *Cancer Cell International*, 16(1), 91.

Visagie, M., Theron, A., Mqoco, T., Vieira, W., Prudent, R., Martinez, A., and Joubert, A. (2013). Sulphamoylated 2-methoxyestradiol analogues induce apoptosis in adenocarcinoma cell lines. *PLoS One*, 8(9), e71935.

Wahba, H. A., and El-Hadaad, H. A. (2015). Current approaches in treatment of triple-negative breast cancer. *Cancer Biology and Medicine*, 12(2), 106.

Wang, W. D., Liu, Y., Su, Y., Xiong, X. Z., Shang, D., Xu, J. J., and Liu, H. J. (2017). Antitumor and apoptotic effects of cucurbitacin a in A-549 lung carcinoma cells is mediated via G2/M cell cycle arrest and M-TOR/PI3K/Akt signalling pathway. *African Journal of Traditional, Complementary and Alternative Medicines*, 14(2), 75-82.

Winter, E., Chiaradia, L. D., Silva, A. H., Nunes, R. J., Yunes, R. A., and Creczynski-Pasa, T. B. (2014). Involvement of extrinsic and intrinsic apoptotic pathways together with endoplasmic reticulum stress in cell death induced by naphthylchalcones in a leukemic cell line: Advantages of multi-target action. *Toxicology in Vitro*, 28(5), 769-777.

Wolber, G., and Sippl, W. (2015). Pharmacophore identification and pseudo-receptor modeling. In The Practice of Medicinal Chemistry (pp. 489-510). Academic Press.

Yi-Long, W. U., Da-Tong, C. H. U., Baohui, H. A. N., Xuyi, L. I. U., Zhang, L., Caicum, Z. H. O. U. and Fukuoka, M. (2012). Phase III, randomized, open-label, first-line study in Asia of gefitinib versus carboplatin/paclitaxel in clinically selected patients with advanced non-small-cell lung cancer: evaluation of patients recruited from mainland China. *Asia-Pacific Journal of Clinical Oncology*, 8(3), 232-243.

Zhang, Y. N., Wu, X. Y., Zhong, N., Deng, J., Zhang, L., Chen, W. and Zhong, C. J. (2014). Stimulatory effects of sorafenib on human non-small cell lung cancer cells in vitro by regulating MAPK/ERK activation. *Molecular Medicine Reports*, 9(1), 365-369.

Chapter 2

Novel estrone analogs inhibit NCIH226 cells proliferation by suppressing EGFR and ERK1/2 pathway as well as arresting G$_1$ phase of the cell cycle.

2.1 Abstract

Lung cancer is the deadliest human cancer globally, with non-small cell lung cancer (NSCLC) being the most frequent type. Epidermal growth factor receptor (EGFR), a central regulator of tumor progression is frequently overexpressed in NSCLC and is a key drug target. Here, we describe the *in-silico* design and synthesis of novel estrone analogs: a hybrid of modified cucurbitacin (Cucs) pharmacophore and estrone base-scaffold as potent inhibitors of NCIH226 cells. Molecular docking studies revealed that most estrone analogs exhibited better potency and binding than the positive controls, erlotinib and sorafenib, when fitted into wild-type EGFR ATP binding site (pdb code: 2ITW). Moreover, two of the analogs, MMA307 and MM320, significantly inhibited the proliferation of NCIH226 cells with IC_{50} dose of 2.88 ± 0.21 and 9.68 ± 0.24 µM respectively, compared to the positive control, sorafenib, IC_{50} molarity of 20.62 ± 1.32 µM. Exposing NCIH226 cells to IC_{50} concentration of MMA307 and MMA320 resulted in downregulation of EGFR and phospho-EGFR expression levels, and suppression of activated MAPK-ERK1/2 signaling proteins; phospho-B-Raf, phospho-MEK1/2 and phospho-ERK1/2. Furthermore, downregulation of cyclin D1 and concomitant upregulation of phospho-cyclin D1 and $p21^{waf1/cip1}$ were observed after the compounds' addition to NCIH226 cells resulted in G_1 phase cell cycle arrest. MMA320 but not MMA307 downregulated the expression levels of Dyrk1B, a checkpoint kinase at the G_1-S phase transition of the cell cycle. To conclude, the present study is the first to report on the antiproliferative potential of novel estrone analogs and provide evidence that MMA307 and MMA320 are promising novel lead candidates for the development of anti-lung cancer drugs.

2.2   Introduction

Lung cancer has the highest mortality rate worldwide and accounts for more than a quarter of all cancer-related deaths (Siegel *et al.,* 2018). Among patients with lung cancer, 25-40% have brain metastases at some point during their disease (Siegel *et al.,* 2018). Non-small cell lung cancer (NSCLC) (~85%) is the most frequent type; "non–small cell" refers to the type of cell within the lung where the cancer originated. In the last few years, the discovery of EGFR as a key driver of NSCLC has led to the classification of patients as either harboring mutations in EGFR kinase domain-mutant EGFR or overexpressed EGFR-EGFR wild-type NSCLC. An estimated 45-70 % of NSCLC cases have EGFR frequently overexpressed (Forcella *et al.,* 2017).

EGFR amplification is an important oncogenic strategy that drives cancer cell proliferation. EGFR is a member of the human epidermal growth factor receptor (HER) family of receptor tyrosine kinases that consists of four members: HER1, HER2, HER3 and HER4. Activation of EGFR through ligand binding promotes receptor dimerization and autophosphorylation which initiates various signaling cascades, one of which is the RAS/RAF/MEK/ERK network. The ERK-MAPK pathway is initiated through the promotion of Ras binding to guanosine triphosphate (GTP), which in turn activates RAF kinases MAPK/extracellular signal-regulated kinases (MEK), and ERK (MacCorkle and Tan, 2005). Activated ERK is thought to translocate into the nucleus, where it phosphorylates and activates numerous targets, elk-1, c-jun, fos, etc. (MacCorkle and Tan, 2005). These transcription factors control the expression of downstream cell cycle

regulators, including cyclin D and p21$^{waf1/cip1}$ as well as Dyrk1B (dual-specificity tyrosine phosphorylation-regulated kinase 1B), a checkpoint kinase important for G_1 to S phase cell cycle transition (MacCorkle and Tan, 2005). Cyclin D overexpression and p21$^{waf1/cip1}$ downregulation are often associated with cancer development. Cyclin D1, a D-type cyclin and well-characterized oncogenic protein, forms active complexes with cyclin-dependent kinases (CDK) 4/6, which phosphorylate and inactivate retinoblastoma tumor suppressor (Rb), leading to the activation of the transcription factor E2F and upregulation of target genes essential for progression from G_1 to S phase of the cell-cycle (Torii *et al.,* 2006). On the other hand, p21$^{waf1/cip1}$ causes G_1 phase cell cycle arrest through phosphorylation of cyclin D1 that leads to its ubiquitination and degradation. Dyrk1B, a G_1-S phase checkpoint kinase, is amplified or overexpressed in certain cancers including NSCLC signifying that it may be an oncogene (Gao *et al.,* 2013; Ashford *et al.,*2014). Dyrk1B is thought to arrest damage tumors in the G_0/G_1 phase to allow their repair in the quiescent state and maintain the clonogenicity of tumors via mediating cyclin D1 turnover and stabilizing p21$^{waf1/cip1}$ (Gao *et al.,* 2013; Ashford *et al.,*2014).

In the past three decades, EGFR has been exploited as a molecular target for two distinct kinds of molecules, monoclonal antibodies (mAbs) and tyrosine kinase inhibitors (TKI). mAbs were thought to be efficacious in EGFR wild-type NSCLC patients while TKIs are effective in NSCLC patients with mutations in the EGFR kinase domain (Imai and Takaoka, 2006). Usually, EGFR wild-type patients with advanced disease are treated with chemotherapy as first-line, and TKIs (gefitinib, erlotinib, afatinib) or mAbs (cetuximab, trastuzumab) as second-line treatment (Nun *et al.,* 2017; Zhang *et al.,* 2014).

It is noteworthy to mention that some clinical trials report that TKIs and mAbs are effective first line agents like chemotherapy in treating EGFR wild-type NSCLCs. Notably, studies by Gridelli *et al.,* 2012; Shepherd *et al.,* 2005 conveyed TKIs or mAbs as beneficial agents against unselected NSCLC patients in terms of response rate and overall survival. Moreover, Zhao *et al.,* 2017 and Scholl *et al.,* 2010 documented that EGFR wild-type NSCLC patients with advanced disease are sensitive to TKIs or mAbs or a combination of TKIs and mAbs. However, recent studies report that most patients eventually experience recurrent disease within 12 to 14 months after anti-EGFR treatment and patients five-year survival after anti-EGFRs exposure is approximately 15% (Wu and Shih, 2018; Ali *et al.,*2013). Additionally, the long-term administration of anti-EGFR therapy accompanies with acquired resistance which limits the treatment efficacy, leading to aggressive tumors and rapid metastasis (Inoue *et al.,*2016; Qi *et al.,* 2018). Thus, in addition to exploring the in-depth drug resistance mechanism of existing drugs, as well as the relationship between EGFR-mediated signaling pathways and tumor specificity, discovering a novel type of targeted agents with improved efficacy and lower toxicity as an alternative therapy to treat these unique patient population is a promising strategy.

Numerous successful anticancer drugs in clinical use are either natural products or their synthetic analogs. In this perspective, cucurbitacins (cucs) and their analogs have become a focus of research because of their capability to significantly inhibit the growth of distinct cancers. Cucs belong to a large family of triterpenoids present in *Cucurbitaceae* plants, and possess many biological activities, with the most relevant without a doubt is anticancer properties toward different cancers (Sikander *et al.,* 2016; Hall *et al.,* 2015;

Chung *et al.,* 2015; Zhang *et al.,* 2014). Notably, cucurbitacin B, its derivative and semisynthetic analogs are documented to induce apoptosis through suppressing Akt and MAPK signaling as well as inhibiting metastasis and invasion in A549 lung cells (Silva *et al.,* 2016). Moreover, Wang and colleagues, 2017 report that cucurbitacin A inhibited the growth of A549 lung cells via arresting the G_2/M phase of cell cycle and modulating Akt signaling. Cucs are secreted in minute quantities in plants and isolating substantial amount remains a challenge. Also, the total synthesis of Cucs is difficult due to the complexity of Cucs structure. Interestingly, there is as structure similarity between Cucs and estrone with a minor difference. Estrone, a major mammalian estrogen, is naturally converted from androstenedione or from testosterone via estradiol and estrone sulfate. Previous studies report that estradiol derivatives possess antimitotic activity. Particularly, a sulphamoylated analog of 2-methoxyoestradiol has been found to be effective against NSCLC due to its increased bioavailability (resist first pass of liver metabolism) (Stander *et al.,* 2013; Stander *et al.,* 2012; Stander *et al.,* 2011). These and similar studies suggest that estrone may be a privileged skeleton upon which pharmacophores can be introduced to generate hybrid analogs with superior pharmacokinetics and improved toxicity. In our research group, estrone analog- a hybrid of modified cucs pharmacophores and estrone base-scaffold are *in silico* designed against important clinical targets including EGFR. In the present study, we report on the design and synthesis of novel estrone analogs, and the compounds inhibition of NCIH226 cells proliferation. We found that two novel analogs labeled as MMA320 and MMA307 inhibited the proliferation of NCIH226 cells. Modulation of EGFR and multiple MAPK-ERK1/2 pathway proteins, as well as deregulation of G_0/G_1 phase cell cycle regulators, were observed in response to the compound's treatment. The

cucurbitacin inspired estrone analogs were dissolved in dimethyl sulfoxide (DMSO) (Fisher Chemical/Fisher Scientific). All other chemicals were of analytical grade.

2.3.2   Design and synthesis of estrone analogs

2.3.2.1   Molecular modeling

Molecular docking of novel estrone analogs into the three-dimensional X-ray structure of wild-type EGFR ATP binding site (PDB code: 2ITW) was carried out using the FRED application (version 2.2.5) as implemented through the graphical user interface of OpenEye® software. The 3D structure of the above protein was downloaded from Protein Data Bank. The three-dimensional structures of the hybrid analogs were constructed using Chem. 3D ultra 12.0 software [Chemical Structure Drawing Standard; Cambridge Soft Corporation, USA (2010)]; compounds were energetically minimized using MMFF94 application with 5000 iterations and minimum RMS gradient of 0.10. All bound water molecules and ligands were eliminated from the proteins. Furthermore, multi-conformers were generated using OMEGA application (version 2.5.1.4) and VIDA application (version 4.1.2) was used as a visualization tool to show the potential binding affinity and binding interactions of the ligands to the receptor (Elshaier *et al.,* 2017). This software package generates consensus scoring which is a filtering process to obtain virtual binding affinity. The lower the consensus score, the better potency and binding affinity of the ligands towards the receptor.

2.3.2.2   Synthesis of MMA307 and MMA320

2.3.2.2.1   General procedure for the preparation of MMA307

Steps 1 to 9 has been previously reported by our research group (Mahnashi, 2017; Kopel *et al.,*2013). Preparation of 10 was carried out as follows: 0.15 g of 9 was dissolved in N, N-dimethylacetamide (0.8 mL) and incubated with sulfamoyl chloride (0.12 g, 0.945 mmol) at 0ºC. Subsequently, the reaction mixture was stirred at room temperature for 18 hrs and the resulting solution extracted with 1:1 mixture of ethyl acetate and water. The residue was purified using silica gel column chromatography (ethyl acetate: n-hexane, 3:7) to isolate compound 10 which was labeled as MMA307 (0.16 g, 91%). MMA307 was characterized by ^{1}H and ^{13}C NMR and high-resolution mass spectroscopies (Mahnashi, 2017).

MMA307 ^{1}H NMR (600 MHz, Chloroform-*d*) δ 8.21 – 8.18 (m, 2H), 7.77 (d, *J* = 15.7 Hz, 1H), 7.71 – 7.67 (m, 2H), 7.25 – 7.21 (m, 1H), 7.10 (d, *J* = 15.7 Hz, 1H), 7.01 (dd, *J* = 8.6, 2.6 Hz, 1H), 6.95 (d, *J* = 2.6 Hz, 1H), 5.03 (s, 2H), 3.98 – 3.89 (m, 1H), 3.83 (s, 1H), 2.78 (qd, *J* = 10.4, 9.7, 4.3 Hz, 2H), 2.29 – 2.21 (m, 2H), 2.16 (dq, *J* = 12.0, 4.2 Hz, 1H), 1.84 – 1.77 (m, 2H), 1.64 – 1.56 (m, 2H), 1.56 – 1.53 (m, 2H), 1.50 (s, 3H), 1.41 – 1.31 (m, 2H), 0.88 (s, 3H).

MMA307 ^{13}C NMR (151 MHz, CDCl$_3$) δ 203.04 (C21), 148.81 (C3), 147.90 (C27), 142.60 (C23), 140.35 (C24), 139.64 (C5), 138.92 (C10), 129.26 (C25, C29), 126.73 (C1),

124.25 (C26,C28), 122.29 (C22), 121.93 (C4), 118.95 (C2), 79.54 (C19), 55.66 (C14),

54.98 (C17), 44.31 (C8), 43.97 (C13), 40.51 (C12), 37.65 (C15), 29.51 (C6), 27.26 (C11),

26.43 (C7), 24.22 (C9), 23.64 (C20), 22.09 (C16), 13.65 (C18).

HR-FT-MS calcd for $C_{29}H_{34}O_7N_2SNa$ 577.1979 found 577.19790.

2.3.2.2.2 General procedure for the preparation of MMA320

Steps 1 to 9 has been previously reported by our research group (Mahnashi, 2017; Kopel *et al.,* 2013). Synthesis of 10 was carried out as follows: to a stirred solution of the 9 (0.3 g, 0.847 mmol), a mixture of tetrahydrofuran and lithium diisopropylamine (LDA) (1.5 mL, 3.05 mmol) were added and the reaction kept at -78 ℃. After that, the reaction mixture was initially stirred for 1 hr, before *para*-trifluoromethyl benzaldehyde (0.206 mL, 1.7 mmol) dissolved in THF added and the resulting mixture warmed to room temperature for 24 hrs. Subsequently, the reaction was quenched with ammonium chloride and the aqueous layer extracted with ethyl acetate, dried over anhydrous sodium sulfate, filtrated, and concentrated under vacuo. Silica gel column chromatography was used to purify the crude material (ethyl acetate: n-hexane, 1:9) to obtain 10 (0.21 g, 61.7%). Pure compound 10 was characterized by NMR and mass spectroscopies and labelled as MMA320 (Mahnashi, 2017).

MMA320   **^{1}H NMR** (600 MHz, Chloroform-*d*) δ 7.77 (d, *J* = 15.8 Hz, 1H), 7.61 – 7.57 (m, 4H), 7.04 – 6.99 (m, 2H), 6.59 (dd, *J* = 8.6, 2.7 Hz, 1H), 6.53 (d, *J* = 2.7 Hz, 1H), 6.02 – 5.88 (m, 1H), 4.32 (s, 1H), 3.67 (d, *J* = 2.3 Hz, 3H), 2.78 (dtd, *J* = 34.0, 17.3, 6.5 Hz,

2H), 2.21 (ddd, J = 15.4, 6.3, 3.4 Hz, 1H), 2.11 (dt, J = 12.8, 3.7 Hz, 1H), 2.03 − 2.00 (m, 1H), 1.81 (dt, J = 12.2, 3.3 Hz, 2H), 1.52 (dd, J = 10.8, 2.4 Hz, 1H), 1.47 − 1.43 (m, 2H), 1.30 (dt, J = 12.2, 6.2 Hz, 1H), 1.11 (td, J = 12.7, 4.4 Hz, 2H), 0.97 (s, 3H).

MMA320 ^{13}C NMR (151 MHz, CDCl$_3$) δ 200.68 (C21), 157.44 (C3), 155.17 (C17), 142.95 (C23), 137.84 (C24), , 132.75 (C5), 132.41 (C10), 132.20 (C27), 129.74 (C1), 128.81 (C25, C29), 126.02 (C22) , 124.66 (C26,C28), 122.86 (C30), 121.09 (C16), 113.83 (C4), 111.37 (C2) , 78.81 (C19) , 57.48 (C31) , 55.18 (C14), 47.86 (C9), 43.93 (C8), 37.09 (C13), 34.49 (C12), 31.23 (C15), 29.69 (C6), 27.59 (C11), 26.27 (C7), 25.26 (C9), 17.21 (C20), 14.16 (C18).

HR-FT-MS calcd for C$_{31}$H$_{33}$O$_3$F$_3$Na 533.2274 found 533.22544.

2.3.3   Cell culture

NCIH226 cell line (a model of EGFR wild-type and p53 mutant NSCLC) was a kind gift from Prof. Xiangming Guan (College of Pharmacy and Allied Health Professions, South Dakota State University, USA). The cells were cultured in Rose Park Memorial Institute (RPMI)-1640 medium supplemented with 10% (v/v) fetal bovine serum (FBS), 100 IU/mL penicillin and 100 µg/mL streptomycin (American Type Culture Collection (ATCC)) at 37˚C equilibrated with 5% (v/v) CO$_2$ in humidified air. The cells for the assays were detached using a solution of trypsin with EDTA (ThermoFisher Scientific).

2.3.4   Cell proliferation assays

2.3.4.1   3-(4,5-dimethylthiazol-2-yl)-2,5-diphenyltetrazolium bromide (MTT) Assay

The effect of 25 novel synthetic estrone analogs on cell viability was tested with MTT reagent as described by Wang *et al.,* 2010 with slight modifications. Briefly, to measure mitochondrial dehydrogenase activities, cells were seeded in 96-well plates at an initial density of 30,000 cells per well. After overnight incubation, cells were treated with different concentrations of compounds in a dose range of 0 - 100 μM. The final DMSO concentration was 0.05%. After 48 hrs of incubation, 20 μL of MTT reagent (5 mg/mL) was added to each well and the formed formazan crystals were dissolved in 250 μL of dimethyl sulfoxide (DMSO). Four independent experiments were completed to determine the mean optical density referred to as cell viability, using a Hidex Sense Beta Plus plate reader (Turku, Finland). Cell viability was expressed as a percentage of DMSO-treated controls.

2.3.4.2   Trypan Blue Exclusion Assay

Cells were seeded in six-well plates at a density of 300,000 cells/well in 3 mL RPMI media and were treated with MMA320, MMA307 and Sorafenib at IC$_{50}$ concentrations for 24 hrs after overnight incubation. Afterward, cells were then detached using trypsin/EDTA and counted with Countess II Automated Cell Counter (ThermoFisher Scientific, USA). At

least two independent experiments were performed to determine the mean value, which is presented as a percentage compared to the DMSO-treated controls.

2.3.5 Flow cytometry for cell cycle analysis

Cells were seeded into six-well plates at a concentration of 300,000 cells/well and allowed to attach in culture overnight, then treated with IC_{50} values of compounds or positive control (sorafenib) for 48 h. Afterward, cells were washed with PBS and harvested. Cell cycle analysis was investigated by adding Vybrant® DyeCycle™ Green Stain (Thermo Fisher Scientific) to 1 mL of cell suspension at a final concentration of 0.0625 μM. After 45 minutes incubation at 37˚C, the samples were analyzed by flow cytometry and compared to DMSO-treated cells. All these experiments were performed on BD Accuri™ C6 flow cytometer (BD Biosciences, San Jose, CA, USA) using BD Accuri™ C6 software, version 1.0.

2.3.6 Protein expression analysis

2.3.6.1 Western Blot

Western blotting was done as previously described by Shin *et al.,* 2008 with slight modification. Briefly, 80% confluent cells were washed three times with PBS prior to

treatment with IC_{50} values of compounds for indicated times. Subsequently, cells were lysed using lysis buffer containing 1% Triton X-100 and 1% Halt™ Protease Inhibitor Cocktail (Thermo Fisher Scientific). Aliquots of lysates containing 20-60 μg of proteins were boiled for 7 min in SDS-PAGE sample buffer supplemented with 5% β-mercaptoethanol, separated on 10% polyacrylamide electrophoresis gels and transferred to nitrocellulose membranes (Bio-Rad Laboratories). After transfer, membranes were incubated with relevant antibodies against EGF Receptor, Phospho-EGF Receptor, B-Raf, Phospho-B-Raf, MEK1/2, Phospho-MEK1/2, ERK1/2, Phospho-ERK1/2, $p21^{Waf1/Cip1}$, Cyclin D1, Phospho-Cyclin D1, Dyrk1B, and either β-actin or GAPDH, loading control, followed by incubation with anti-mouse or anti-rabbit DyLight conjugated (680 or 800 nm) secondary antibodies. Membranes were scanned with LICOR Odyssey® Fc Imaging System (Lincoln, Nebraska, United States) and blots analyzed by Fiji software (Image J, Java 1.8.0).

2.3.6.2 In-Cell Western (ICW) Assay

ICW was carried out in accordance with manufacturers instruction with slight modifications. Briefly, about 40,000 cells per well were seeded in 96-well black walled plate with clear bottom for overnight attachment. Cells were then washed three times with PBS prior to treatment with MMA307 (IC_{50} value) for indicated times. Subsequently, cells were fixed with 3.7% formaldehyde solution, permeabilized with 0.1% Triton X-100 solution and blocked with fish gel buffer (1×) prior to primary antibody addition. Wells

were then incubated with the relevant antibodies EGF Receptor, Phospho-EGF Receptor, MEK1/2, Phospho-MEK1/2, ERK1/2, Phospho-ERK1/2, Dyrk1B, and GAPDH, loading control, overnight followed by incubation with anti-mouse or anti-rabbit DyLight conjugated (680 or 800 nm) secondary antibodies. Images were acquired using LICOR Odyssey® Fc Imaging System (Lincoln, Nebraska, United States) and image quantification done by Fiji software (Image J, Java 1.8.0).

2.3.7 Statistical Analysis

Microsoft® Excel® for Windows, version 16.0., was used for the calculation of mean and standard deviation values of different experiments and plotting of bar or line graphs. Mean IC_{50} values were compared by one-way Analysis of Variance (ANOVA) using GraphPad Prism 5.01 (San Diego, USA) and values with $p < 0.05$ were considered statistically significant.

2.4 Results and Discussion

Installing various modified cucurbitacin functionalities and other pharmacophores onto the estrone scaffold resulted in unique hybrid analogs. To validate the potential of these designed estrone analogs against wild-type NSCLC, molecular docking was performed by fitting the designed hybrid analogs and reference compounds (erlotinib and

sorafenib) into the ATP binding site of EGFR (PDB codes: 2ITW) crystallized from wild-type NSCLC. The results were plotted as a line-scatter graph (Figure 2.1), which mainly displays the corresponding consensus scores of the molecular docking studies. Compared to erlotinib and sorafenib, it was clearly observed that most estrone analogs showed lower consensus scores (a measure of better binding and potency) against the wild-type EGFR ATP binding site. Furthermore, Figure 2.2 and 2.3 showed EGFR with the binding mode of compounds MMA307, containing sulfamoyl and paranitrophenyl groups, and MMA320, with *para*-trifluoromethylphenyl and methoxy substituents that exhibited potent antiproliferative activity *in vitro* compared to sorafenib. Previous studies by Yun *et al.,* 2007 suggested that hydrogen bonding towards the amino acid residue, MET793A, in the EGFR kinase domain may be a key interaction in achieving effective drug potency. We observed that the positive controls, erlotinib (Tarceva) showed hydrogen bonding from the pyrimidine-N_2 towards MET793A and sorafenib (Nexavar) showed hydrogen bonding from pyridine-N, methyl-H and carbonyl-O towards THR854A and THR790A, respectively but registered a higher consensus score (Figure 2.4 and 2.5). Analyzing compound MMA320 in the EGFR-binding site revealed hydrogen bonding from the methoxy carbonyl-O on the substituent group towards the amino acid residue THR854A (Figure 2.3). However, examining MMA307 enriched with functionalities capable of hydrogen bonding within the EGFR kinase domain demonstrated hydrophobic-hydrophobic (cation-π) interactions towards the amino acid residue, LYS745A (Figure 2.2). Both MMA320 and MMA307 recorded lower consensus scores compared to the positive controls. The hydrogen bonding exhibited by MMA320 toward THR854A and the cation-π interactions exhibited by MMA307 toward LYS745A demonstrate a strong and

unique binding mode and suggest that interactions between the compounds pharmacophore and THR854A and LYS745A residues in the EGFR ATP binding site may be key in estrone analogs achieving drug potency. These results could provide a molecular-level foundation to illustrate that MMA307 and MMA320 can bind well at the active site of activated EGFR. These findings are supported by their lower IC_{50} concentration compared to sorafenib from the *in vitro* antiproliferative assays. Directed sulfamoylation on compound 9 afforded 10 (MMA307) in 91% yield after column chromatography (scheme 2.1) and the addition of *para*-trifluoromethyl benzaldehyde to the hydroxyl methyl ketone diastereomeric mixture yielded 61.7% of MMA320 after purification with silica gel column chromatography (Scheme 2.2). These pure compounds were characterized by NMR and mass spectrometry techniques with the ^{1}H and ^{13}C chemical shifts as well as accurate masses documented in the method section. MMA307 was named as (8S,9S,13S,14S,17S)-7,8,9,11,12,13,14,15,16,17-decahydro-17-((R,E)-2-hydroxy-5-(4-nitrophenyl)-3-oxopent-4-en-2-yl)-13-methyl-6H-cyclopenta[a]phenanthren-3-yl sulfamate and MMA320 named as (R,1E)-1-(4-(trifluoromethyl)phenyl)-4-((8S,9S,13S,14S)-7,8,9,11,12,13,14,15-octahydro-3-methoxy-13-methyl-6H-cyclopenta[a]phenanthren-17-yl)-4-hydroxypent-1-en-3-one (Figure 2.6).

Subsequently, estrone analogs effect on the proliferation of NCIH226 cells were determined by the MTT assay after 48 hrs. Overall, the compounds showed a significant growth inhibitory effect toward the NCIH226 cells. Particularly, MMA287, MMA306, MMA307, MMA320 and MMA321 showed significant ($p < 0.001$ to $p < 0.05$) antiproliferative activity against NCIH226 cells at IC_{50} doses of 11.82 ± 0.65, 17.41 ± 1.56,

2.88 ± 0.21, 9.68 ± 0.24 and 14.57 ± 0.31 µM, respectively (Table 2.1). MMA307 and MMA320 were at least two to seven-fold more potent than the standard anticancer drug sorafenib and were chosen for further studies. Morphological changes were evaluated after NCIH226 cells were treated with IC_{50} concentrations of MMA307, MMA320, and sorafenib (positive control). Compared with DMSO-control cells, the majority of the compound-treated NCIH226 cells changed from spindle to either round- (observed for MMA307 and sorafenib) or rod-shaped (observed for MMA320) (Figure 2.7 A) showing the compounds growth modulatory effects. Furthermore, the growth inhibitory effects of MMA307 and MMA320 at their IC_{50} doses were confirmed by the trypan blue exclusion assay; shows increased cell membrane permeability for trypan blue dye by dead cells. NCIH226 cells were treated for 24 hrs and no significant cell death as measured by trypan blue stained cells were observed for MMA307 (Figure 2.7 B). A slight but statistically insignificant increase in NCIH226 cell death was observed for both MMA320 and sorafenib. It is well known that several cucurbitacin classes and their derivatives, estrone analogs as well as anti-EGFRs with anticancer properties exhibit their cytotoxic effects on tumor cells by inhibiting cell proliferation or inducing cell death (Wang *et al.,* 2017; Ahmed *et al.,* 2017; Ahmed *et al.,* 2014; Kutkowska *et al.,* 2017). Comparing data obtained through cell viability (MTT, trypan blue and morphological changes) and Vybrant® Dye Cycle™ Green staining, we were able to distinguish between the two possible effects of the estrone analogs: inhibition of cell proliferation and induction of cell death. Our findings showed that, even though treatment with MMA320 leads to some amount of cell death, the predominant effect of estrone analogs administration to NCIH226 cells is the inhibition of cell proliferation. These results are supported by initial apoptosis (annexin v staining of

phosphatidyl serine) detection using propidium iodide staining where no significant cell death (data not shown) induced by MMA307 and MMA320 treatments are detected. These observations were not unexpected considering the fact that NCIH226 cells (EGFR wild-type and p53 mutant) overexpress EGFR which is mainly involved in cell proliferation pathways instead of cell death pathways. Moreover, the significant G_1 phase cell cycle arrest (Figure 2.8) induced by MMA307 and MMA320 treatment against NCIH226 cells offer support to the idea that these compounds inhibit cell proliferation rather than induce cell death. Our findings are in line with studies by Ahmed *et al.,* 2017, Ahmed *et al.,* 2014 and Kutkowska *et al.,* 2017 that report the antiproliferative effects of different estrone derivatives and anti-EGFRs against distinct cancer cell lines *in vitro*.

As a result of significant ($p < 0.05$) G_1 phase cell cycle arrest (results are summarized in Figure 2.8) induced by MMA307 and MMA320 compared to sorafenib, we analyzed the expression levels of known downstream G_1 cell cycle regulators. It has been reported that Dyrk1B phosphorylates cyclin D1 to promote its ubiquitination and degradation in the proteasome whereas $p21^{Waf1/Cip1}$ is stabilized, impacting the G_1 phase cell cycle (Gao *et al.,* 2013; Ashford *et al.,* 2014; Visagie *et al.,* 2017). We observed that cyclin D1 levels were decreased while $p21^{Waf1/Cip1}$ levels were increased following treatment with IC_{50} amounts of MMA307 and MMA320 in a time-dependent manner (Figure 2.11 – 2.12). Moreover, treatment with the compounds lead to increased phosphorylation of cyclin D1 (at phosphorylation site T286) in a time-dependent manner (Figure 2.11 – 2.12). Cyclin D1 overexpression and $p21^{waf1/cip1}$ downregulation have been shown to be important for cancer progression through the G_1-S phase transition.

Alternatively, phosphorylation of cyclin D1 leads to its turnover, marked by its ubiquitination and degradation in the proteasome. We report for the first time that, MMA307 and MMA320 treatments to NCIH226 cells lead to significant downregulation of cyclin D1 levels, whereas the opposite effect was seen for phospho-cyclin D1 (T286) and p21$^{waf1/cip1}$. Aside p21$^{waf1/cip1}$, Dyrk1B can phosphorylate cyclin D1 on either T286 or T288 (Gao *et al.,* 2013; Ashford *et al.,* 2014) to arrest damaged tumor cells and to allow cellular repair in a quiescent state, to ultimately maintain cell survival. Interestingly, the above studies report that Dyrk1B performs dissimilar functions in arresting G_1 phase of the cell cycle in distinct cancer types. Of note, in a panel of NSCLC cell lines, Dyrk1B overexpression was associated with colony formation and cell survival whereas its knockdown leads to opposing effect (Chen *et al.,* 2017; Friedman, 2007; Gao *et al.,* 2009). Along with other studies by Deng *et al.,* 2006 and Mercer and Friedman, 2006, it has been suggested that pharmacological inhibition of Dyrk1B sensitizes cancer cells to various chemotherapeutic agents and maybe an ideal strategy for treating cancers. Consistent with our findings we observed that MMA320 but not MM307 administration to NCIH226 cells resulted in Dyrk1B inhibition over the 24 hr time course (Figure 2.11 – 2.12). While the status of selected G_1 phase cell cycle regulators was analyzed in this study, the functions of other proteins are likely modulated, and therefore, the antiproliferative effects of the estrone analogs reported here may not be solely due to these proteins alone.

Furthermore, we demonstrated that MMA307 and MMA320 inhibit NCIH226 cell proliferation by targeting directly the expression levels of EGFR, suppressing its phosphorylation in a time-dependent manner, followed by inhibition of its downstream

MAPK (ERK1/2) pathway proteins which are dependent on activated EGFR. Genetic analyses of various NSCLC revealed that EGFR and its immediate downstream targets, the MAPK signaling cascades, are frequently overexpressed or mutated during cell proliferation (Scrima *et al.,* 2017). Constitutive EGFR-mediated signaling and the extent of ERK1/2 activation are usually correlated with poor prognosis and aggressiveness of NSCLC, respectively (Scrima *et al.,* 2017). Previous studies by Iida *et al.,* 2013 and Wheeler *et al.,* 2008 reported that sym004 (a mixture of antibodies) or TKIs impacted EGFR phosphorylation at tyrosine 1173 (Y1173), and this position is important in activating the MAPK pathway. Therefore, this phosphorylation site was chosen for further analysis. We observed that treating NCIH226 cells with MMA320 and MMA307 resulted in significant inhibition of EGFR and activated EFGR (Y1173) expression levels in a time-dependent pattern (Figure 2.9 – 2.10). Concomitantly, activated ERK1/2 pathway proteins, specifically, BRaf (S445), MEK1/2 (S217/221) and ERK1/2 (T202/Y204) expression levels (Figure 2.9 – 2.10), were downregulated in a time-dependent manner when NCIH226 cells were treated with MMA307 and MMA320. Our findings agree with that made by earlier reports (Abou-Salim *et al.,* 2019; Elgazwi, 2018). It must be acknowledged that EGFR is a major receptor that triggers numerous downstream pathways, and therefore it is likely that other proliferation pathways that are activated by EGFR were equally inhibited by MMA307 and MMA320 administration.

2.5   Conclusion

We report for the first time the synthesis of novel estrone analogs-a hybrid of modified Cucs pharmacophore and estrone-base scaffold. These analogs were initially designed against wild-type EGFR ATP binding site *in silico*. Among these, MMA307 and MMA320 demonstrated better potency and binding towards EGFR kinase domain *in silico*, and significantly inhibited the proliferation of NCIH226 cells *in vitro*. The antiproliferation effect could be ascribed in part to suppression of EGFR and its downstream ERK1/2 signaling pathway, and to the arrest of the G_1 phase of the cell cycle. Derivatives of estrone have been reported to be multitargeted antitumor agents (Solum *et al.,* 2015), and such types of anticancer agents are of current interest towards the potential development of remedies against cancer, including NSCLC. The results presented herein provide novel information on such lead compounds. Taken together, the present study suggest that estrone analogs may be the potential novel therapeutic agents that can be beneficial to wild-type NSCLC patients.

2.6 References

A. Ali, J. R. Goffin, A. Arnold, P. M. Ellis, Survival of patients with non-small-cell lung cancer after a diagnosis of brain metastases. Curr. Oncol. 20(2013), 300.

A. Inoue, K. Yoshida, S. Morita, F. Imamura, T. Seto, I. Okamoto, K. Nakagawa, N. Yamamoto, S. Muto, M. Fukuoka, Characteristics and overall survival of EGFR mutation-positive non-small cell lung cancer treated with EGFR tyrosine kinase inhibitors: a retrospective analysis for 1660 Japanese patients. Jpn. J. Clin. Oncol. 46(2016), 462-467.

A. L. Ashford, D. Oxley, J. Kettle, K. Hudson, S. Guichard, S. J. Cook, P. A. Lochhead, A novel DYRK1B inhibitor AZ191 demonstrates that DYRK1B acts independently of GSK3β to phosphorylate cyclin D1 at Thr286, not Thr288. Biochem. J. 457(2014), 43-56.

A. Stander, F. Joubert, A. Joubert, Docking, synthesis, and in vitro evaluation of antimitotic estrone analogs. Chem. Biol. Drug Des. 77(2011), 173-181.

C. Chen, R. Ju, J. Shi, W. Chen, F. Sun, L. Zhu, L. Guo, Carboxyamidotriazole Synergizes with Sorafenib to Combat Non–Small Cell Lung Cancer through Inhibition of NANOG and Aggravation of Apoptosis. J. Pharmacol. Exp. Ther. 362(2017), 219-229.

C. Gridelli, F. Ciardiello, C. Gallo, R. Feld, C. Butts, V. Gebbia, P. Maione, F. Morgillo, G. Genestreti, A. Favaretto, A.N. Leighl, First-line erlotinib followed by second-line cisplatin-gemcitabine chemotherapy in advanced non–small-cell lung cancer: The TORCH randomized trial. J. Clin. Oncol. 30(2012), 3002-3011.

C. H. Yun, T. J. Boggon, Y. Li, M. S. Woo, H. Greulich, M. Meyerson, M. J. Eck, Structures of lung cancer-derived EGFR mutants and inhibitor complexes: mechanism of activation and insights into differential inhibitor sensitivity. Cancer Cell. 11(2007), 217-227.

D. L. Wheeler, S. Huang, T. J. Kruser, M. M. Nechrebecki, E. A. Armstrong, S. Benavente, P. M. Harari, Mechanisms of acquired resistance to cetuximab: role of HER (ErbB) family members. Oncogene. 27(2008), 3944.

D. Zhao, X. Chen, N. Qin, D. Su, L. Zhou, Q. Zhang, X. Li, X. Zhang, M. Jin, J. Wang, The prognostic role of EGFR-TKIs for patients with advanced non-small cell lung cancer. Sci. Rep. 7(2017), 40374.

E. Friedman, Mirk/Dyrk1B in cancer. J. Cell Biochem. 102(2007), pp.274-279.

E. J. Solum, J. J. Cheng, I. Sylte, A. Vik, T. V. Hansen, Synthesis, biological evaluation and molecular modeling of new analogs of the anti-cancer agent 2-methoxyestradiol: potent inhibitors of angiogenesis. RSC Adv.5(2015), 32497-32504.

F. A. Shepherd, J. Rodrigues Pereira, T. Ciuleanu, E. H. Tan, V. Hirsh, S. Thongprasert, D. Campos, S. Maoleekoonpiroj, M. Smylie, R. Martins, M. van Kooten, Erlotinib in previously treated non–small-cell lung cancer. N. Engl. J. Med. 353(2005), 123-132.

Forcella, M., Oldani, M., Epistolio, S., Freguia, S., Monti, E., Fusi, P., and Frattini, M. (2017). Non-small cell lung cancer (NSCLC), EGFR downstream pathway activation and TKI targeted therapies sensitivity: Effect of the plasma membrane-associated NEU3. PLoS One, 12(10), e0187289.

https://openprairie.sdstate.edu/etd/2640

I. T. Silva, F. C. Geller, L. Persich, S. E. Dudek, K. L. Lang, M. S. B. Caro, F. J. Durán, E. P. Schenkel, S. Ludwig, C. M. O. Simões, Cytotoxic effects of natural and semisynthetic cucurbitacins on lung cancer cell line A549. Invest. New Drugs. 34(2016), 139-148.

J. A. Hall, S. Seedarala, N. Rice, L. Kopel, F. Halaweish, B. S. Blagg, Cucurbitacin D is a disruptor of the HSP90 chaperone machinery. J. Nat. Prod. 78(2015), 873-879.

J. Gao, Y. Zhao, Y. Lv, Y. Chen, B. Wei, J. Tian, Z. Yang, F. Kong, J. Pang, J. Liu, H. Shi, Mirk/Dyrk1B mediates G_0/G_1 to S phase cell cycle progression and cell survival involving MAPK/ERK signaling in human cancer cells. Cancer Cell Int. 13(2013), 2.

J. Gao, Z. Zheng, B. Rawal, M. J. Schell, G. Bepler, E. B. Haura, Mirk/Dyrk1B, a novel therapeutic target, mediates cell survival in non-small cell lung cancer cells. Cancer Biol. Ther. 8(2009), 1671-1679.

J. Kutkowska, L. Strzadala, A. Rapak, Synergistic activity of sorafenib and betulinic acid against clonogenic activity of non-small cell lung cancer cells. Cancer Sci. 108(2017), 2265-2272.

J. S. Shin, S. W. Hong, S. L. O. Lee, T. H. Kim, I. C. Park, S. K. An, S. S. Lee, Serum starvation induces G_1 arrest through suppression of Skp2-CDK2 and CDK4 in SK-OV-3 cells. Int. J. Oncol. 32(2008), 435-439.

K. Imai, A. Takaoka, Comparing antibody and small-molecule therapies for cancer. Nat. Rev. Cancer, 6(2006), 714.

L. C. Kopel, M. S. Ahmed, F. T. Halaweish, Synthesis of novel estrone analogs by incorporation of thiophenols via conjugate addition to an enone side chain. Steroids. 78(2013), 1119-25.

L. M. Sholl, Y. Xiao, V. Joshi, B. Y. Yeap, L. A. Cioffredi, D. M. Jackman, C. Lee, P. A. Jänne, N. I. Lindeman, EGFR mutation is a better predictor of response to tyrosine kinase inhibitors in non–small cell lung carcinoma than FISH, CISH, and immunohistochemistry. Am. J. Clin. Pathol. 133(2010), 922-934.

M. A. Abou-Salim, M. A. Shaaban, M. K. A. El Hameid, Y. A. Elshaier, F. Halaweish, Design, synthesis and biological study of hybrid drug candidates of nitric oxide releasing cucurbitacin-inspired estrone analogs for treatment of hepatocellular carcinoma. Bioorg. Chem. 85(2019), 515-533.

M. H. Mahnashi, Design, Synthesis and Biological Screening of Novel Cucs inspired Estrone Analogues Towards Treatment of Hepatocellular Carcinoma Electronic Theses and Dissertations. (2017), 1182. Retrieved from https://openprairie.sdstate.edu/etd/1182

M. Iida, T. M. Brand, M. M. Starr, C. Li, E. J. Huppert, N. Luthar, D. L. Wheeler, Sym004, a novel EGFR antibody mixture, can overcome acquired resistance to cetuximab. Neoplasia. 15(2013), 1196-1206.

M. Qi, Y. Tian, W. Li, D. Li, T. Zhao, Y. Yang, Q. Li, S. Chen, Y. Yang, Z. Zhang, L. Tang, ERK inhibition represses gefitinib resistance in non-small cell lung cancer cells. Oncotarget. 9(2018), 12020.

M. S. Ahmed, F. El-Senduny, J. Taylor, F. T. Halaweish, Biological screening of cucurbitacin inspired estrone analogs targeting mitogen-activated protein kinase (MAPK) pathway. Chem. Biol. Drug Des. 90(2017), 478-484.

M. S. Ahmed, L. C. Kopel, F. T. Halaweish, Structural Optimization and Biological Screening of a Steroidal Scaffold Possessing Cucurbitacin-Like Functionalities as B-Raf Inhibitors. ChemMedChem. 9(2014), 1361-1367.

M. Scrima, F. Z. Marino, D. M. Oliveira, C. Marinaro, E. La Mantia, G. Rocco, G. Botti, Aberrant signaling through the HER2-ERK1/2 pathway is predictive of reduced disease-free and overall survival in early stage non-small cell lung cancer (NSCLC) patients. J. Cancer. 8(2017), 227.

M. Sikander, B. B. Hafeez, S. Malik, A. Alsayari, F. T Halaweish, M. M. Yallapu, M. Jaggi, Cucurbitacin D exhibits potent anti-cancer activity in cervical cancer. Sci. Rep. 6(2016), 36594.

M. Visagie, T. Mqoco, A. Joubert, Sulphamoylated estradiol analogue induces antiproliferative activity and apoptosis in breast cell lines. Cell Mol. Biol. Lett. 17(2012), 549.

M. Zhang, Z. G. Bian, Y. Zhang, J. H. Wang, L. Kan, X. Wang, P. Liang Kan, P. He, Cucurbitacin B inhibits proliferation and induces apoptosis via STAT3 pathway inhibition in A549 lung cancer cells. Mol. Med. Rep. 10(2014), 2905-2911.

P. Wang, S. M. Henning, D. Heber, Limitations of MTT and MTS-based assays for measurement of antiproliferative activity of green tea polyphenols. PLoS One. 5(2010), 10202.

R. A. MacCorkle, T. H. Tan, Mitogen-activated protein kinases in cell-cycle control. Cell Biochem. Biophys. 43(2005), 451-461.

R. L. Siegel, K. D. Miller, S. A. Fedewa, D. J. Ahnen, R. G. Meester, A. Barzi, A. Jemal, Cancer statistics, 2017. CA Cancer J. Clin. 67(2017), 177-193.

S. E. Mercer, E. Friedman, Mirk/Dyrk 1B. Cell Biochem. Biophys. 45(2006). 303-315.

S. Elgazwi, Study of Anti-proliferative Activity of Cucurbitacins Inspired Estrone Analogs on Hepatocellular Carcinoma. Electronic Theses and Dissertations. (2018), 2640.

S. G. Wu, J. Y. Shih, Management of acquired resistance to EGFR TKI–targeted therapy in advanced non-small cell lung cancer. Mol. Cancer. 17(2018), 38.

S. O. Chung, Y. J. Kim, S. U. Park, An updated review of cucurbitacins and their biological and pharmacological activities. EXCLI. J. 14(2015), 562.

S. Torii, T. Yamamoto, Y. Tsuchiya, E. Nishida, ERK MAP kinase in G_1 cell cycle progression and cancer. Cancer Sci. 97(2006), 697-702.

S. Vicent, J. M. Lopez-Picazo, G. Toledo, M. D. Lozano, W. Torre, C. Garcia-Corchon, L. M. Montuenga, ERK1/2 is activated in non-small-cell lung cancer and associated with advanced tumours. Br. J. Cancer. 90(2004), 1047.

S. Zhao, Z. X. Qiu, L. Zhang, W. M. Li, Prognostic values of ERK1/2 and p-ERK1/2 expressions for poor survival in non-small cell lung cancer. Tumor Biol. 36(2015), 4143-4150.

Stander, B.A., Joubert, F., Tu, C., Sippel, K.H., McKenna, R. and Joubert, A.M., 2013. Signaling pathways of ESE-16, an antimitotic and anticarbonic anhydrase estradiol analog, in breast cancer cells. PLoS One, 8(1), p. e53853.

Stander, B.A., Joubert, F., Tu, C., Sippel, K.H., McKenna, R. and Joubert, A.M., 2012. *In vitro* evaluation of ESE-15-ol, an estradiol analogue with nanomolar antimitotic and carbonic anhydrase inhibitory activity. PLoS One. 7(12), e52205.

W. D. Wang, Y. Liu, Y. Su, X. Z. Xiong, D. Shang, J. J. Xu, H.J. Liu, Antitumor and apoptotic effects of cucurbitacin a in A-549 lung carcinoma cells is mediated via G2/M cell cycle arrest and M-TOR/PI3K/Akt signalling pathway. Afr. J. Tradit. Complement Altern. Med. 14(2017), 75-82.

X. Deng, D. Z. Ewton, S. Li, A. Naqvi, S. E. Mercer, S. Landas, E. Friedman, The kinase Mirk/Dyrk1B mediates cell survival in pancreatic ductal adenocarcinoma. Cancer Res. 66(2006), 4149-4158.

X. Nan, C. Xie, X. Yu, J. Liu, EGFR TKI as first-line treatment for patients with advanced EGFR mutation-positive non-small-cell lung cancer. Oncotarget. 8(2017), 75712.

Y. A. Elshaier, M. A. Shaaban, M. K. A. El Hamid, M. H. Abdelrahman, M. A. Abou-Salim, S. M. Elgazwi, F. Halaweish, Design and synthesis of pyrazolo [3, 4-d] pyrimidines:

Nitric oxide releasing compounds targeting hepatocellular carcinoma. Bioorg. Med. Chem. 25(2017), 2956-2970.

Y. N. Zhang, X. Y. Wu, N. Zhong, J. Deng, L. Zhang, W. Chen, X. Li, C. J. Zhong, Stimulatory effects of sorafenib on human non-small cell lung cancer cells in vitro by regulating MAPK/ERK activation. Mol. Med. Rep. 9(2014), 365-369.

Tables and Figures
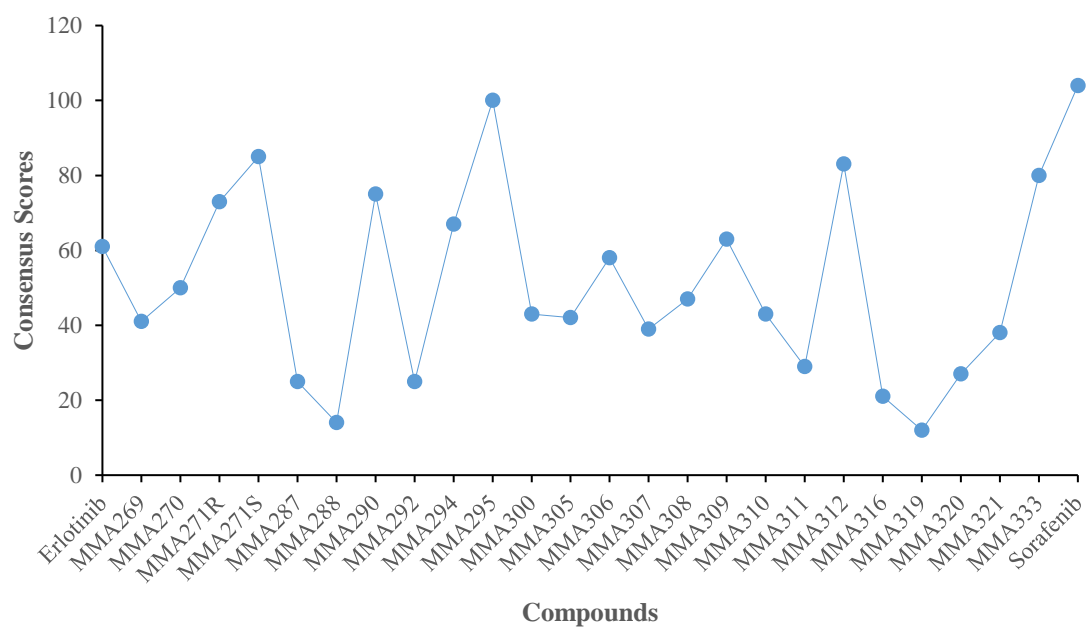
Figure 2.1 Molecular docking study of designed estrone analogs against EGFR binding site (Pdb: 2ITW). Scatter plot of compounds consensus scores generated by VIDA application.
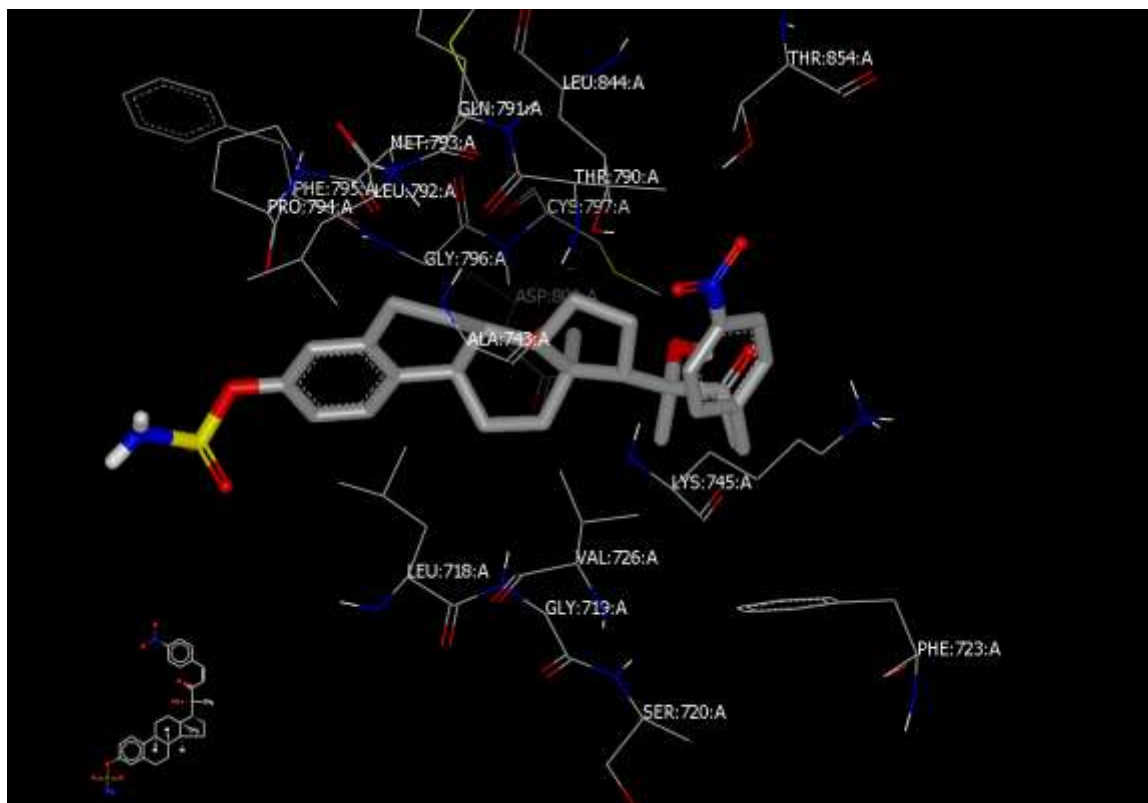
Figure 2.2 3D visual representation of MMA307 docked against EGFR binding site (Pdb: 2ITW). There is a cation-π interaction between LYS745A of 2ITW and para-nitrophenyl aromatic ring of MMA307
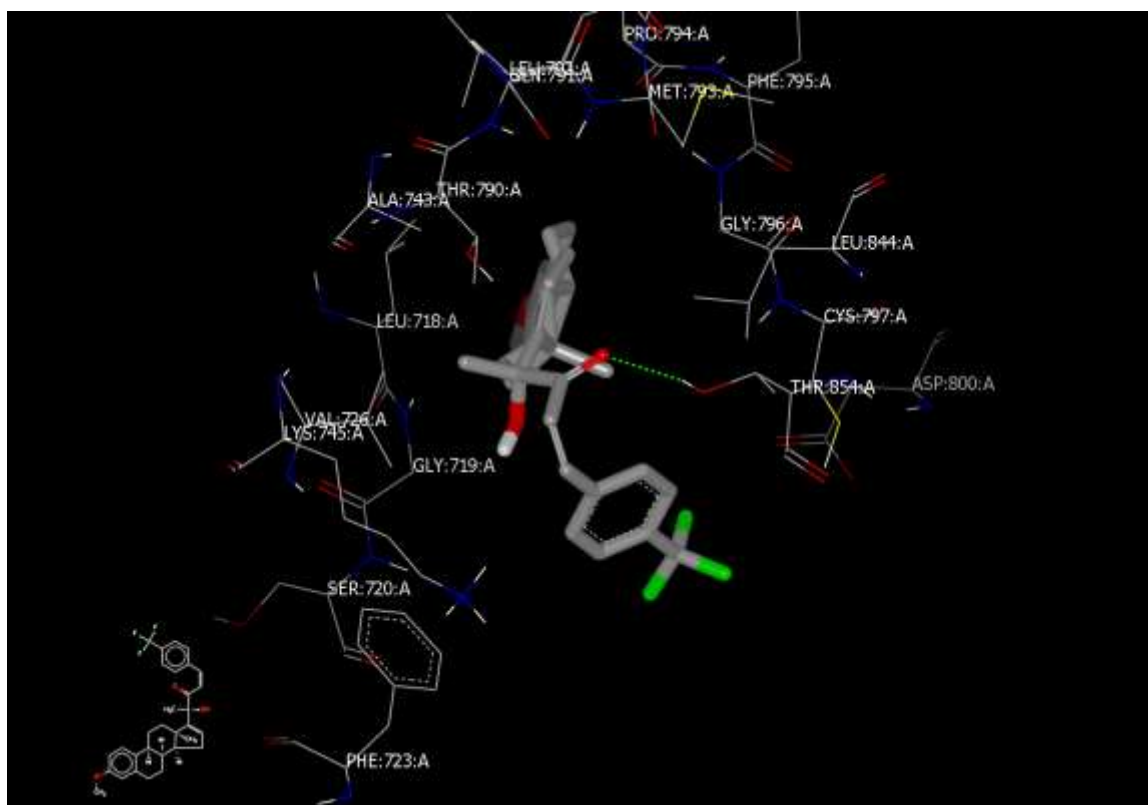
Figure 2.3 3D visual representation of MMA320 docked against EGFR binding site (Pdb: 2ITW). The dashed green line shows hydrogen bonding from the carbonyl-O of MMA320 towards THR854A of 2ITW. Also, there is a cation-π interaction between LYS745A of 2ITW and para-trifluoro phenyl ring of MMA307.
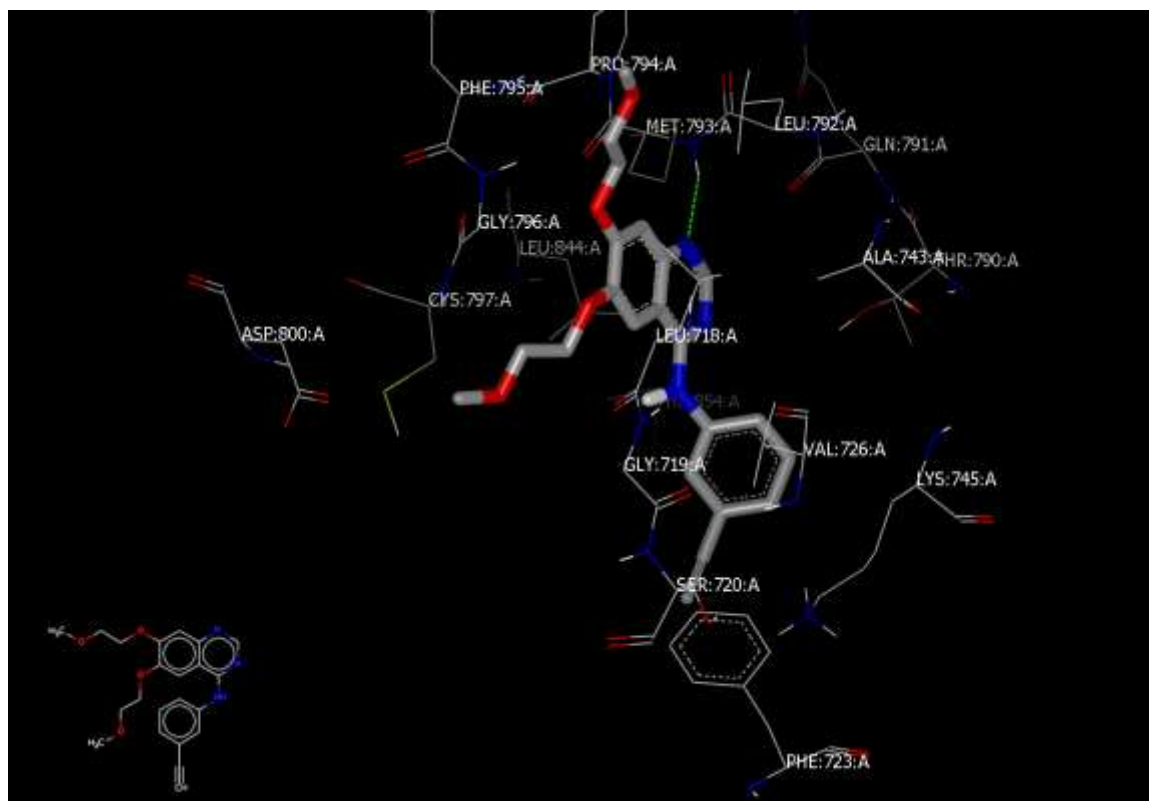
Figure 2.4 3D visual representation of erlotinib docked against EGFR binding site (Pdb: 2ITW). The dashed green line shows hydrogen bonding from the pyrimidine-N_2 of erlotinib towards MET793A of 2ITW binding site.
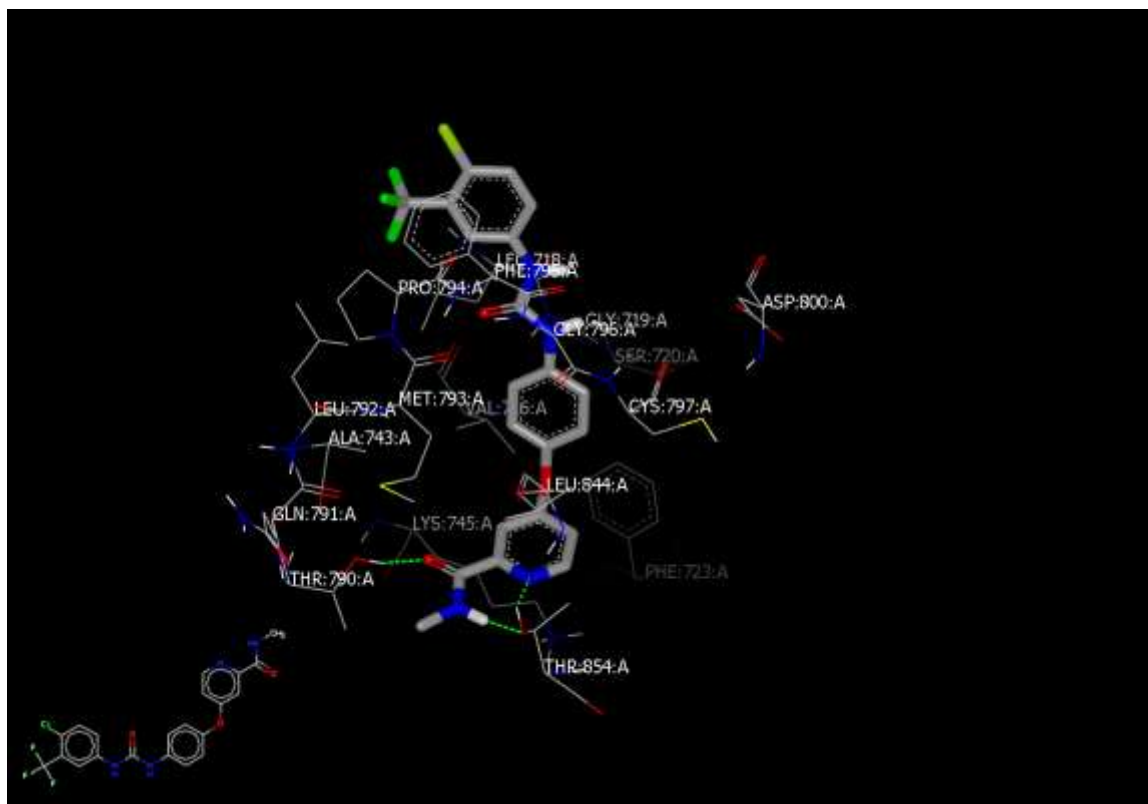
Figure 2.5. 3D visual representation of sorafenib docked against EGFR binding site (Pdb: 2ITW). The dashed green line shows hydrogen bonding from the pyridine-N and methyl-H of sorafenib towards THR854A as well as from the carbonyl-O towards THR790A of 2ITW binding site.
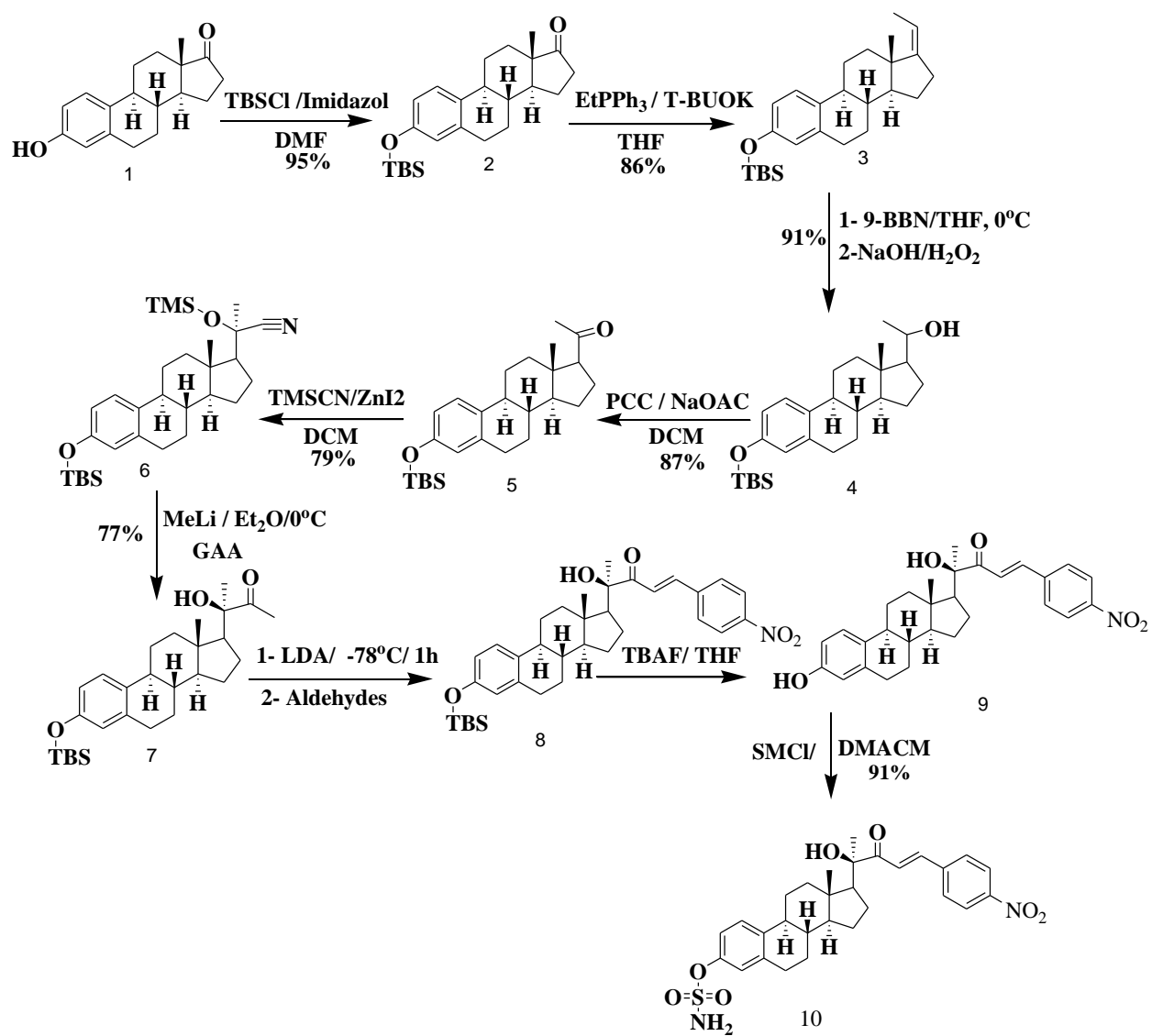
Scheme 2.1 Synthesis route of MMA307.
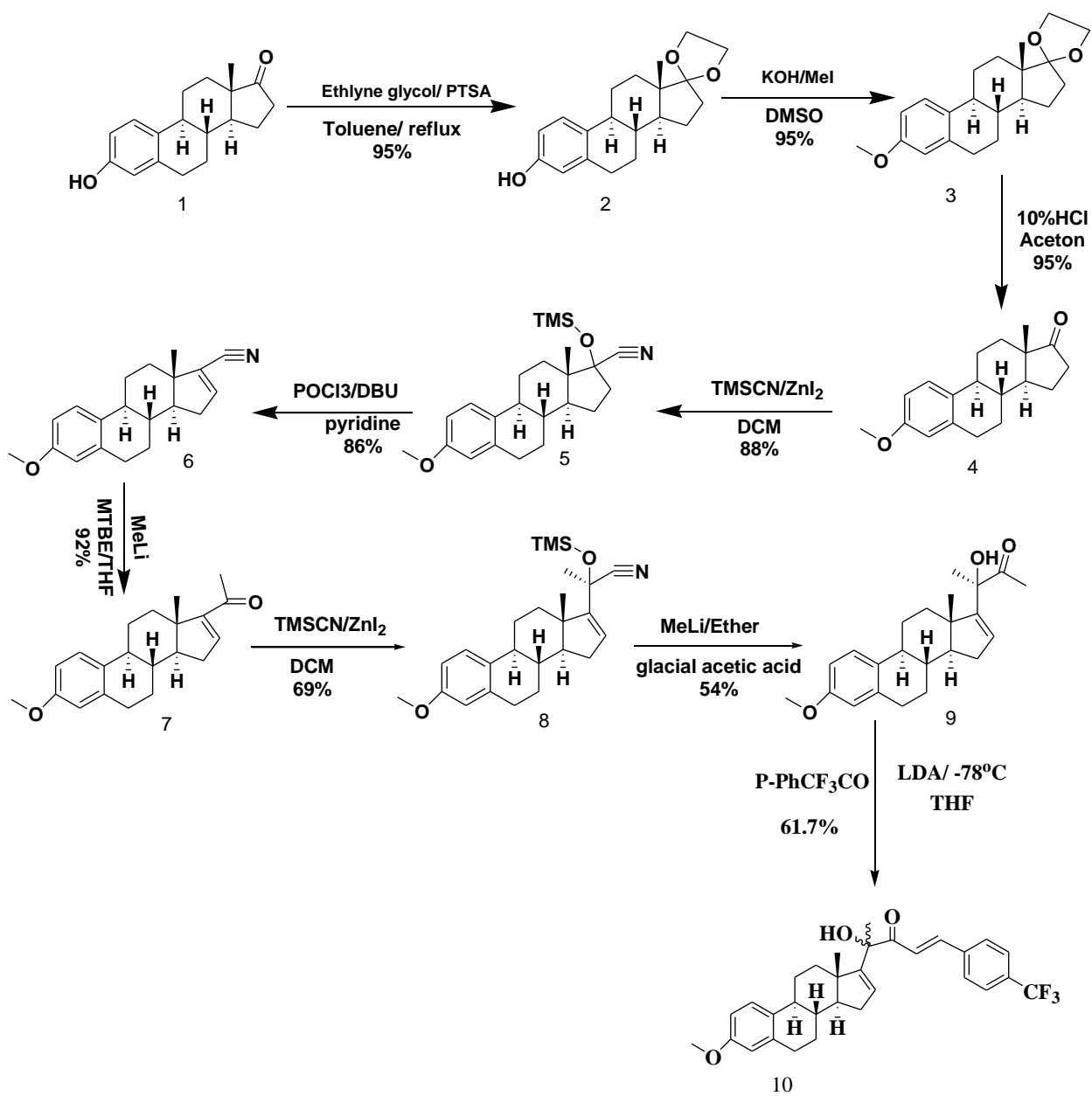
Scheme 2.2 Synthesis route of MMA320.
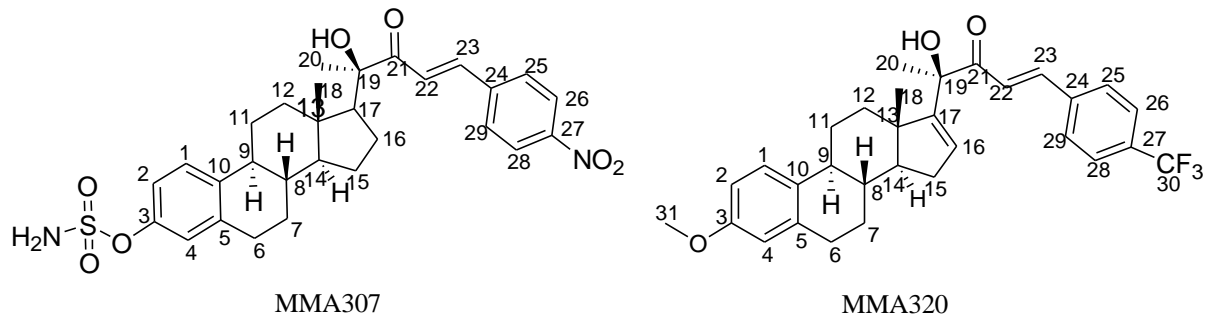
Figure 2.6 Structures of MMA307 and MMA320. MMA307 was named as (8S,9S,13S,14S,17S)-7,8,9,11,12,13,14,15,16,17-decahydro-17-((R,E)-2-hydroxy-5-(4-nitrophenyl)-3-oxopent-4-en-2-yl)-13-methyl-6H-cyclopenta[a]phenanthren-3-yl sulfamate and MMA320 named as (R,1E)-1-(4-(trifluoromethyl)phenyl)-4-((8S,9S,13S,14S)-7,8,9,11,12,13,14,15-octahydro-3-methoxy-13-methyl-6H-cyclopenta[a]phenanthren-17-yl)-4-hydroxypent-1-en-3-one.

Table 2.1 Inhibitory effects of estrone analogs against NCIH226 cell proliferation.

Compound	IC$_{50}$ (µM)
MMA228	99.8 ± 0.28^c
MMA269	10.41 ± 0.46^b
MMA270	$> 100^c$
MMA271(R)	19.43 ± 0.79^d
MMA271(S)	40.39 ± 1.65^b
MMA287	11.82 ± 0.65^b
MMA290	$>100^c$
MMA292	$>100^c$
MMA300	17.41 ± 1.56^a
MMA306	17.42 ± 0.56^a
MMA307	2.88 ± 0.21^c
MMA308	$>100^c$
MMA309	$>100^c$
MMA310	$>100c$
MMA311	45.46 ± 0.71^b
MMA312	20.64 ± 1.66^d
MMA313	$>100^c$
MMA316	$>100^c$
MMA319	$>100^c$
MMA320	9.68 ± 0.24^b
MMA321	14.57 ± 0.31^b
MMA323	$>100^c$
MMA327	$>100^c$
MMA334	42.02 ± 1.57^b
Sorafenib	20.62 ± 1.32
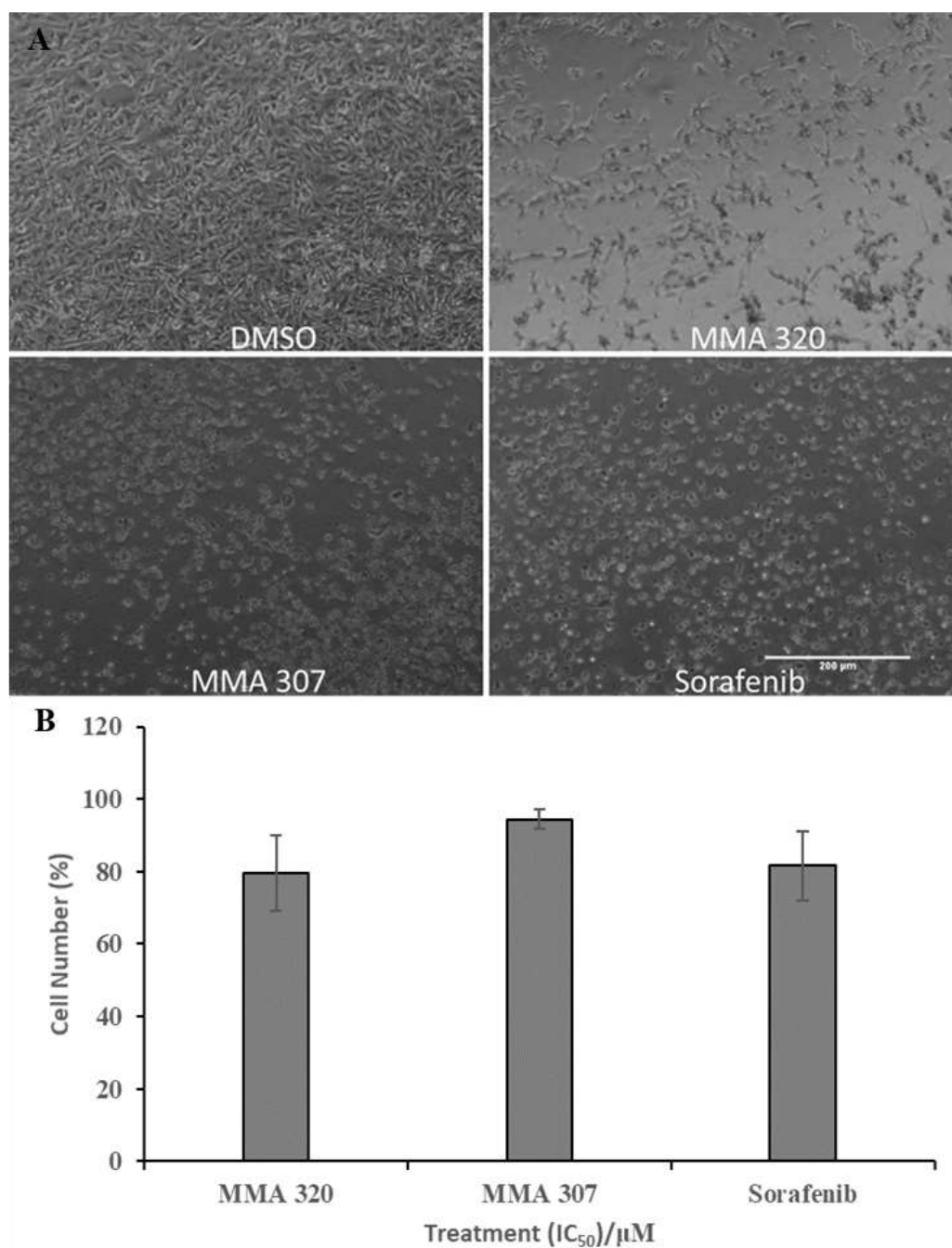
Figure 2.7 Growth inhibitory effects on NCIH226 after treatment with IC$_{50}$ values of estrone analogs. (A) Morphological changes in NCIH226 cells after treatment with 0.05% DMSO, MMA320, MMA307 and sorafenib. Images were acquired with ×4 objective lens of Evos XL cell imaging system (ThermoFisher Scientific), scale bar = 200 µm. (B). Trypan blue cell counting after 24 hrs. The number of cells was determined by counting and expressed as mean % ± SD of two independent experiments with n=2 per condition in each experiment.
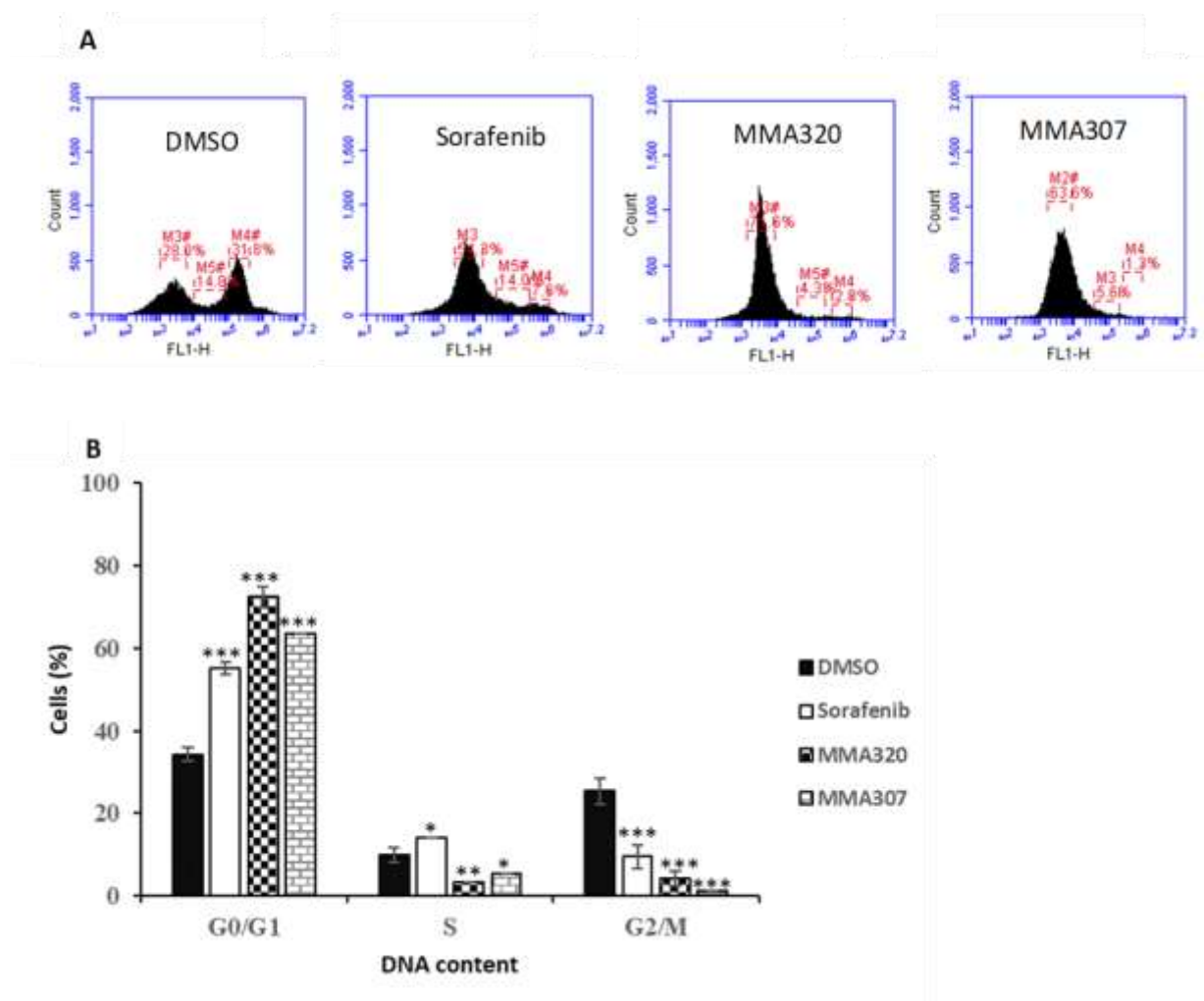
Figure 2.8 Estrone analogs exposure resulted in G_1-phase cell cycle arrest. NCIH226 cells were treated with IC_{50} values of estrone analogs and analyzed after 48 hrs by flow cytometry. (**A**) Distribution of cells in distinct phases of the cell cycle. MMA320 shows the highest arrest of G_0/G_1 phase of the cell cycle compared to the negative control, DMSO. (**B**) The bar graphs show Mean ± SD of the percentages of NCIH226 cells in the indicated phases of the cell cycle (G_0/G_1, S and G_2/M). At least three independent experiments were performed. $^*p < 0.05$, $^{**}p < 0.01$, $^{***}p < 0.001$ significant differences in cell cycle arrest compared to DMSO control.
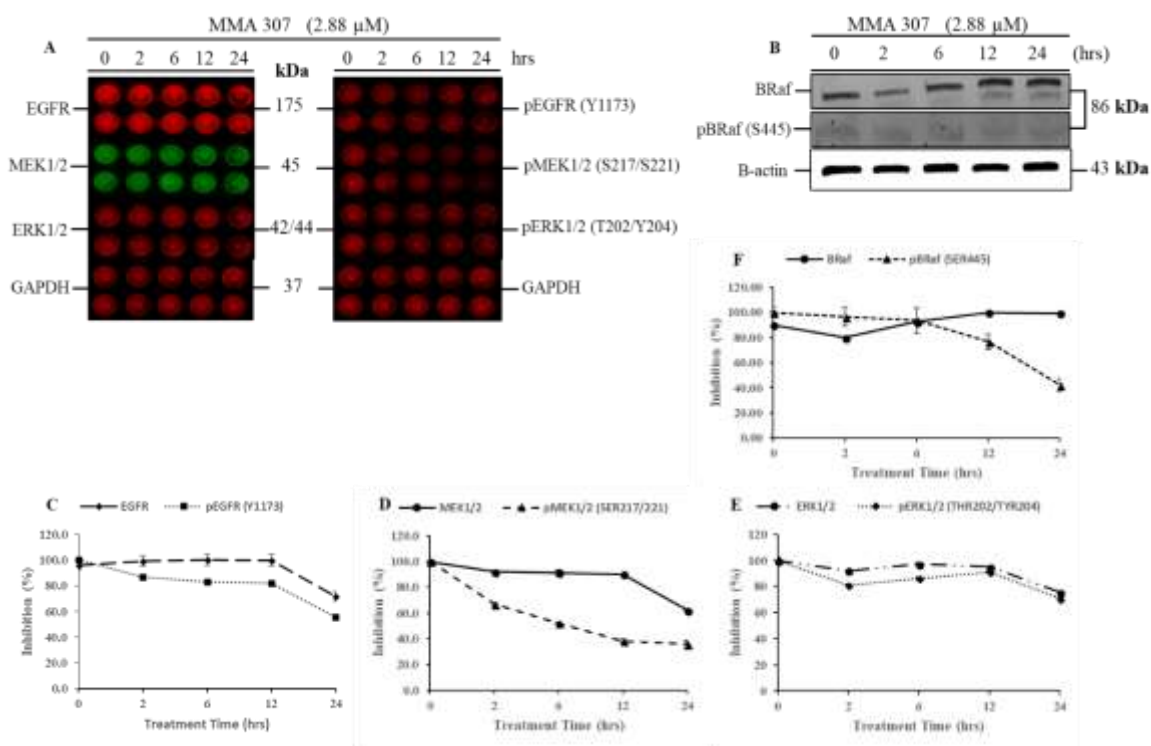
Figure 2.9 EGFR and multiple MAPK-ERK1/2 effector molecules are inhibited in NCIH226 cells by MMA307 treatment. (**A**) MMA307 inhibited EGFR and pEGFR, as well as multiple downstream MAPK-ERK1/2 effector molecules, detected through In Cell Western (ICW) assay. After treatment with MMA307 (2.88 μM), fixed cells were incubated with specific antibodies for each protein. The cells were washed and incubated with DyLight conjugated (680 or 800 nm) detection antibodies, and plates scanned with LICOR Odyssey® Fc imaging system to measure the levels of total and phosphorylated proteins. Quantitation of proteins was completed using scanned images from Fiji software. (**B**) Cell extracts were also fractionated on SDS-PAGE, followed by immunoblot analysis for the indicated proteins. β-Actin was examined as a loading control for each immunoblot analysis. (**C-F**) Data points are represented as the mean of duplicate and SD of two independent experiments.
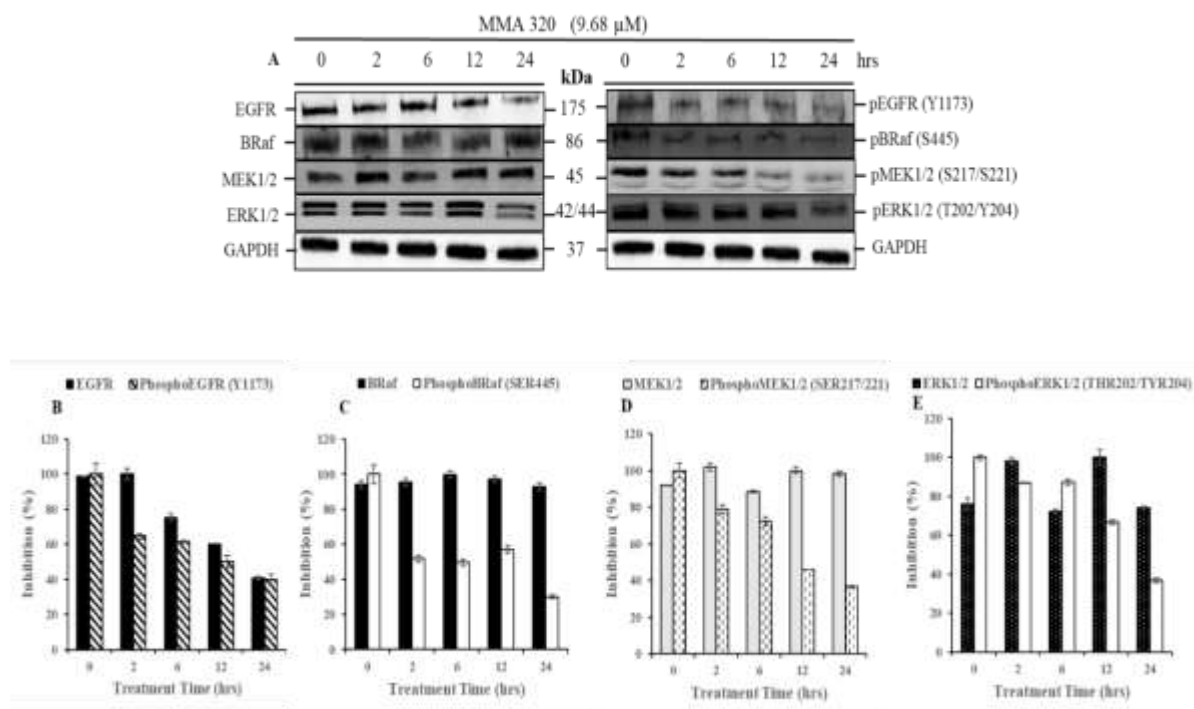
Figure 2.10 Effects of MMA320 treatments on EGFR and multiple MAPK-ERK1/2 effector molecules in NCIH226 cells. (**A**) Cells were treated for indicated times with 9.68 μM MMA320. Cell lysates were analyzed by SDS-PAGE, transferred to nitrocellulose membranes and use of the corresponding primary antibodies against specific proteins and GAPDH as loading controls. Blots are representative examples of at least two independent experiments. LICOR Odyssey® Fc imaging system analysis of bands comparing the relative levels of proteins after time-course treatment with MMA320 as compared to DMSO control. (**B-E**) Bar graphs are means ± SD from at least two independent experiments.
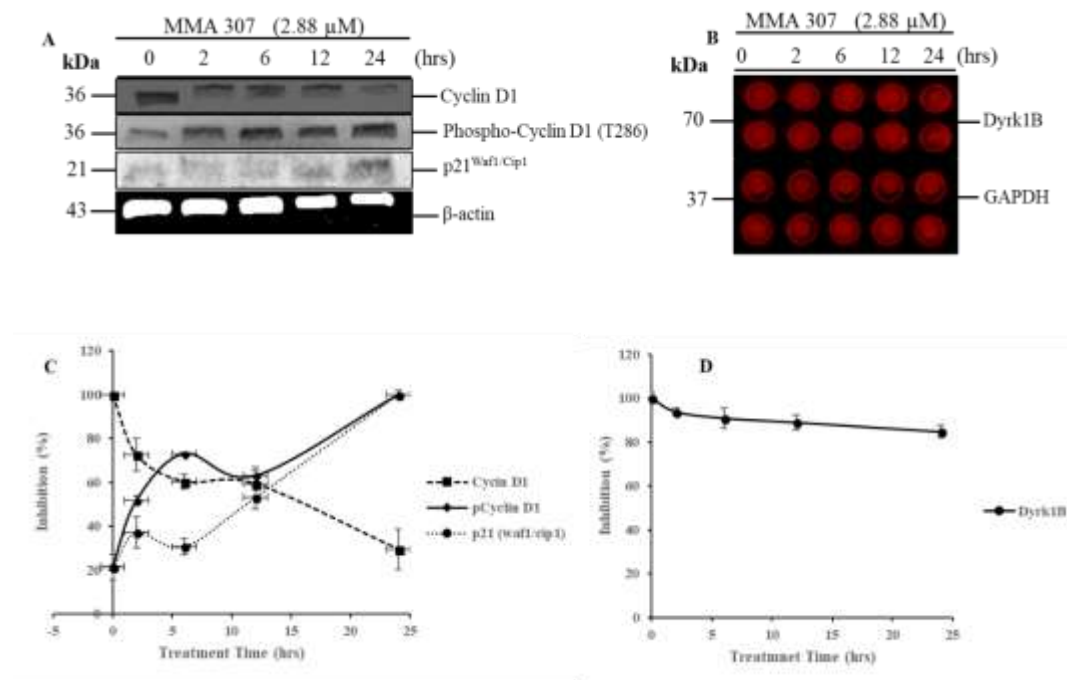
Figure 2.11 Effects on G_1 phase cell cycle regulators after treatment with MMA307 in NCIH226 cells. (**A-B**) Cells were treated for indicated times with 2.88 μM MMA307. Cell lysates or fixed cells were analyzed by western blot or ICW and use of the corresponding primary antibodies against specific proteins and β-Actin or GAPDH as loading controls. LICOR Odyssey® Fc imaging system analysis of bands comparing the relative levels of proteins after time-course treatment with MMA320 as compared to DMSO control. Blots or ICW images are representative examples of at least two independent experiments. (**C-D**) Line graphs are means ± SD from at least two independent experiments.
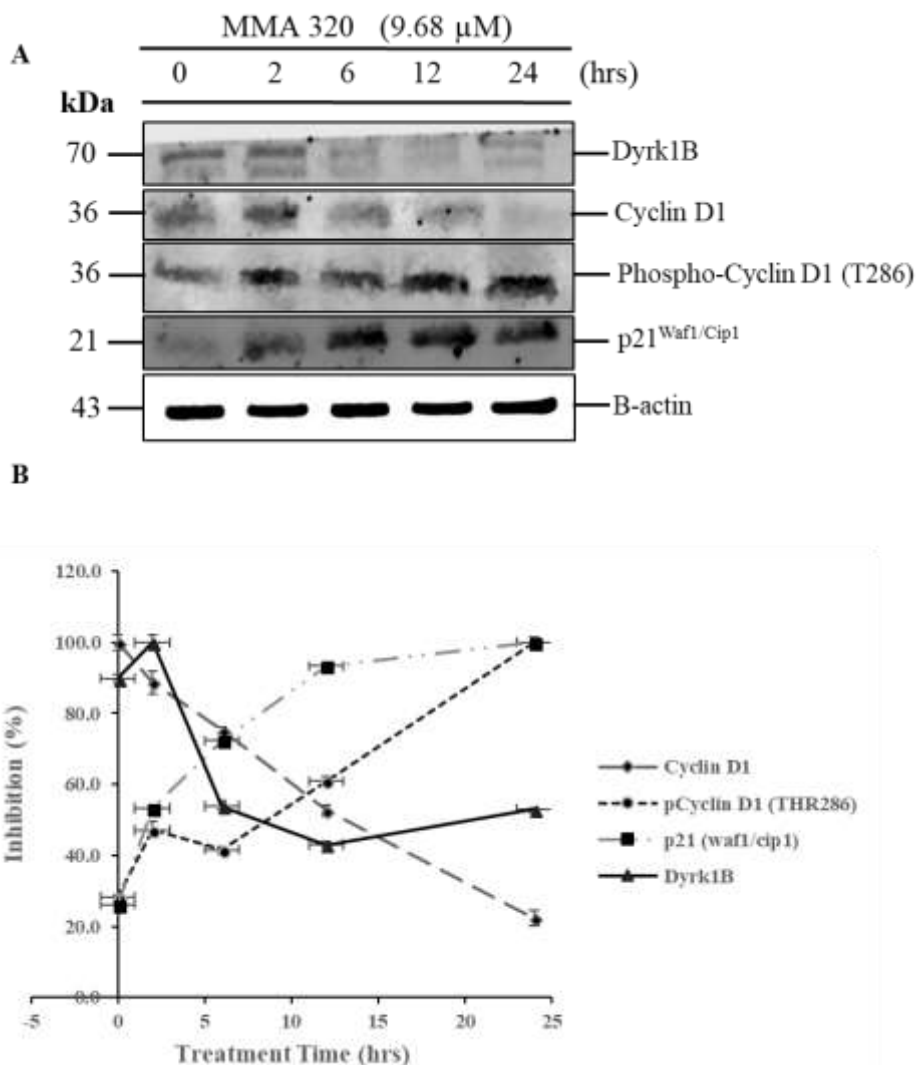
Figure 2.12 Effects on G_1 phase cell cycle regulators after treatment with MMA320 in NCIH226 cells. (A) Cells were treated for indicated times with 9.68 µM MMA320 for indicated times. Cell lysates were analyzed by SDS-PAGE gels, transferred to nitrocellulose membranes and use of the corresponding primary antibodies against Dyrk1B, cyclin D1, p-cyclin D1, p21$^{waf1/cip1}$ and β-actin as loading controls. LICOR Odyssey® Fc imaging system analysis of bands comparing the relative levels of proteins after time-course treatment with MMA320 as compared to DMSO control. Blot images are representative examples of at least two independent experiments. (B) Line graphs are means ± SD from at least two independent experiments.

Chapter 3

Estrone hybrids with modified cucurbitacin pharmacophores induce growth inhibition and apoptosis via suppressing EGFR, Akt/mTOR and ERK1/2 pathways in triple negative breast cancer cells.

3.1   Abstract

Triple-negative breast cancer (TNBC) is a subtype of breast cancer with an aggressive phenotype which shows high metastatic capability and poor prognosis. The aggressive behavior of TNBC may involve aberrant EGFR expression and activation of its downstream PI3K/Akt/mTOR and RAF/ERK signaling which has received considerable attention as druggable targets in recent times. Currently, no targeted therapy has been approved for treating TNBC. Previous studies from our research group showed that estrone analogs with cucurbitacin pharmacophores and nitric oxide releasing properties inhibited the proliferation of several type of cancers. In this study, we report that novel estrone analogs with modified cucurbitacin pharmacophores exhibited cytotoxic killing towards TNBC cells through multiple mechanisms, inhibition of cell proliferation and induction of mitochondrial apoptosis. Molecular docking studies were carried out with OpenEye software. The MTT cell viability assay was used to perform cytotoxicity studies. Morphological changes and cell cycle arrest were carried out by microscopy and flow cytometric techniques, respectively. Annexin V assay was used to evaluate initial apoptosis induction in MDA-MB-468 cells, and In-cell western assay was used to detect the expression levels of apoptotic, cell cycle and EGFR and its downstream AKT and ERK1/2 pathways associated proteins. We demonstrated that MMA307 and MMA321 showed strong potency towards the EGFR kinase domain (pdb code: 1M17) *in silico* and exhibited cation-π and hydrogen bonding interactions towards amino acid residues within the ATP binding site. MMA307 was over tenfold more cytotoxic than sorafenib when dosed to MDA-MB-468 cells and MMA321 was almost twenty-fold more potent than sorafenib.

Moreover, condensed nuclei with fragmented chromatin, phosphatidylserine flip and modulated expression of proteins within the intrinsic apoptosis pathway (Apaf1, cytochrome c, caspases 3 and 9) confirms mitochondrial apoptosis and suggest MMA307 and MMA321 induced apoptosis via caspase-dependent pathways. Also, MMA307 and MMA321 downregulated cyclin D1 expression levels contributing to G_1 phase cell cycle arrest. Furthermore, both compounds inhibited the expression of EGFR and activated EGFR (Y1068); Activated proteins within the RAF/ERK and AKT/mTOR pathways were downregulated upon MMA307 and MMA321 treatment. Particularly, pARaf, pERK1/2, pAKT, pmTOR and p70S6Kα were all suppressed. Taken together, we report for the first time that estrone analogs with modified cucurbitacin pharmacophores may be an effective therapy for TNBC, which urgently needs novel treatment options. Further studies are needed to develop these novel candidates as targeted agents for TNBC.

Keywords: TNBC; EGFR; Estrone analogs; MDA-MB-468; Apoptosis; Cell cycle

3.2   Introduction

Breast cancer is the most common invasive cancer in women globally and the leading cause of cancer-related death (Bray *et al.*, 2018). Breast cancers can be categorized into four main subtypes in accordance to the pattern of genetic profiling. Two are derived from hormone receptor expression, thus estrogen receptor (ER)-positive tumors, luminal A and B, and the remaining two are derived from lack of hormone receptor expression, thus ER-negative tumors, basal-like and HER2 positive (Berrocal, 2017). Triple-negative breast cancer (TNBC) is a basal-like subtype of breast cancer that accounts for about 20% of all breast cancers (Dai *et al*., 2015; Uscanga-Perales *et al*., 2016; Lee and Djamgoz, 2018). In comparison with other breast cancer subtypes, TNBC is a heterogeneous disease with a higher metastasis rate, worse prognosis, and higher relapse risk (Uscanga-Perales *et al*., 2016, Podo *et al*., 2016). Also, brain metastasis is mainly the results of TNBC progression (Feng *et al*, 2018). This disease stage has no effective therapeutic option partially due to the poor penetration of drugs across the blood-brain barrier. Therefore, TNBC has attracted increasing amounts of attention in oncology research. Currently, the major therapies for breast cancer include surgery, radiation therapy, hormone therapy and chemotherapy. Surgery and radiotherapy are local therapy methods for the treatment of cancer. Because of the high metastasis and relapse rates of TNBC, new therapeutic modalities need to be discovered for TNBC treatment. Contrary to this, TNBC cannot be treated by hormone therapy because it lacks or has low expression of estrogen receptor (ER), progesterone receptor, and human epidermal growth factor receptor 2 (HER2) (Ma *et al*., 2017). Despite

several possible targeted agents been studied in the last two decades, currently, there are no targeted therapies approved by the FDA and other agencies around the globe for treating TNBC (Yue *et al*, 2018). Hence, standard chemotherapy, especially anthracycline-based agents, remains the first option of current TNBC treatment strategies (Cortazar *et al*., 2014), but there is still a substantial risk for recurrence and aggressive disease progression (Székely *et al*., 2017; Wahba and El-Hadaad, 2015). Thus, it is urgent to discover highly effective and low toxic targeted treatment strategies for TNBC.

Natural products are often regarded as sources of phytochemicals or leads for the discovery of novel drugs. Phytochemicals are naturally occurring secondary metabolites-biologically active compounds found in plants, animals, microorganisms and marine organisms which have capabilities of inhibiting various diseases including cancer. Notable examples include the vinca alkaloids vincristine and vinblastine isolated from *Catharanthus roseus,* as well as taxol isolated from *Taxus brevifolia,* for the treatment of various cancers (Acheampong *et al*, 2017; Acheampong *et al*, 2015; Larbie *et al*, 2015). In the face of worldwide disease challenges, natural products research and development potentially play a key function in innovative drug discovery. About 33% of FDA-approved drugs over the past two decades are based on natural products or their derivatives and these have transformed medicine (Thomford *et al*, 2018). In particular, Stander *et al*, 2011, Botes *et al*, 2018, report that 2-Methoxyestradiol (2ME), an endogenous metabolite of 17β-estradiol, and its sulphamoylated derivative (Visagie *et al*, 2013; Verwey *et al*, 2016; van Vuuren *et al*, 2019) possess both antiangiogenic and anti-breast cancer effects *in vitro* and *in vivo*.

However, 17β-estradiol promotes the proliferation of various cancers (Verwey *et al*, 2016). This suggests that estradiol may be a privileged scaffold upon which modifications can be done to generate lead candidates with improved potency and pharmacokinetic properties as well as reduced toxicities. In our research group, estrone, an isomer of estradiol, is used as a starting material to synthesize novel estrone analogs. Many of our estrone derivatives, especially those bearing cucurbitacin side chains have been documented to exhibit potent cytotoxic effects against distinct cancers (Ahmed *et al*, 2017; Elshaier *et al*, 2017; Ahmed *et al*, 2014; Kopel *et al*, 2013). Also, Sara *et al*, 2018 reported on the cytotoxic effect and EGFR/MAPK pathway suppression capabilities by the novel estrone analogs with cucurbitacin side chains against wild-type and resistant HepG2 cell lines. In addition, Amr and colleagues, 2019, reported that novel estrogen analogs effectively bind to EGFR *in vitro* and *in vivo* and were cytotoxic against MCF-7 cells but not towards MCF-10A cells alluding to their selectivity.

In the current research, we showed that several estrone analogs were effective in inducing growth inhibition, cell cycle arrest and apoptosis in the TNBC model MDA-MB-468 cells. Also, we determined the effect of MMA307 and MMA321 on EGFR and its downstream PI3K/Akt/mTOR (PAM) and RAF/ERK pathways, because both represent the main signaling pathways responsible for cell metabolism, survival and proliferation and are often activated in TNBC (Ignacio *et al*., 2018; Chen and Costa, 2018; Foidart *et al*., 2019). We revealed that MMA307 and MMA321 suppression of MDA-MB-468 cells growth could be as a result of multiple factors including inhibition of EGFR and its downstream PAM

and MAPK pathways; induction of mitochondrial apoptosis and suppression of cell cycle progression.

3.3   Materials and methods

3.3.1   Reagents and chemicals

Antibodies against EGF Receptor (D38B1) XP®, Phospho-p44/42 MAPK (Erk1/2) (Thr202/Tyr204) (197G2), Cyclin D1 (92G2), Phospho-Akt (Ser473) were purchased from Cell Signaling Technology (Danvers, MA, USA); goat anti-rabbit and goat anti-mouse horseradish peroxidase conjugate (HRP) secondary antibodies, phospho-cyclin D1 (Thr286) (A537487), Phospho-A-Raf (Ser299) were from Thermo Fisher Scientific (Waltham, MA, USA); Phospho-EGF Receptor (Tyr1068), Phospho-p70S6 Kinase α, Dyrk1B, caspase 9, caspase 3, PARP1, cleaved PARP1, Bcl-2, APAF1, cytochrome C and GAPDH were from Santa Cruz Biotechnology Inc. (Dallas, Texas, USA). Phosphate buffered saline (PBS) and trypan blue solution were from Thermo Fisher Scientific (Waltham, MA, USA). RealTime-Glo™ Annexin V apoptosis and necrosis assay (JA1011) kit was from Promega (Madison, WI, USA). PI/RNase staining buffer was purchased from BD Biosciences (San Jose, CA, USA). Compounds cytotoxicity was evaluated through measurement of mitochondrial dehydrogenase activities with 3-(4,5-dimethylthiazol-2-yl)-2,5-diphenyltetrazolium bromide (MTT) reagent (Sigma-Aldrich, St. Louis, MO, USA). Hoechst 33342 stain for evaluating chromatin condensation and nuclear fragmentation was

purchased from Thermo Fisher Scientific (Waltham, MA, USA). Sorafenib (positive control) (Selleckchem, Houston, TX, USA) and novel triazole derived estrone analogs were dissolved in dimethyl sulfoxide (DMSO) (Fisher Chemical/Fisher Scientific). Western Lightning Plus-ECL, Enhanced Chemiluminescence Substrate for protein detection was purchased from PerkinElmer (Waltham, Massachusetts, USA). All other chemicals were of biological and analytical grade.

3.3.2   Design and synthesis of estrone analogs

3.3.2.1   Molecular modeling

Fitting novel estrone analogs into the 3D X-ray structure of EGFR kinase domain (PDB code: 1M17) was carried out using the FRED application (version 2.2.5) as implemented through the graphical user interface of OpenEye® software. The 3D structure of the above protein was downloaded from Protein Data Bank (pdb) and prepared with the make receptor software. The three-dimensional structures of the estrone analogs were constructed using Chem. 3D ultra 12.0 software [Chemical Structure Drawing Standard; Cambridge Soft corporation, USA (2010)], then they were energetically minimized with MMFF94 application with 5000 iterations and minimum RMS gradient of 0.10. All bound water molecules and ligands were eliminated from the proteins. Furthermore, multi-conformers were generated using OMEGA application (version 2.5.1.4) and the VIDA application (version 4.1.2) was used as a visualization tool to show the potential binding

affinity and binding interactions of the ligands to the receptor (Elshaier *et al*, 2017). This software package generates consensus scoring which is a filtering process to obtain virtual binding affinity. The lower the consensus score, the better binding affinity of the ligands towards the receptor.

3.3.2.2   Synthesis of MMA307 and MMA320

3.3.2.2.1   General procedure for the preparation of MMA307

Steps 1 to 9 has been previously reported by our research group (Ahmed *et al*, 2014; Kopel *et al*, 2013). Preparation of 10 was carried out as follows: 0.15 g of 9 was dissolved in N, N-dimethylacetamide (0.8 mL) and incubated with sulfamoyl chloride (0.12 g, 0.945 mmol) at 0ºC. Subsequently, the reaction mixture was stirred at room temperature for 18 hrs and the resulting solution extracted with 1:1 mixture of ethyl acetate and water. The residue was purified using silica gel column chromatography (ethyl acetate: n-hexane, 3:7) to isolate compound 10 which was labeled as MMA307 (0.16 g, 91%). MMA307 was characterized by ^{1}H and ^{13}C NMR and high-resolution mass spectroscopies (Mahnashi, 2017).

MMA307 ^{1}H NMR (600 MHz, Chloroform-d) δ 8.21 – 8.18 (m, 2H), 7.77 (d, J = 15.7 Hz, 1H), 7.71 – 7.67 (m, 2H), 7.25 – 7.21 (m, 1H), 7.10 (d, J = 15.7 Hz, 1H), 7.01 (dd, J = 8.6, 2.6 Hz, 1H), 6.95 (d, J = 2.6 Hz, 1H), 5.03 (s, 2H), 3.98 – 3.89 (m, 1H), 3.83 (s, 1H), 2.78 (qd, J = 10.4, 9.7, 4.3 Hz, 2H), 2.29 – 2.21 (m, 2H), 2.16 (dq, J = 12.0, 4.2 Hz, 1H),

1.84 – 1.77 (m, 2H), 1.64 – 1.56 (m, 2H), 1.56 – 1.53 (m, 2H), 1.50 (s, 3H), 1.41 – 1.31 (m, 2H), 0.88 (s, 3H).

MMA307 ^{13}C NMR (151 MHz, CDCl3) δ 203.04 (C21), 148.81 (C3), 147.90 (C27), 142.60 (C23), 140.35 (C24), 139.64 (C5), 138.92 (C10), 129.26 (C25, C29), 126.73 (C1), 124.25 (C26,C28), 122.29 (C22), 121.93 (C4), 118.95 (C2), 79.54 (C19), 55.66 (C14), 54.98 (C17), 44.31 (C8), 43.97 (C13), 40.51 (C12), 37.65 (C15), 29.51 (C6), 27.26 (C11), 26.43 (C7), 24.22 (C9), 23.64 (C20), 22.09 (C16), 13.65 (C18).

HR-FT-MS calcd for C29H34O7N2SNa 577.1979 found 577.19790.

3.3.2.2.2 General procedure for the preparation of MMA321

Steps 1 to 9 has been previously reported by our research group (Ahmed *et al*, 2014; Kopel *et al*, 2013). Synthesis of 10 was carried out as follows: to a stirred solution of the 9 (0.4g, 1.13 mmol), a mixture of tetrahydrofuran and lithium diisopropylamine (LDA) (2.034mL, 4.068 mmol) were added and the reaction kept at -78 ºC. Afterwards, the reaction mixture was initially stirred for 1 hr, before para-nitrobenzene (0.242mL, 2.26mmol) dissolved in THF added and the resulting mixture warmed to room temperature for 24 hrs. Subsequently, the reaction was quenched with ammonium chloride and the aqueous layer extracted with ethyl acetate, dried over anhydrous sodium sulfate, filtrated, and concentrated under vacuum. Silica gel column chromatography was used to purify the crude material (ethyl acetate: n-hexane, 1:9) to obtain 10 (0.29g, 52.7%). Pure compound

10 was characterized by NMR and mass spectroscopies and labeled as MMA321 (Mahnashi, 2017).

MMA321 ^{1}H NMR (400 MHz, Chloroform-d) δ 8.14 (m, 2H), 7.75 (m, 1H), 7.61 (m, 2H), 7.12 (s, 1H), 7.08 – 6.96 (m, 2H), 6.59 – 6.52 (m, 1H), 6.49 (d, 1H), 5.95 (d, 1H), 4.24 (s, 1H), 3.64 (s, 3H), 2.79- 2.73 (m, 2H), 2.20-2.10 (m, 2H), 2.01 (m, 1H), 1.79 (d, 1H), 1.48 – 1.35 (m, 1H), 1.32 – 1.13 (m, 3H), 1.08 (m, 1H), 0.94 (s, 3H), 0.85- 0.76 (m, 4H).

MMA321 ^{13}C NMR (101 MHz, Chloroform-d) δ 200.45, 157.40, 154.95, 148.73, 141.74, 140.35, 137.79, 132.62, 129.97, 129.24, 125.96, 124.20, 122.58, 113.78, 111.35, 78.89, 57.48, 55.14, 47.83, 43.91, 37.05, 34.67, 34.54, 31.60, 31.24, 29.65, 27.57, 26.25, 25.29, 25.18, 22.67, 17.19, 14.16.

HR-FT-MS calcd for C30H33O5N1Na1 510.2251 found 510.22454.

3.3.3 Cell culture

MDA-MB-468 (a model for TNBC with amplified EGFR) was a kind gift from Dr. Rachel Willand Charnley (South Dakota State University, Department of Chemistry and Biochemistry). The cells were cultured in Dulbecco's Modified Eagle Medium (DMEM) supplemented with 10% (v/v) fetal bovine serum (FBS), antibiotic-antimycotic (Gibco™, ThermoFisher Scientific) at 37˚C equilibrated with 5% (v/v) CO_2 in humidified air. The

cells for the assays were detached using a solution of trypsin with EDTA (ThermoFisher Scientific).

3.3.3.1   Cytotoxicity assay

3.3.3.1.1   3-(4,5-dimethylthiazol-2-yl)-2,5-diphenyltetrazolium bromide (MTT) Assay

The effect of novel synthetic estrone analogs on cell viability was tested with MTT reagent as described by Wang *et al*, 2010, with slight modifications. Briefly, to measure mitochondrial dehydrogenase activities, cells were seeded into wells on 96-well plates at an initial density of 30, 000 cells per well. After overnight incubation, cells were treated with different concentrations of compounds in a dose range of 0 - 100 μM. The final DMSO concentration was 0.05%. After 48 hrs of incubation, 20 μL   of MTT reagent (5 mg/mL) was added to each well and the formed formazan crystals were dissolved in 250 μL   of dimethyl sulfoxide (DMSO). Four independent experiments were completed to determine the mean optical density referred to as cell viability, using a Hidex Sense Beta Plus plate reader (Turku, Finland). Cell viability was expressed as a percentage of DMSO-treated controls.

3.3.3.2   Flow cytometry for cell cycle analysis

MDA-MB-468 cells were seeded into six-well plates at a concentration of 300, 000 cells/ well and allowed to attach in culture overnight, then treated with IC_{50} molarity of compounds or positive control (sorafenib) for 48 h. Afterward, cells were washed with PBS and harvested. Cell cycle analysis was investigated by adding propidium iodide (PI) stain (Thermo Fisher Scientific) to 1 mL of cell suspension. Briefly, harvested cells were fixed in 70% ethanol and incubated at 4ºC for 4hrs. Subsequently, the cells were cleaned of alcohol and stained with RNase free PI solution, the cell suspension was incubated in the dark for 45 minutes at room temperature. The samples were analyzed by flow cytometry and compared to DMSO-treated cells. All these experiments were performed on CytoFLEX flow cytometer, serial no. AW35216 (Beckman Coulter Life Sciences, Indianapolis, IN, USA) using CyExpert software, version 1.2.

3.3.3.3   Apoptosis analysis

3.3.3.3.1   Annexin V assay

The annexin v assay was performed in accordance with the manufacturers' protocol with slight modifications. Briefly, MDA-MB-468 cells were seeded into wells on a 96-white plate with a clear bottom at an initial density of 30,000 cells for overnight attachment. Afterward, the cells were incubated with the IC_{50} concentrations of compounds for 12 hrs. Subsequently, the RealTime-Glo™ Annexin V Apoptosis reagent (Promega, Madison, WI) was prepared (sequentially mix Annexin NanoBiT® Substrate, $CaCl_2$, Annexin V-SmBiT

and Annexin V-LgBiT in a prewarmed media) and added to the reaction set up before incubating for additional 1 hr. Luminescence was measured afterward using Hidex Sense Beta Plus plate reader (Turku, Finland). Apoptosis was expressed as a percentage relative to DMSO-treated controls.

3.3.3.3.2 Morphological analysis with fluorescence microscopy

To further evaluate the apoptotic activity of the estrone analogs, nuclear staining with the DNA-binding dye Hoechst-33342 was performed in accordance with the manufacturers' protocol. In brief, MDA-MB-468 cells were plated into wells on 96-well plates and treated with IC_{50} concentrations of compounds for 12 hrs. Cells were washed with PBS and incubated with Hoechst-33342 (10μg/mL) for 15 min in the dark, then images were acquired using Cytation 3 imaging multi-mode reader (BioTek Instruments, Inc., Waltham, MA, USA) with 4× objective lens (excitation 352 nm, emission 461 nm). Apoptotic cells were identified by condensation of chromatin and fragmentation of nuclei with Gen5 software version 3.03.

3.3.3.4 Protein expression analysis

3.3.3.4.1 In-Cell Western (ICW) Assay

Proteins involved in apoptosis, cell cycle progression, EGFR, and its downstream MAP kinase and Akt pathways were quantified by ICW. This technique was carried out in accordance with the manufacturer's instruction with slight modifications. Briefly, about 50,000 cells per well were seeded into 96-well white-walled plate with clear bottom for overnight attachment. Afterward cells were washed three times with PBS and depleted of serum for six hours. Cells were then treated with varying concentrations of compounds in serum-free media for six hours before stimulating with 100nM of EGF for one hour. Subsequently, cells were fixed with 3.7% formaldehyde solution, permeabilized with 0.1% Triton X-100 solution and blocked with fish gel buffer (1×) prior to primary antibody addition. Wells were then incubated with the relevant antibodies EGF Receptor (D38B1) XP®, Phospho-p44/42 MAPK (Erk1/2) (Thr202/Tyr204) (197G2), Cyclin D1 (92G2), Phospho-Akt (Ser473), Phospho-A-Raf (Ser299), Phospho-EGF Receptor (Tyr1068), Phospho-p70S6 Kinase α, caspase 9, caspase 3, PARP1, cleaved PARP1, Bcl-2, APAF1, cytochrome C and GAPDH (loading control) overnight followed by an hour incubation with goat anti-mouse or goat anti-rabbit horseradish peroxidase conjugated secondary antibodies. Finally, the cell mixture was incubated with enhanced chemiluminescence substrate (Western Lightning Plus-ECL) for a few minutes before chemiluminescence was measured using Hidex Sense Beta Plus plate reader (Turku, Finland). Protein expression levels were normalized to the housekeeping gene, GAPDH, and expressed as a percentage.

3.3.4 Statistical Analysis

Microsoft® Excel® for Windows, version 16.0., was used for the calculation of mean and standard deviation values of different experiments and plotting of bar or line graphs. Mean IC_{50} values were compared by one-way analysis of variance (ANOVA) and multiple comparisons were done by the Dunnett Test using GraphPad Prism 5.01 (San Diego, USA) and values with $p < 0.01$ or $p < 0.001$ were considered statistically significant.

3.4   Results

3.4.1   Docking simulations

To demonstrate whether the designed estrone analogs can target EGFR dependent breast cancers, an initial *in silico* molecular docking studies were carried out by fitting the designed analogs and reference compound (erlotinib) into the ATP binding site of the EGFR kinase domain (PDB codes: 1M17). The obtained results were plotted as a line-scatter graph (Figure 3.1), which mainly displays the corresponding consensus scores of the molecular docking studies. Compared with the reference drug, erlotinib, it was clearly observed that most estrone analogs showed lower consensus scores (a measure of better binding and improved potency) when fitted into the EGFR kinase domain. Furthermore, the binding mode of MMA307 and MMA321 revealed that MMA307 fitted into the hydrophobic pocket of the EGFR kinase domain and demonstrated hydrophobic interaction towards the ATP binding site. However, MMA321 demonstrated hydrogen bonding towards THR830A, ASP831A and LYS721A residues within the ATP binding site of 1M17 (Figures 3.3 – 3.4). Also, these compounds exhibited potent cytotoxic effects against

MDA-MB-468 cells *in vitro* compared to sorafenib. The addition of a sulfamoyl moiety to compound 9 afforded 10 (MMA307) in 91% yield after column chromatography (scheme 3.1), and the addition of para-nitrobenzene to the hyroxyl methyl ketone diastereomeric mixture yielded 52.7% of MMA321 after purification with silica gel column chromatography (Scheme 3.2). These pure compounds were characterized by NMR and mass spectrometry techniques with the ^{1}H and ^{13}C chemical shifts as well as accurate masses reported above. In terms of IUPAC nomenclature, MMA307 was named as (8S,9S,13S,14S,17S)-7,8,9,11,12,13,14,15,16,17-decahydro-17-((R,E)-2-hydroxy-5-(4-nitrophenyl)-3-oxopent-4-en-2-yl)-13-methyl-6H-cyclopenta[a]phenanthren-3-yl sulfamate and MMA321 named as 4-Hydroxy-4-(3-methoxy-13-methyl-7,8,9,11,12,13,14,15,16,17-decahydro-6H-cyclopenta[a]phenanthren-17-yl)-1-(4-nitro-phenyl)-pent-1-en-3-one (Figure 3.5).

3.4.2   Estrone analogs exhibit cytotoxic effects against MDA-MB-468 cells

To determine the cytotoxic effects of the estrone analogs against TNBC cell lines, the viability of MDA-MB-468 cells initially treated with a dose range of $0 - 100$ µM was analyzed using the MTT cell viability assay after 48 hrs. Overall, the compounds did show a significant cytotoxic effect toward the MDA-MB-468 cells within the dose range tested after 48 hrs and therefore IC_{50} values were calculated. Most of the compounds were very effective than the positive control-sorafenib in exhibiting cytotoxic killing towards MDA-MB-468 cells. Particularly, MMA300, MMA307, MMA320 and MMA321 recorded IC_{50} concentrations of 0.89 ± 0.10, 0.85 ± 0.00, 1.71 ± 0.01 and 0.56 ± 0.01 µM, respectively

compared to sorafenib IC_{50} molarity of 10.09 ± 0.68 µM (Table 3.1). MMA321 was almost twenty fold more potent whereas MMA307 was more than tenfold more potent compared to sorafenib in exhibiting their cytotoxic effect. Therefore, in the subsequent experiments the IC_{50} concentrations of MMA307 and MMA321, a highly effective and low toxicity dose was used. Mechanisms pertaining to programmed cell death, apoptosis, and that involved in inhibition of proliferation were investigated.

3.4.3   Estrone analogs induce apoptosis in TNBC cells

3.4.3.1   RealTime-Glo™ Annexin V assay

The apoptosis-inducing effect of MMA307 and MMA321 in MDA-MB-468 cells were evaluated by RealTime-Glo™ Annexin V apoptosis and necrosis luminescent assay. The detection reagent contains Annexin V-LgBiT and Annexin V-SmBiT (NanoBiT) fusion proteins and a profluorescent DNA dye. In healthy cells, most of the phosphatidylserine (PS) is confined to the inner leaflets of the cell membrane, fewer fusion proteins bind to PS and less luminescence is recorded. In apoptotic cells, PS is exposed to the outer leaflet of the cell membrane, more fusion proteins bind to PS and increased luminescence is measured. Increased luminescence corresponds to increased apoptosis. Exposing MDA-MB-468 cells to MMA307 and MMA321, resulted in increased apoptosis in a dose-dependent manner (Figure 3.6 A). Notably, both compounds induced apoptosis in MDA-MB-468 cells within 12 hrs of drug incubation similar to the positive control, camptothecin.

3.4.3.2   Morphological analysis with fluorescence microscopy

The morphological changes in cell nuclei of MDA-MB-468 cells within 12 hrs after treatment with MMA307 and MMA321 showed significant shape alterations when compared to 0.05% DMSO control. As shown in Figure 3.6 B, the control or untreated cells appeared as intact oval shape and the nuclei were stained with a less bright blue fluorescence (due to the Hoechst 33342 dye). Cells treated with tested compounds exhibited typical features of apoptosis such as cell shrinkage, chromatin condensation, and nuclear fragmentation in multiple, segregated bodies, the formation of apoptotic bodies, and cell decrement. The apoptotic nuclei clearly showed highly condensed or fragmented chromatin that was uniformLy fluorescent. MMA307 and MMA321, as well as sorafenib treatments, resulted in increased apoptotic cells (condensed chromatin, indicated by arrows) compared to the DMSO control.

3.4.3.3   Estrone analogs induce apoptosis via the mitochondrial pathway

To further study the effects of MMA307 and MMA321 on apoptosis, ICW assay was performed to detect changes in protein expression involved in the apoptosis pathway. As shown in Figure 4 and 5, exposure of MDA-MB-468 cells to the compounds resulted in increased expressions of cytochrome C and apoptotic protease activating factor 1 (APAF1), which are markers of mitochondrial apoptosis. Furthermore, we observed decreased

expression of B-Cell Lymphoma 2 (Bcl-2) protein when TNBC cells were treated with both compounds (Figure 3.7). Also, when the compounds were administered to cells an elevated expression caspase-3 and -9 were increased post-treatment with MMA307 and MMA321 (Figure 3.8). All these results indicate that MMA307 and MMA321 could effectively induce apoptosis in MDA-MB-468 cells via the mitochondrial pathway and in a caspase-dependent manner.

3.4.4 Estrone analogs inhibit the proliferation of MDA-MB-468 cells through G_1 phase cell cycle arrest

To elucidate the antiproliferative effects of MMA307 and MMA321 on MDA-MB-468 cells, the cell cycle distribution was the first mechanism examined by propidium iodide (PI) stain and distinct populations analyzed by flow cytometry. Cell-cycle population distribution of MDA-MB-468 cells exposed to DMSO (Figure 3.9 A) showed an average of 3% in the G_0/G_1 phase, 1.5% in the S phase, and 95.5% in the G_2/M phase. Treating MDA-MB-468 cells with sorafenib resulted in enrichment of cells within G_0/G_1 phase, 15.43%. Also, accumulation of cells in the S phase was 4.35% and G_2/M phase 81.59%. Exposure of cells to MMA307 resulted in significant accumulation of cells within G_0/G_1 phase, an average of 42.3%; there was decrease enrichment of cells in the G_2/M phase, an average of 47.2% was observed. Similarly, exposure of MDA-MB-468 cells to MMA321 resulted in significant enrichment of cells within the G_0/G_1 phase of the cell cycle. It arrested an average of 58.11% of cells in the G_0/G_1 phase and a lower number of cells (an average of 29%) in the G_2/M phase.

3.4.4.1 G_1 phase cell cycle associated proteins are modulated post estrone analogs exposure

As a result of the significant ($p < 0.05$) cell cycle arrest induced by the estrone analogs, we analyzed the expression levels of known G_0/G_1 phase cell cycle proteins. In-Cell Western approach was adopted to establish our findings. Cyclin D1 plays a vital role in regulating the progression of cell cycle within the G_1 phase. We observed that MMA307 and MMA321 administration towards MDA-MB-468 cells resulted in the suppression of cyclin D1 expression levels in a concentration-dependent manner within 12 hrs (Figure 3.9B). These findings are in line with the significant G_0/G_1 phase cell cycle arrest recorded above.

3.4.5 EGFR and its downstream signaling pathways are inhibited after TNBC exposure to estrone analogs

We evaluated the expression levels of total and activated (phosphorylated) forms of EGFR by ICW (Figure 3.10). Higher levels of EGFR were detected in the EGF only treated cells compared to the compound plus EGF treated cells, depicting EGFR downregulation. Similarly, levels of phosphorylated EGFR (Y1068) were also increased in the EGF only treated cells compared to EGF plus compound treated cells. EGFR and phosphorylated EGFR (Y1068) expression levels were downregulated in a concentration-dependent manner post MMA307 and MMA321 exposure. The purpose of EGFR autophosphorylation within tyrosine residues, especially Y1173 and Y1068, is to activate

signaling pathways such as PI3K/AKT and RAS/MAPK pathways involved in cell proliferation, survival and angiogenesis (Romano *et al*, 2011). Next we investigated the activation of these pathways by quantifying activated (phosphorylated) forms of ERK1/2- and AKT-associated pathway proteins. Decreased amounts of phospho-ARaf (S299) and phospho-ERK1/2 (T202/Y204) (Figure 7) were clearly detected in MDA-MB-468 cells when exposed to MMA307 and MMA321 together with 100 nM of EGF in a dose-dependent manner. Similarly, phospho-AKT (S473), phospho-mTOR (S2448) and phospho-p70S6Kα (S411) expression levels (Figure 3.11) were downregulated in concentration-dependent manner in the presence of estrone analogs and 100nM of EGF. Based on the low expression levels of activated ERK- and AKT-associated proteins, RAS/MAPK and PI3K/AKT signaling pathways were downregulated in MDA-MB-468 cell line upon estrone analogs treatment. This could be one of the key reasons underlying the observed growth inhibition in TNBC cells.

3.5   Discussion

This study revealed that estrone analogs exhibit cytotoxic killing in TNBC cells through inhibition of cell proliferation and induction of apoptosis. The mechanisms of antiproliferation involved cell cycle arrest, suppression of EGFR and blocking of its downstream RAS/MAPK and PI3K/AKT pathways whereas the mechanism of cell death studied was that of mitochondrial apoptosis. Therefore, MMA307 and MMA321 have a good antitumor effect against TNBC cells *in vitro*.

Installing various modified cucurbitacin pharmacophores and other moieties onto the estrone scaffold yielded unique hybrid analogs. Among these MMA307, containing sulfamoyl and paranitrophenyl groups, and MMA321, possessing paranitrophenyl and methoxy substituents, exhibited acceptable potency *in silico* and stronger cytotoxic effects *in vitro*. Previous studies by Stamos *et al*, 2002 suggested that hydrogen bonding towards the amino acid residue, MET 769A, alongside other hydrophobic interactions in the EGFR kinase domain are important for a drug to elicit cytotoxic effects. Our findings revealed that the reference compound, erlotinib, showed hydrogen bonding from the pyrimidine-N_2 towards MET 769A (Figure 3.2) and registered a lower consensus score (a measure of effective binding and drug potency). However, examining the analog MMA307, enriched with pharmacophores capable of donating and accepting hydrogen bonds within the EGFR kinase domain, we observed hydrophobic-hydrophobic (cation-π) interactions between the steroidal aromatic ring and the amino acid residue, LYS721A (Figure 3.3). Also, analyzing the analog MMA321 within the EGFR binding site revealed hydrogen bonding from the nitro-O on the substituent group towards the amino acid residue THR830A (Figure 3.4). The hydrogen bonding exhibited by MMA321 towards THR830A and the cation-π interactions exhibited by MMA307 towards LYS721A demonstrate a strong and unique binding mode and suggest that interactions with THR830A and LYS721A residues in the EGFR kinase domain may be key in the estrone analogs achieving *in vitro* and *in vivo* drug potency. These results could provide a molecular level foundation to illustrate that MMA307 and MMA320 can bind well towards the EGFR kinase active site. These findings

are further supported by their lower IC_{50} concentrations compared to sorafenib from the cell viability assay *in vitro*.

Estrone analogs have been exploited as anticancer agents in clinical trials and basic research for some time now. Nolte *et al*, 2018 report that 2-methylestradiol and its sulfamoyl derivative induced mitochondrial apoptosis in radiation-exposed MCF-7 (model for estrogen positive breast cancer) cells. Also, studies by Sara, 2018 documented that estrone analogs with cucurbitacin pharmacophores inhibited the proliferation of hepatocellular carcinoma via induction of apoptosis and suppression of EGFR and its downstream MAP kinase signaling. In addition, estrone derivatives synthesized by our research group, especially those bearing cucurbitacin side chains and that possessing nitric oxide-releasing capabilities have been documented to exhibit potent cytotoxic effects against distinct cancers (Ahmed *et al*, 2017; Elshaier *et al*, 2017; Ahmed *et al*, 2014; Kopel *et al*, 2013; Abou-Salim *et al*, 2019). Also, Felix and colleagues (unpublished data) revealed that these new estrone hybrids inhibited the proliferation of EGFR-wild-type NSCLC (NCIH226 cells) via suppressing EGFR and MAP kinase signaling. Furthermore, Verwey *et al*, 2016 reported that sulphamoylated estradiol derivative exhibited cytotoxic effects through the induction of autophagy in MCF-7 and MDA-MB-231 cells. From all the studies involving the use of estrone analogs, only Verwey and colleagues, 2016 have tested estradiol analogs against MDA-MB-231 cells (a model for TNBC cells) for their autophagic cell death effects. The current study sought to investigate the anticancer potential of novel estrone hybrids against MDA-MB-468 cells. MDA-MB-468 cell line is

a typical TNBC model that possesses stronger drug resistance and has higher rates of recurrence and metastasis due to overexpression of EGFR. Currently, there is no targeted agent approved for the treatment of TNBC. From this research, we showed for the first time that most of our estrone hybrids were more potent that reference compound sorafenib. Especially, MMA307 and MMA321 were over 10-fold and 20-fold, respectively potent than the positive control sorafenib (Table 3.1).

Apoptosis mechanism is a complex process of programmed cell death that is regulated by different cell signals. This mechanism is initiated and executed through two major pathways, namely, the extrinsic and intrinsic pathways (Elmore, 2007). The extrinsic pathway is triggered by extracellular ligands binding to cell surface death receptors. The intrinsic pathway is initiated by a variety of intracellular factors generated when cells are stressed. The BCL-2 family of proteins play a key role in regulating the intrinsic pathway. BCL-2 protects the cell against apoptosis, but BAX and the BCL-2 homologous killer, BAK, induce cellular apoptosis through the mitochondria (Alberts *et al*, 2002). This requires the release of cytochrome c which activates APAF1 through the formation of an apoptosome. Both the intrinsic and extrinsic pathways have a final common pathway, which involves activation of the effector caspases (caspase-3/7) by initiator caspases (caspase 8 for extrinsic pathway and caspase 9 for intrinsic pathway) (Dewangan *et al*, 2018). Finally, caspase 3 cleaves and inactivates PARP-poly (ADP-ribose) polymerase-which is important for damaged DNA repair (Soldani and Scovassi, 2002). Therefore, the expression of BCL-2, cytochrome c, active caspase-3 and 9, cleaved PARP become

important mitochondrial apoptosis indicators. In this research, we first analyzed PS flipping which occurs during early apoptosis. Viable cells contain phosphatidylserine (PS), located within the inner leaflet of the cell membrane. PS flips to the outer leaflet of the lipid bilayer and becomes exposed on the cell surface during apoptosis. This allows for the binding of annexin V dye. Analyzing MDA-MB-468 treated cells with real-time annexin V assay, it was observed that MMA307 and MMA321 induced PS translocation within 12 hrs in a dose-dependent fashion when compared to camptothecin, positive control (Figure 3.6A). Subsequently, morphological changes, thus chromatin condensation, induced by the estrone analogs were analyzed by fluorescence microscopy after staining cells with Hoechst 33342. Chromatin condensation paralleled by DNA fragmentation is one of the most important criteria which are used to identify apoptotic cells. Both MMA307 and MMA321 as well as sorafenib, clearly induced chromatin condensation within 12 hrs of drug treatment (Figure 3.6 B). Furthermore, we demonstrated that cytochrome c, APAF1, active caspase-3 and -9 expression levels were increased (Figures 3.7 and 3.8) but BCL-2 expression levels were decreased (Figure 3.7) in MMA307 and MMA321 treated cells. These findings suggest that these compounds induced mitochondrial or intrinsic apoptosis in MDA-MB-468 cells.

Altered cell division is a hallmark of cancer. Targeting the cell cycle has proven to be a key strategy in treating breast cancer, and several drugs targeting this pathway have been approved by the FDA (Lo *et al*, 2017). The interaction among cyclins, cyclin-dependent kinases (CDKs) and cyclin-dependent kinase inhibitors (CKIs) play a fundamental role in

cell cycle progression (Uroz *et al*, 2018). Cyclin D and its specific CDKs are the crucial regulators in the G_1 phase of cell division. It has been documented that cyclin D is an oncogene whose overexpression may be associated with poor prognosis in TNBC (Ly *et al*, 2017). Cells will usually synthesize cyclin D in response to the mitogenic stimulation. An increased amount of cyclin D interacts with CDK4/6 to phosphorylate the inhibitory protein retinoblastoma (Rb) in the G_1 phase, which leads to the dissociation of Rb from the transcription factor E2F and promote E2F-dependent transcription. E2F activation could promote a series of subsequent events that favor DNA replication and expression of cyclin E and CDK2 (Bertoli *et al*, 2013) which transitions cells into the G_2/M phase. Phosphorylating cyclin D by cyclin-dependent kinase inhibitors, p^{21} and p^{27}, leads to cell cycle arrest within the G_1 phase. In the present study, the expression levels of cyclin D1 were downregulated in MDA-MB-468 cells after MMA307 and MMA321 treatment (Figure 3.9 B), suggesting that their significant G_0/G_1 phase cell cycle arrest (Figure 3.9 A) was at least partially mediated via suppression of cyclin D1. It must be mentioned that while the status of selected G_1 phase cell cycle activator, cyclin D1, was analyzed in this study, the functions of other G_1 phase proteins were likely modulated as well, and therefore, the antiproliferative effects of the estrone analogs reported here may not be solely due to these proteins.

EGFR is a central regulator of cell proliferation through multiple downstream targets. Dysregulation of EGFR signaling has been implicated in cancer. Phosphorylation of EGFR on Y1068 creates docking sites for the adaptor protein, Grb2, leading to activation of the

MAPK/ERK cascade, and a binding site for Gab1, which recruits the p85 subunit of phosphatidylinositol 3-kinase (PI 3-kinase), leading to AKT activation (Yamaoka *et al*, 2011). EGFR is overexpressed and genetically amplified in one-third of metastatic or recurrent breast cancers, and this has been inversely correlated with relapse-free survival (Nagaria *et al*, 2017). The Ras/MAPK pathway is initiated through the promotion of Ras binding to guanosine triphosphate (GTP), which in turn activates RAF kinases MAPK/extracellular signal-regulated kinases (MEK), and ERK (Slomovitz and Coleman, 2012). Activated ERK is thought to translocate into the nucleus, where it phosphorylates and activates transcription factors like elk-1, c-jun, fos, etc. that regulate the cell cycle. The PI3K/Akt pathway is an important regulator of cell growth and survival through multiple downstream targets and it has been shown that AKT could promote the activation of mTOR through either mTORC1 or mTORC2 complex, which in turn, activates the p70S6 kinase and promote cell growth (Manning and Toker, 2017). In the present study, MMA307 and MMA321 decreased the expression of EGFR and activated EGFR (Y1068) (Figure 3.10). Also, the expression levels of phosphorylated ARaf, phosphorylated ERK1/2, phosphorylated AKT, phosphorylated mTOR and phosphorylated p70S6 kinase were reduced upon MDA-MB-468 cells exposure to MMA307 and MMA321 (Figures 3.10 and 3.11). Our findings reveal that MMA307 and MMA321 might have inhibited TNBC cells growth via impacting EGFR, Raf/MAPK, and Akt/mTOR signaling pathway.

3.6   Conclusion

The present study gives preliminary convincing results on novel estrone analogs favorable cytotoxic effects against TNBC *in vitro*. However, the mechanisms by which these novel estrone analogs show anticancer effects and its direct target have never been exploited before, which prompted further investigations. This study revealed that the estrone analogs induced mitochondrial apoptosis, arrested G_1 phase of the cell cycle, suppressed activated EGFR and its downstream MAPK and AKT signaling. To the best of our knowledge, there was no report about estrone analogs with modified cucurbitacin side chains having potential applications in treating TNBC which possesses a high risk of brain metastasis. Our work lays a foundation for using these new estrone analogs to treat TNBC, which currently lacks any effective treatment options. Therefore, our results suggested that MMA307 and MMA321 might be potential therapeutic agents for treating TNBC, which deserves further investigation.

3.7 References

Abou-Salim, M. A., Shaaban, M. A., El Hameid, M. K. A., Elshaier, Y. A., and Halaweish, F. (2019). Design, synthesis and biological study of hybrid drug candidates of nitric oxide releasing cucurbitacin-inspired estrone analogs for treatment of hepatocellular carcinoma. *Bioorganic Chemistry*, 85, 515-533.

Acheampong, F., Reilly, J., Larbie, C., Spencer, M., Gunderson, K., Appiah-Opong, R., and Voytek, S. (2017). Methoxy-flavones identified from Ageratum conyzoides induce caspase-3 and-7 activations in Jurkat cells. *Journal of Medicinal Plants Research*, 11(38), 583-590.

Acheampong, F., Tuffour, I., Larbie, C., Appiah-Opong, R., and Arthur, F. K. (2015). In vitro antioxidant and anticancer properties of Hydroethanolic extracts and fractions of Ageratum conyzoides. *European Journal of Medicinal Plants*. 7(4), 205-214.

Ahmed, M. S., El-Senduny, F., Taylor, J., and Halaweish, F. T. (2017). Biological screening of cucurbitacin inspired estrone analogs targeting mitogen-activated protein kinase (MAPK) pathway. *Chemical Biology and Drug Design*, 90(3), 478-484.

Ahmed, M. S., Kopel, L. C., and Halaweish, F. T. (2014). Structural Optimization and Biological Screening of a Steroidal Scaffold Possessing Cucurbitacin-Like Functionalities as B-Raf Inhibitors. *ChemMedChem*, 9(7), 1361-1367.

Alberts, B., Johnson, A., Lewis, J., Raff, M., Roberts, K., and Walter, P. (2002). Programmed cell death (apoptosis). In Molecular Biology of the Cell. 4th edition. Garland Science.

Amr, A. E. G. E., Elsayed, E. A., Al-Omar, M. A., Badr Eldin, H. O., Nossier, E. S., and Abdallah, M. M. (2019). Design, Synthesis, Anticancer Evaluation and Molecular Modeling of Novel Estrogen Derivatives. *Molecules*, 24(3), 416.

Berrocal, J. K. (2017). Current Approaches to Triple-Negative Breast Cancer. *American Journal of Hematology/Oncology®*, 13(6).

Bertoli, C., Skotheim, J. M., and De Bruin, R. A. (2013). Control of cell cycle transcription during G1 and S phases. *Nature reviews Molecular Cell Biology*, 14(8), 518.

Botes, M., Jurgens, T., Riahi, Z., Visagie, M., van Vuuren, R. J., Joubert, A. M., and van den Bout, I. (2018). A novel non-sulphamoylated 2-methoxyestradiol derivative causes detachment of breast cancer cells by rapid disassembly of focal adhesions. *Cancer Cell International*, 18(1), 188.

Bray, F., Ferlay, J., Soerjomataram, I., Siegel, R. L., Torre, L. A., and Jemal, A. (2018). Global cancer statistics 2018: GLOBOCAN estimates of incidence and mortality worldwide for 36 cancers in 185 countries. *CA: a Cancer Journal for Clinicians*, *68*(6), 394-424.

Chen, Q. Y., and Costa, M. (2018). PI3K/Akt/mTOR signaling pathway and the biphasic effect of arsenic in carcinogenesis. *Molecular Pharmacology*, 94(1), 784-792.

Cortazar, P., Zhang, L., Untch, M., Mehta, K., Costantino, J. P., Wolmark, N., and Swain, S. M. (2014). Pathological complete response and long-term clinical benefit in breast cancer: the CTNeoBC pooled analysis. *The Lancet*, 384(9938), 164-172.

Dai, X., Li, Y., Bai, Z., and Tang, X. Q. (2015). Molecular portraits revealing the heterogeneity of breast tumor subtypes defined using immunohistochemistry markers. *Scientific Reports*, 5, 14499.

Dewangan, J., Srivastava, S., Mishra, S., Pandey, P. K., Divakar, A., and Rath, S. K. (2018). Chetomin induces apoptosis in human triple-negative breast cancer cells by promoting calcium overload and mitochondrial dysfunction. *Biochemical and Biophysical Research Communications*, 495(2), 1915-1921.

Elgazwi, S. (2018). Study of Anti-proliferative Activity of Cucurbitacins Inspired Estrone Analogs on Hepatocellular Carcinoma. Electronic *Theses and Dissertations*. 2640. https://openprairie.sdstate.edu/etd/2640

Elmore, S. (2007). Apoptosis: a review of programmed cell death. *Toxicologic Pathology*, 35(4), 495-516.

Elshaier, Y. A., Shaaban, M. A., El Hamid, M. K. A., Abdelrahman, M. H., Abou-Salim, M. A., Elgazwi, S. M., and Halaweish, F. (2017). Design and synthesis of pyrazolo [3, 4-d] pyrimidines: Nitric oxide releasing compounds targeting hepatocellular carcinoma. *Bioorganic and Medicinal Chemistry*, 25(12), 2956-2970.

Feng, Z., Xia, Y., Gao, T., Xu, F., Lei, Q., Peng, C., and Wang, R. (2018). The antipsychotic agent trifluoperazine hydrochloride suppresses triple-negative breast cancer tumor growth and brain metastasis by inducing G0/G1 arrest and apoptosis. *Cell Death and Disease*, 9(10), 1006.

Foidart, P., Yip, C., Radermacher, J., Blacher, S., Lienard, M., Montero-Ruiz, L., and Coibion, M. (2019). Expression of MT4-MMP, EGFR, and RB in Triple-Negative Breast Cancer Strongly Sensitizes Tumors to Erlotinib and Palbociclib Combination Therapy. *Clinical Cancer Research*, 25(6), 1838-1850.

Ignacio, R. M. C., Gibbs, C. R., Lee, E. S., and Son, D. S. (2018). The TGFα-EGFR-Akt signaling axis plays a role in enhancing proinflammatory chemokines in triple-negative breast cancer cells. *Oncotarget*, 9(50), 29286.

Kopel, L. C., Ahmed, M. S., and Halaweish, F. T. (2013). Synthesis of novel estrone analogs by incorporation of thiophenols via conjugate addition to an enone side chain. *Steroids*, 78(11), 1119-1125.

Larbie, C., Abotsi, P., Appiah-Opong, R., Acheampong, F., Tuffour, I., Uto, T., and Opoku-Mensah, E. (2015). Anti-proliferative effect of Amaranthus Viridis Linn. on human leukemic cell lines-a preliminary study. *International Journal of Biological and Pharmaceutical Research.* 6(3), 236-243

Lee, A., and Djamgoz, M. B. (2018). Triple negative breast cancer: emerging therapeutic modalities and novel combination therapies. *Cancer Treatment Reviews*, 62, 110-122.

Lo, Y. C., Senese, S., France, B., Gholkar, A. A., Damoiseaux, R., and Torres, J. Z. (2017). Computational cell cycle profiling of cancer cells for prioritizing FDA-approved drugs with repurposing potential. *Scientific Reports*, 7(1), 11261.

Ly, T., Whigham, A., Clarke, R., Brenes-Murillo, A. J., Estes, B., Madhessian, D., and Lamond, A. I. (2017). Proteomic analysis of cell cycle progression in asynchronous cultures, including mitotic subphases, using PRIMMUS. *Elife*, 6, e27574.

Ma, H., Ursin, G., Xu, X., Lee, E., Togawa, K., Duan, L., and Simon, M. S. (2017). Reproductive factors and the risk of triple-negative breast cancer in white women and African-American women: a pooled analysis. *Breast Cancer Research*, 19(1), 6.

Manning, B. D., and Toker, A. (2017). AKT/PKB signaling: navigating the network. *Cell*, 169(3), 381-405.

Nagaria, T. S., Shi, C., Leduc, C., Hoskin, V., Sikdar, S., Sangrar, W., and Greer, P. A. (2017). Combined targeting of Raf and Mek synergistically inhibits tumorigenesis in triple negative breast cancer model systems. *Oncotarget*, 8(46), 80804.

Nolte, E., Joubert, A., Lakier, R., Van Rensburg, A., and Mercier, A. (2018). Exposure of Breast and Lung Cancer Cells to a Novel Estrone Analog Prior to Radiation Enhances Bcl-2-Mediated Cell Death. *International Journal of Molecular Sciences*, 19(10), 2887.

Podo, F., Santoro, F., Di Leo, G., Manoukian, S., De Giacomi, C., Corcione, S., and Preda, L. (2016). Triple-Negative versus Non–Triple-Negative Breast Cancers in High-Risk Women: Phenotype Features and Survival from the HIBCRIT-1 MRI-Including Screening Study. *Clinical Cancer Research*, 22(4), 895-904.

Slomovitz, B. M., and Coleman, R. L. (2012). The PI3K/AKT/mTOR pathway as a therapeutic target in endometrial cancer. *Clinical Cancer Research*, 18(21), 5856-5864.

Soldani, C., and Scovassi, A. I. (2002). Poly (ADP-ribose) polymerase-1 cleavage during apoptosis: an update. *Apoptosis*, 7(4), 321-328.

Stamos, J., Sliwkowski, M. X., and Eigenbrot, C. (2002). Structure of the epidermal growth factor receptor kinase domain alone and in complex with a 4-anilinoquinazoline inhibitor. *Journal of Biological Chemistry*, 277(48), 46265-46272.

Stander, A., Joubert, F., and Joubert, A. (2011). Docking, synthesis, and in vitro evaluation of antimitotic estrone analogs. *Chemical Biology and Drug Design*, 77(3), 173-181.

Székely, B., Silber, A. L., and Pusztai, L. (2017). New Therapeutic Strategies for Triple-Negative Breast Cancer: Page 2 of 2. *Oncology*, 31(2).

Thomford, N., Senthebane, D., Rowe, A., Munro, D., Seele, P., Maroyi, A., and Dzobo, K. (2018). Natural products for drug discovery in the 21st century: Innovations for novel drug discovery. *International Journal of Molecular Sciences*, 19(6), 1578.

Uroz, M., Wistorf, S., Serra-Picamal, X., Conte, V., Sales-Pardo, M., Roca-Cusachs, P., and Trepat, X. (2018). Regulation of cell cycle progression by cell–cell and cell–matrix forces. *Nature Cell Biology*, 20(6), 646.

Uscanga-Perales, G. I., Santuario-Facio, S. K., and Ortiz-López, R. (2016). Triple negative breast cancer: Deciphering the biology and heterogeneity. *Medicina Universitaria*, 18(71), 105-114.

van Vuuren, R. J., Botes, M., Jurgens, T., Joubert, A. M., and van den Bout, I. (2019). Novel sulphamoylated 2-methoxy estradiol derivatives inhibit breast cancer migration by disrupting microtubule turnover and organization. *Cancer Cell International*, 19(1), 1.

Verwey, M., Nolte, E. M., Joubert, A. M., and Theron, A. E. (2016). Autophagy induced by a sulphamoylated estrone analogue contributes to its cytotoxic effect on breast cancer cells. *Cancer Cell International*, 16(1), 91.

Visagie, M., Theron, A., Mqoco, T., Vieira, W., Prudent, R., Martinez, A., and Joubert, A. (2013). Sulphamoylated 2-methoxyestradiol analogues induce apoptosis in adenocarcinoma cell lines. *PLoS One*, 8(9), e71935.

Wahba, H. A., and El-Hadaad, H. A. (2015). Current approaches in treatment of triple-negative breast cancer. *Cancer Biology and Medicine*, 12(2), 106.

Wang, P., Henning, S. M., and Heber, D. (2010). Limitations of MTT and MTS-based assays for measurement of antiproliferative activity of green tea polyphenols. *PloS One*, 5(4), e10202.

Yamaoka, T., Frey, M. R., Dise, R. S., Bernard, J. K., and Polk, D. B. (2011). Specific epidermal growth factor receptor autophosphorylation sites promote mouse colon epithelial cell chemotaxis and restitution. *American Journal of Physiology-Gastrointestinal and Liver Physiology*, 301(2), G368-G376.

Yue, X., Li, M., Chen, D., Xu, Z., and Sun, S. (2018). UNBS5162 induces growth inhibition and apoptosis via inhibiting PI3K/AKT/mTOR pathway in triple negative breast cancer MDA-MB-231 cells. *Experimental and Therapeutic Medicine*, 16(5), 3921-3928.

Tables and Figures
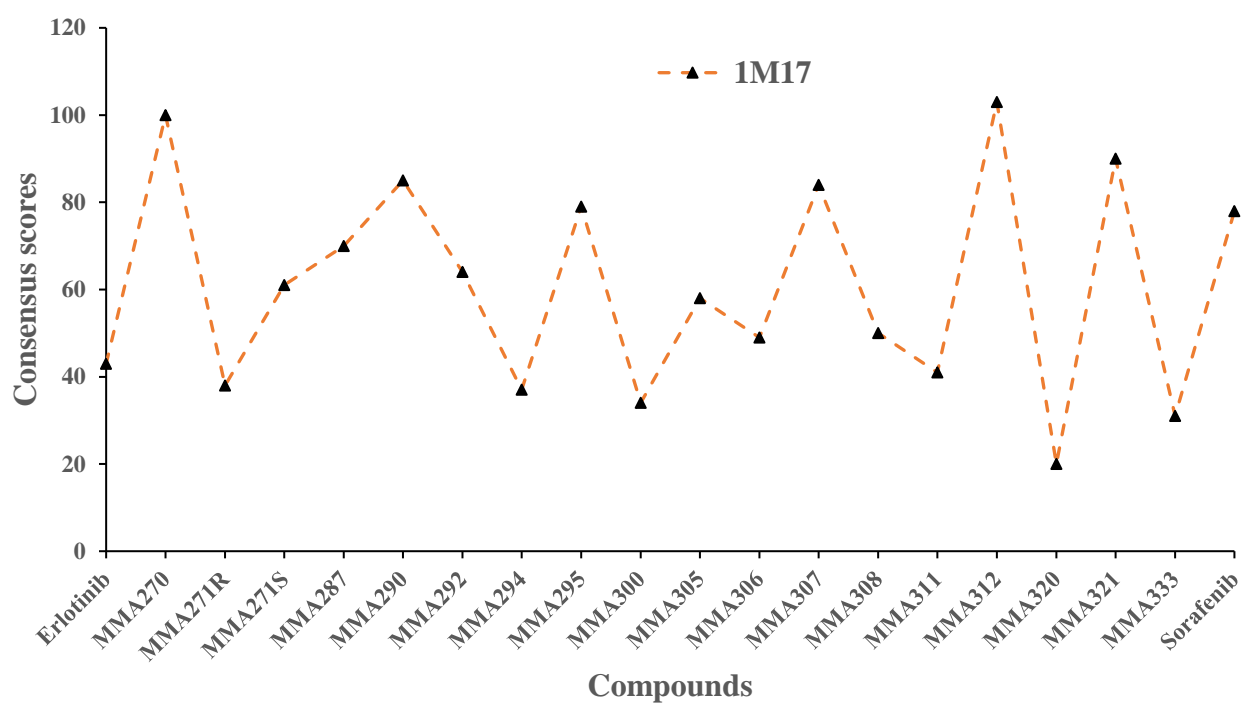
Figure 3.1 Molecular docking study of designed estrone analogs against EGFR binding site (Pdb: 1M17). Scatter plot of compounds consensus scores generated by VIDA application.
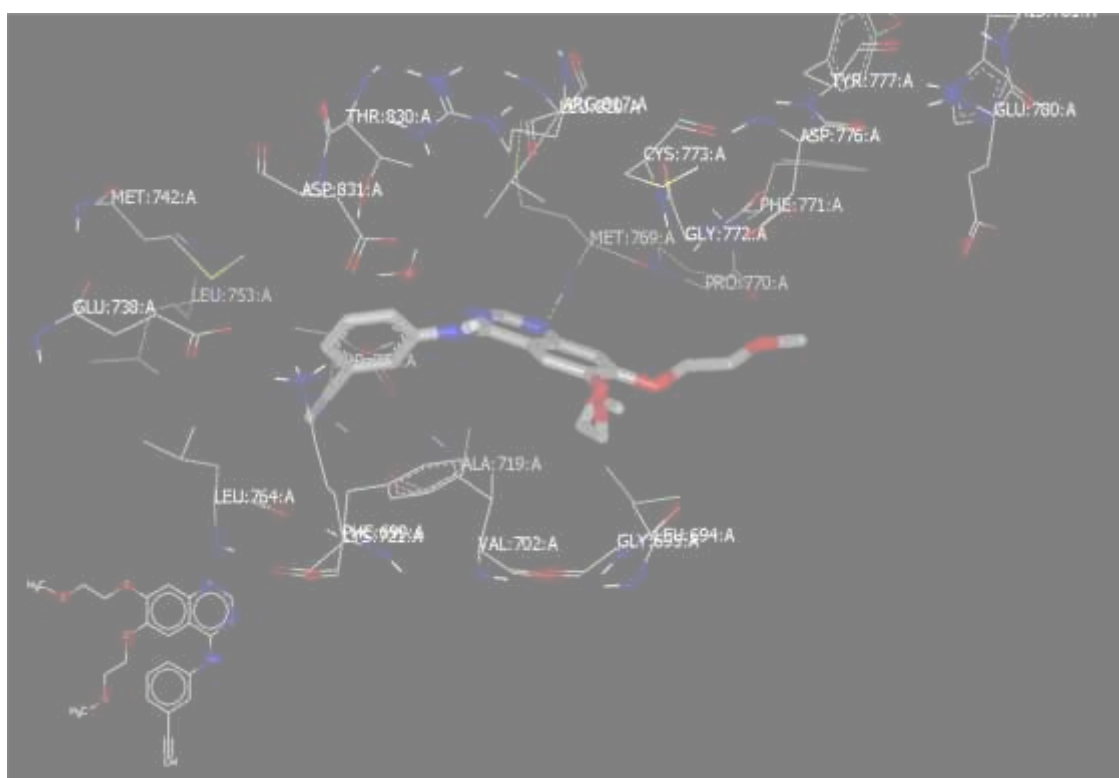
Figure 3.2 3D visual representation of reference drug, erlotinib, docked against EGFR binding site. There is hydrogen bonding from the pyrimidine-N2 of erlotinib towards MET769A of 1M17 binding site.
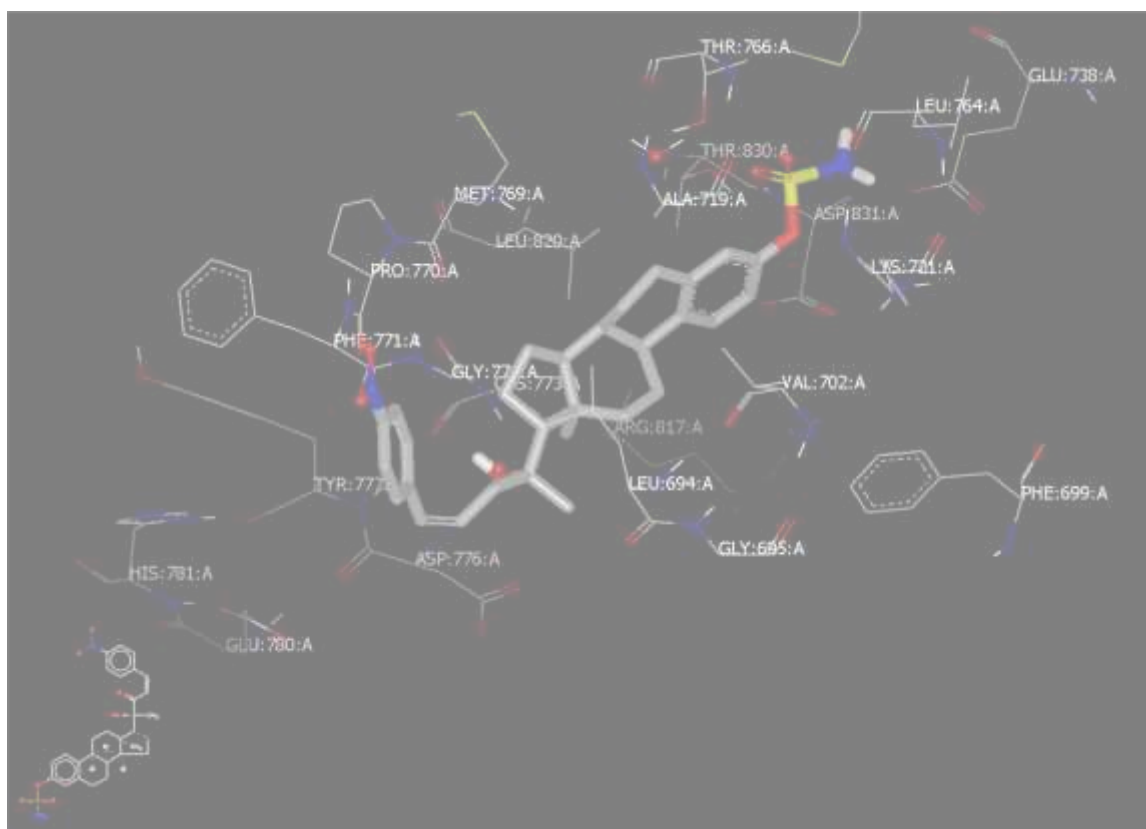
Figure 3.3 3D visual representation of MMA307 docked against EGFR binding site (Pdb: 1M17). There is cation-π interactions between LYS721A of 1M17 and the steroidal aromatic ring of MMA307.
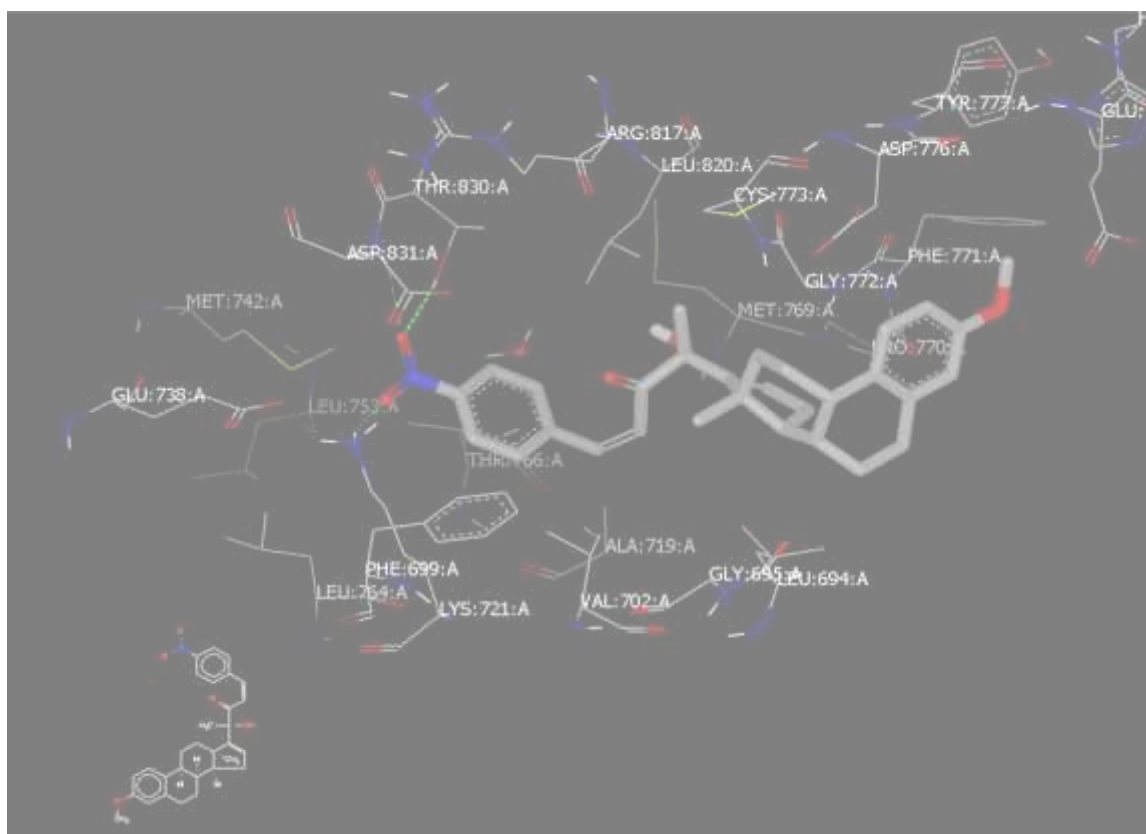
Figure 3.4 3D visual representation of MMA321 docked against EGFR binding site (Pdb: 1M17). The dashed green line shows hydrogen bonding from the Nitro-O of MMA321 towards THR830A of 1M17.

Table 3.1 Cytotoxic effects of estrone analogs against the viability of MDA-MB-468 cells in vitro.

|	IC$_{50}$ Values (µM)
Compound	**MDA-MB-468**
MMA228	$44.51 \pm 2.06^{***}$
MMA271(R)	4.39 ± 0.07
MMA271(S)	4.06 ± 0.00
MMA287	$2.51 \pm 0.12^{**}$
MMA290	$24.95 \pm 0.05^{***}$
MMA292	$> 50^{***}$
MMA294	5.48 ± 0.18
MMA295	$2.98 \pm 0.17^{**}$
MMA300	$0.89 \pm 0.10^{***}$
MMA305	$27.00 \pm 3.56^{***}$
MMA306	9.43 ± 0.07
MMA307	$0.85 \pm 0.00^{***}$
MMA308	$34.68 \pm 0.59^{***}$
MMA311	8.82 ± 0.08
MMA312	7.45 ± 0.09
MMA320	$1.71 \pm 0.01^{***}$
MMA321	$0.56 \pm 0.01^{***}$
MMA323	> 50
MMA327	$49.81 \pm 4.50^{***}$
MMA334	9.98 ± 0.30
Sorafenib	10.09 ± 0.68

Cytotoxic activities (IC$_{50}$, µM) of estrone analogs against MDA-MB-468 cells *in vitro*. IC$_{50}$ values were calculated by non-linear regression analysis. Values represent Mean $\pm$ SD of quadruplicate experiment (n = 4). *** represent the significant differences in cytotoxic effects of estrone analogs compared to sorafenib (positive control). *** $p < 0.001$ was considered as statistically significant.
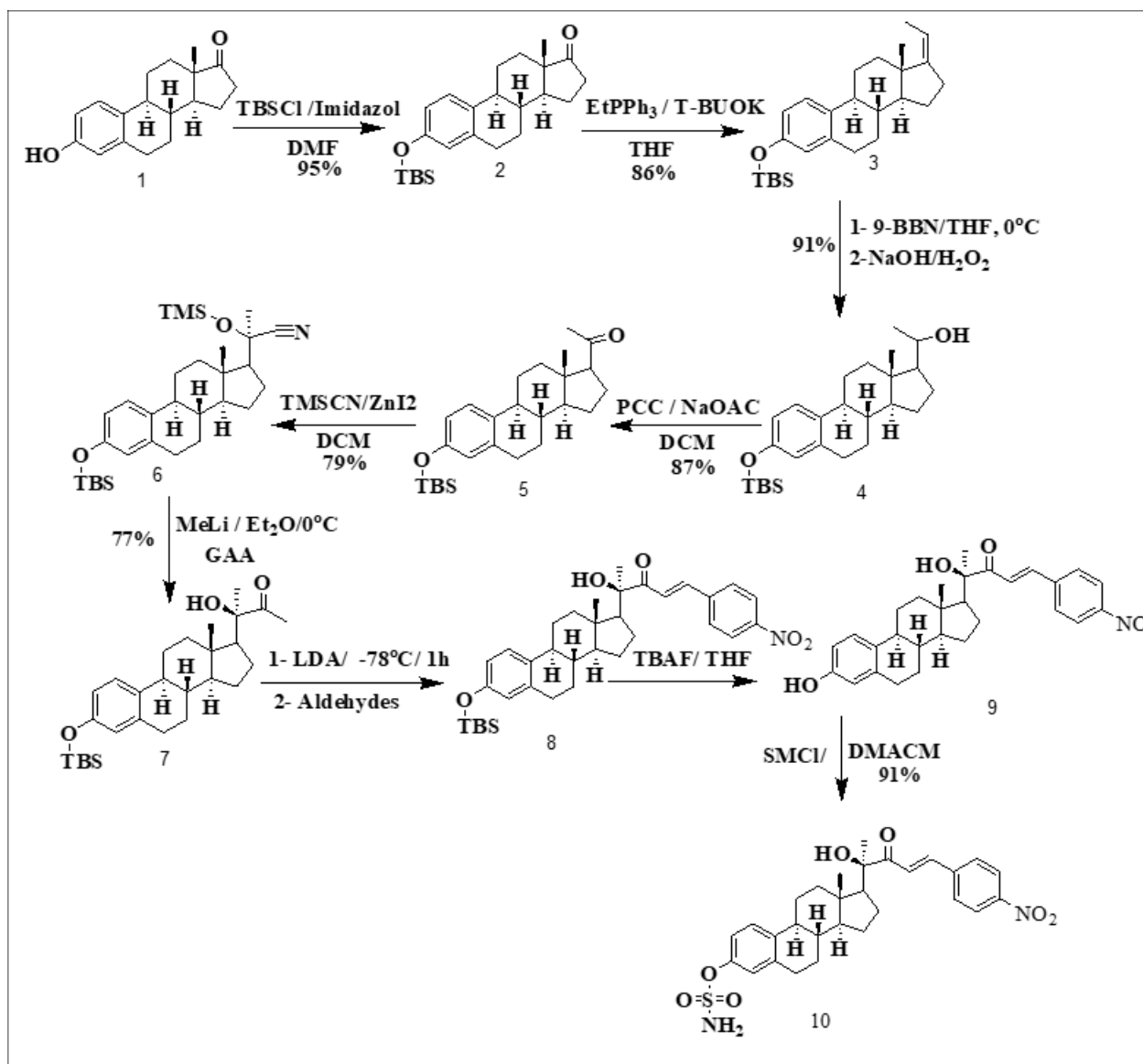
Scheme 3.1 Synthesis route for MMA307.
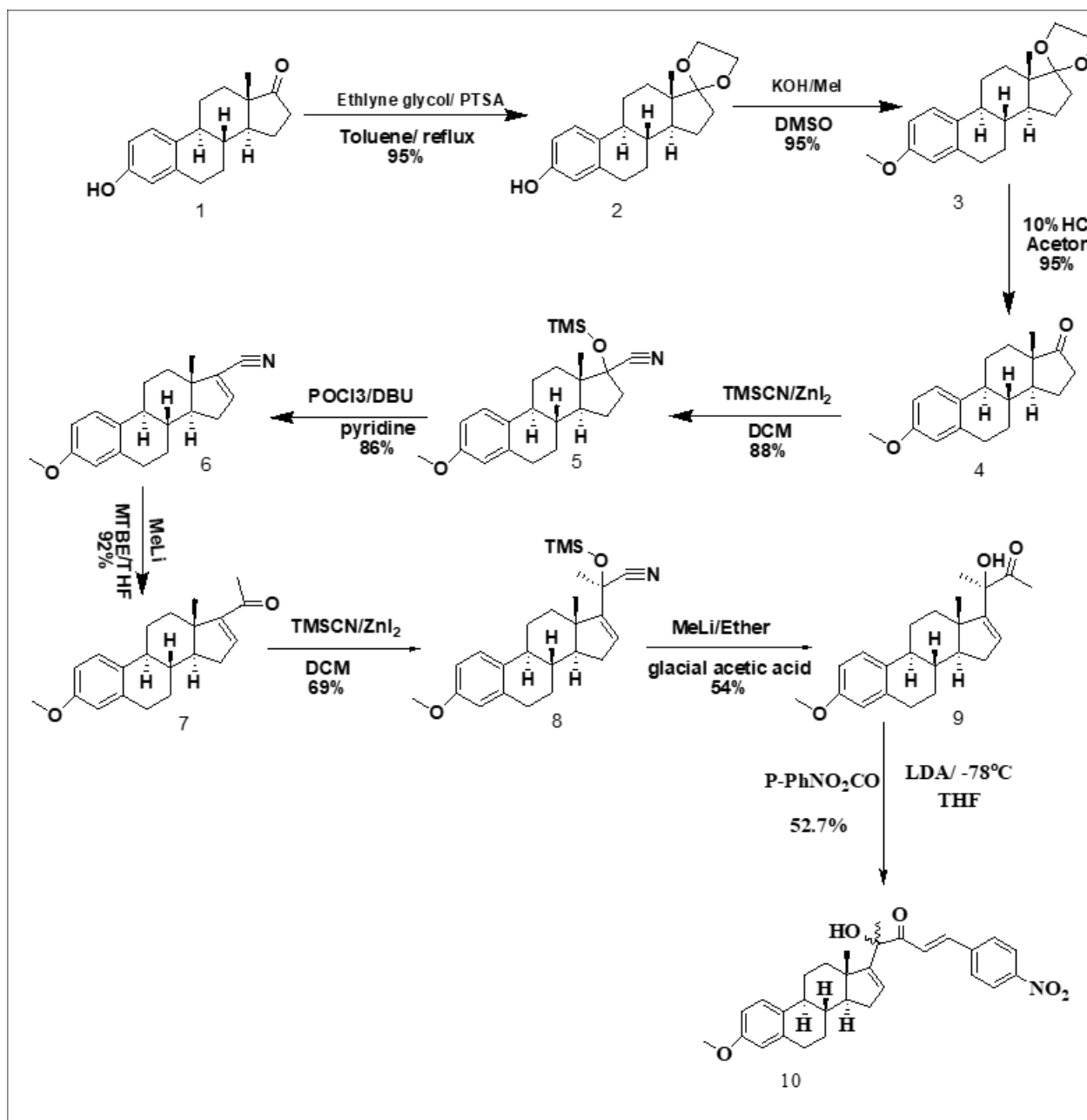
Scheme 3.2 Synthesis route for MMA321.
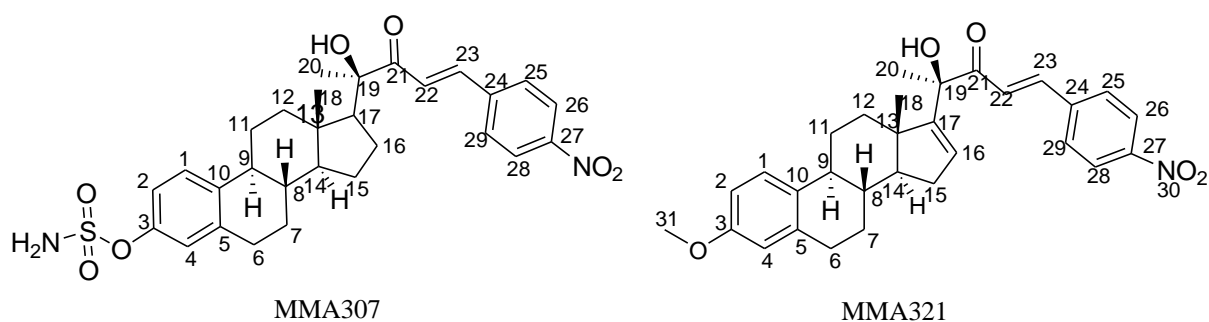
Figure 3.5 Structures of MMA307 and MMA321. MMA307 was named as (8S,9S,13S,14S,17S)-7,8,9,11,12,13,14,15,16,17-decahydro-17-((R,E)-2-hydroxy-5-(4-nitrophenyl)-3-oxopent-4-en-2-yl)-13-methyl-6H-cyclopenta[a]phenanthren-3-yl sulfamate and MMA321 named as 4-Hydroxy-4-(3-methoxy-13-methyl-7,8,9,11,12,13,14,15,16,17-decahydro-6H-cyclopenta[a]phenanthren-17-yl)-1-(4-nitro-phenyl)-pent-1-en-3-one.
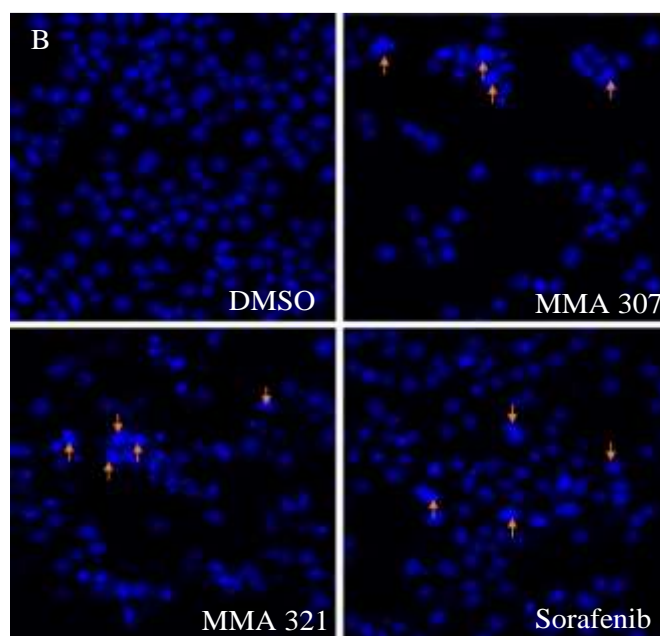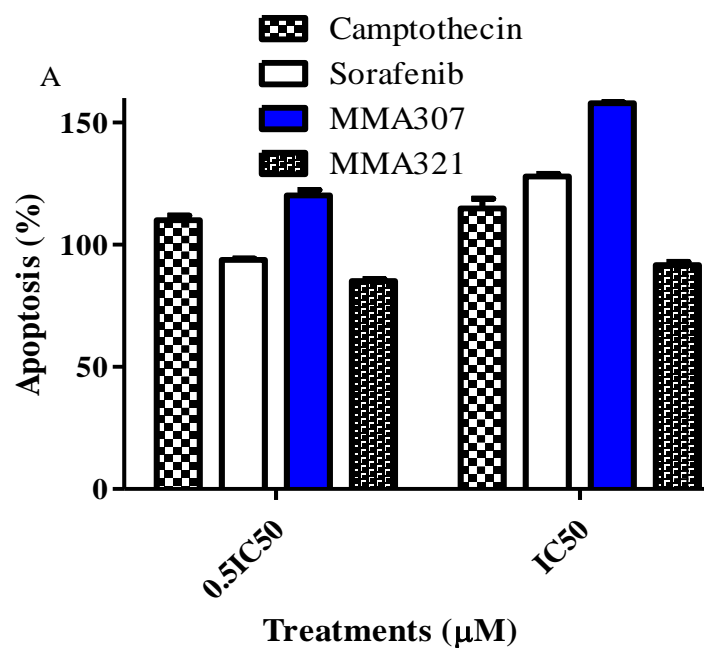
Figure 3.6 Initial apoptosis induction and chromatin condensation observed in MDA-MB-468 cells assayed by Annexin V and Hoechst staining, respectively. (A) Cells were treated with 0.5IC50 and IC50 of MMA307, MMA321 or positive control, camptothecin for 12 hrs. The cells were then incubated with Annexin V reagent and luminescence measured by a luminometer. At least two independent experiments were performed in triplicate. (B) MDA-MB-468 cells were treated with 0.05% DMSO, IC50 doses of MMA307, MMA321 or positive control, sorafenib. Apoptotic cells exhibited chromatin condensation.
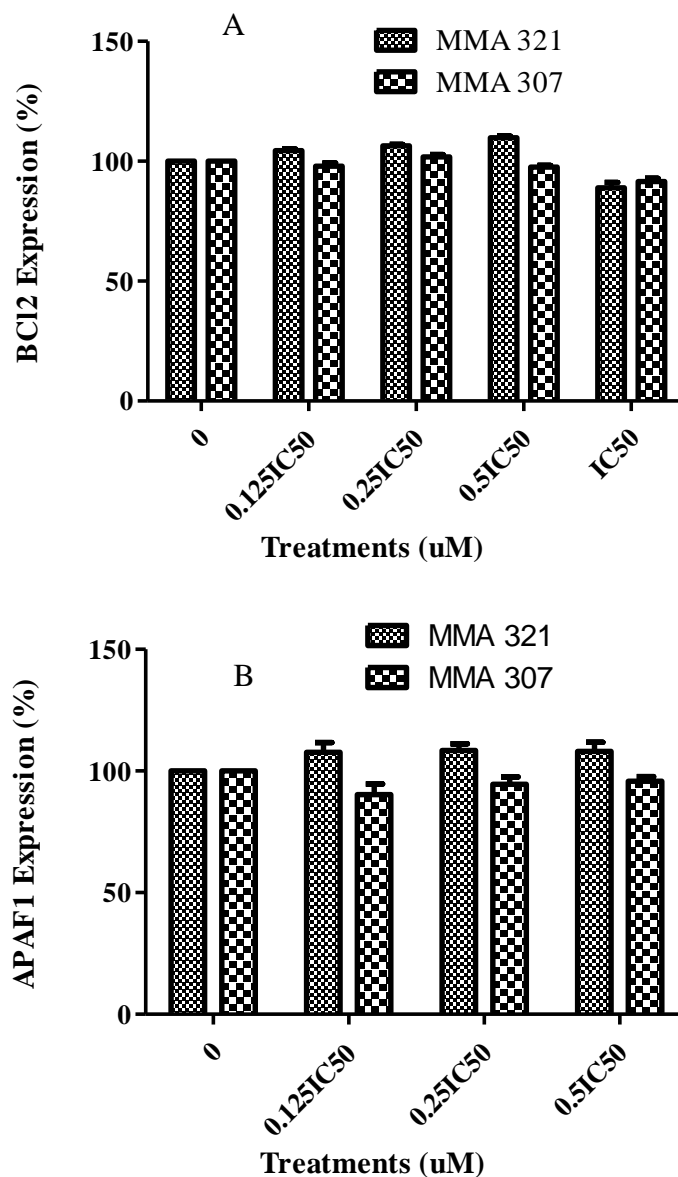
Figure 3.7 Expression levels of cytosolic BCl2 and APAF1 in MDA-MB-468 cells assayed by In-Cell Western (ICW). After treatment with MMA307 and MMA321 in a dose-dependent manner, fixed cells were incubated with specific primary antibodies for each protein. The cells were washed and incubated with goat anti-rabbit horseradish peroxidase conjugated secondary antibodies, and cell mixture was incubated with enhanced chemiluminescence substrate (Western Lightning Plus-ECL) for few minutes before chemiluminescence was measured using a Hidex Sense Beta Plus plate reader (Turku, Finland). Quantitation of proteins was completed with Excel and expression levels of APAF1 and BCl2 normalized to GAPDH. At least two independent experiments were performed. (**A**) BCl2 (**B**) APAF1.
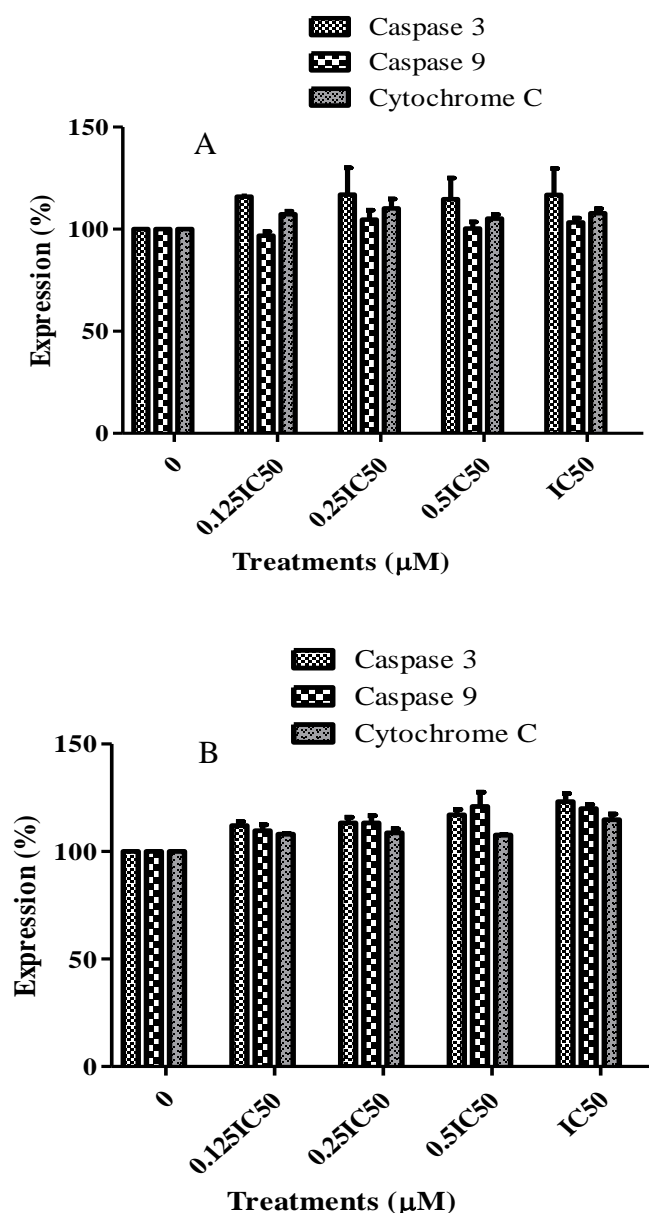
Figure 3.8 Expression levels of cytosolic BCl2 and APAF1 in MDA-MB-468 cells assayed by In-Cell Western (ICW). After treatment with MMA307 and MMA321 in a dose-dependent manner, fixed cells were incubated with specific primary antibodies for each protein. The cells were washed and incubated with goat anti-rabbit horseradish peroxidase conjugated secondary antibodies, and cell mixture was incubated with enhanced chemiluminescence substrate (Western Lightning Plus-ECL) for few minutes before chemiluminescence was measured using Hidex Sense Beta Plus plate reader (Turku, Finland). Quantitation of proteins was completed with Excel and expression levels of caspase 3, 9 and cytochrome C normalized to GAPDH. At least two independent experiments were performed. (**A**) MMA307 (**B**) MMA321
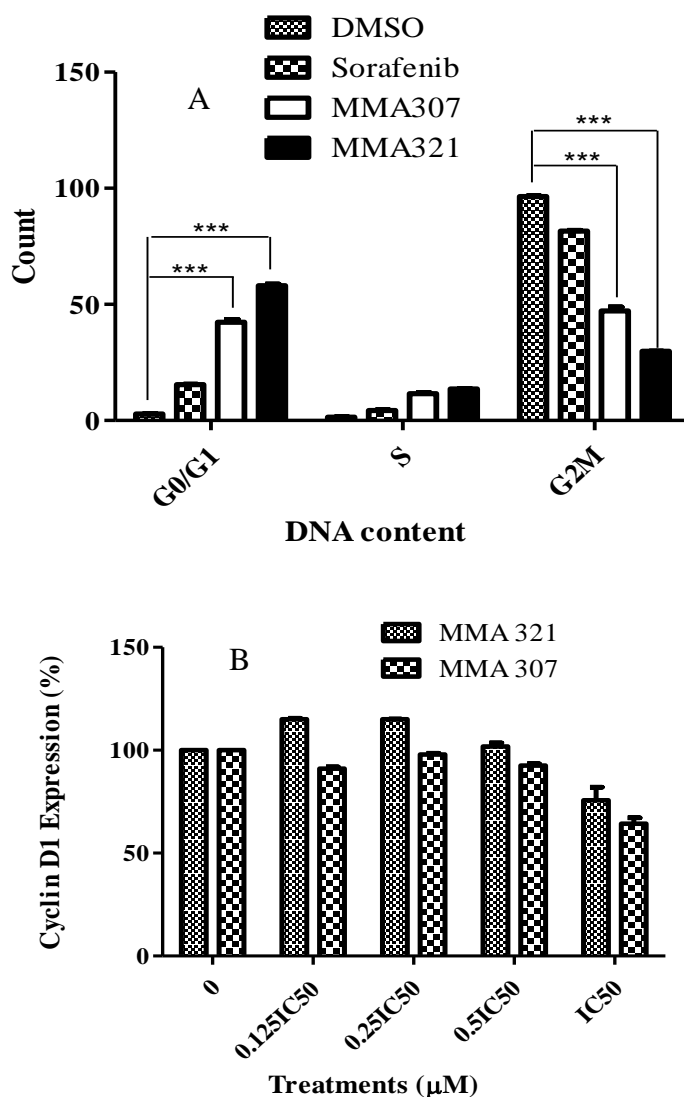
Figure 3.9 Estrone analogs exposure resulted in G_1 phase cell cycle arrest. MDA-MB-468 cells were treated with IC_{50} concentrations of estrone analogs and analyzed after 48 hrs by flow cytometry. (**A**) Distribution of cells in distinct phases of the cell cycle. MMA307, MMA321 and sorafenib, positive control, showed G_0/G_1 phase cell cycle arrest compared to the negative control, DMSO. (**B**) Cells were treated with indicated concentrations, fixed and analyzed by ICW. Wells were incubated with appropriate primary antibodies and subsequently incubated with Western Lightning Plus-ECL for few minutes before chemiluminescence was measured using Hidex Sense Beta Plus plate reader (Turku, Finland). The expression levels of cyclin D1 was normalized to GAPDH. The bar graphs for cell cycle distribution show Mean ± SD of the percentages of MDA-MB-468 cells in the indicated phases of the cell cycle (G_0/G_1, S and G_2/M). At least three independent experiments were performed. ***$p < 0.001$ significant differences in cell cycle arrest compared to DMSO control.
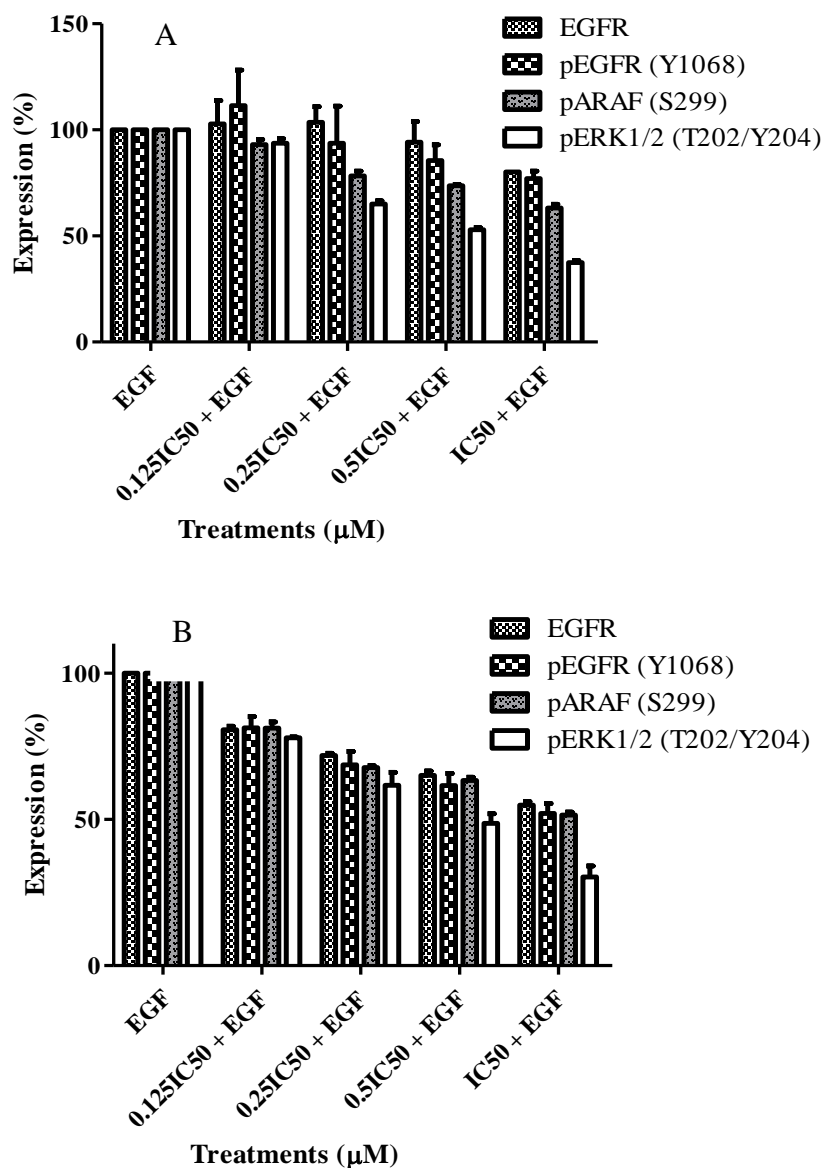
Figure 3.10 Effect of estrone analogs treatment on EGFR and downstream ERK1/2 effector molecules in MDA-MB-468 cells. Cells were treated with varying IC_{50} concentrations for 6 hrs followed by 100 nM of EGF for 1 hr, fixed and analyzed by ICW. Wells were incubated with appropriate primary antibodies, washed and incubated with goat anti-rabbit or goat anti-mouse horseradish peroxidase conjugated secondary antibodies, and cell mixture was incubated with enhanced chemiluminescence substrate (Western Lightning Plus-ECL) for few minutes before chemiluminescence was measured using Hidex Sense Beta Plus plate reader (Turku, Finland). Quantitation of proteins was completed with Excel and expression levels of EGFR, pEGFR (Y1068), pARaf (S299) and pERK1/2 (T202/Y204) normalized to GAPDH. At least two independent experiments were performed. (**A**) MMA307 (**B**) MMA321.

Figure 3.11 Effect of estrone analogs treatment on Akt signaling in MDA-MB-468 cells. Cells were treated with varying IC_{50} concentrations for 6 hrs followed by 100 nM of EGF for 1 hr, fixed and analyzed by ICW. Wells were incubated with appropriate primary antibodies, washed and incubated with goat anti-rabbit or goat anti-mouse horseradish peroxidase conjugated secondary antibodies, and cell mixture was incubated with enhanced chemiluminescence substrate (Western Lightning Plus-ECL) for few minutes before chemiluminescence was measured using Hidex Sense Beta Plus plate reader (Turku, Finland). Quantitation of proteins was completed with Excel and expression levels of EGFR, pEGFR (Y1068), pARaf (S299) and pERK1/2 (T202/Y204) normalized to GAPDH. At least two independent experiments were performed. (**A**) MMA307 (**B**) MMA321.

Chapter 4

Exposure of Triple Negative Breast Cancer cells to Novel Triazole Derived Estrone Analogs Enhance Mitochondrial Apoptosis Induction and EGFR Suppression.

4.1   Abstract

Previously estrone analogs have been examined as effective clinical agents targeting cancers including triple negative breast cancer (TNBC). However, no estrone analog nor other agent is currently approved as targeted therapy for TNBC. In this study we describe the synthesis and biological activity of novel triazole derived estrone analogs (Fz series) targeting EGFR in MDA-MB-231 (a model for TNBC) cells *in vitro*; knowledge that will pave a way for future clinical applications for these cytotoxic compounds. Molecular docking studies were carried out with OpenEye software. The MTT as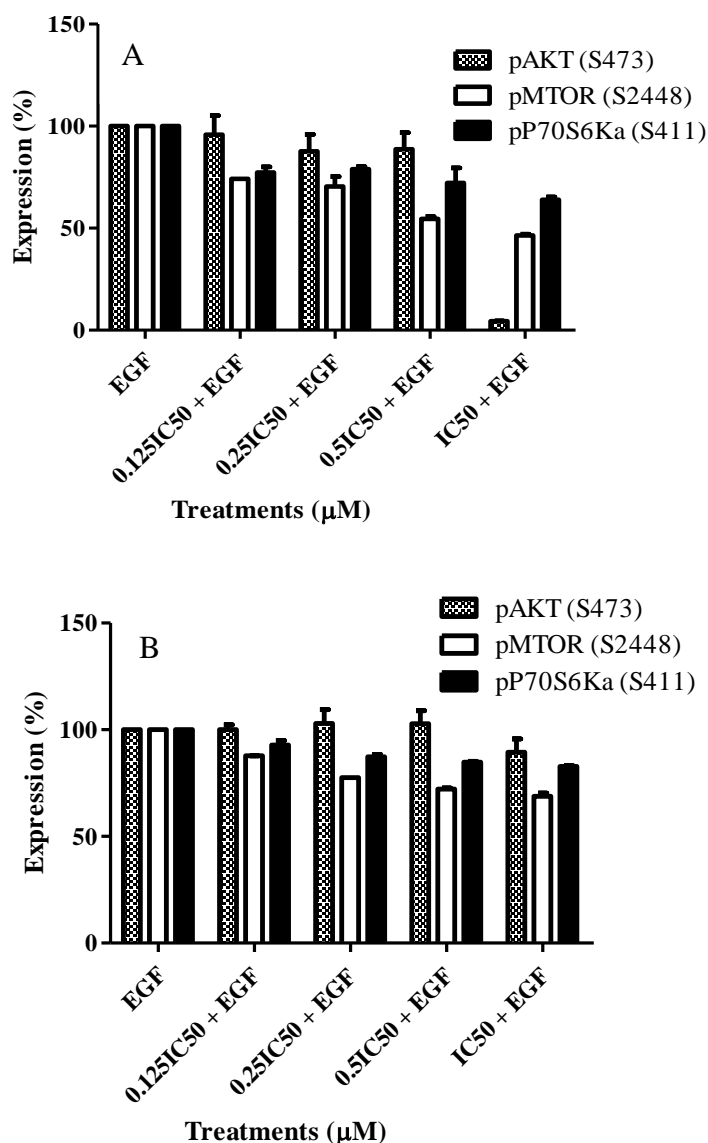say was used to perform cytotoxicity studies. Morphological changes and cell cycle arrest were carried out by microscopy and flow cytometric techniques. Annexin V assay was used to evaluate initial apoptosis induction in MDA-MB-231 cells and In-cell western assay was used to detect the expression levels of apoptotic, cell cycle and EGFR and its downstream AKT and ERK1/2 associated proteins. We demonstrated that Fz25 showed strong binding affinity towards the EGFR kinase domain (pdb code: 1M17) *in silico*, like the reference compound, erlotinib, but exhibited hydrogen bonding towards different amino acid residues. Fz200 showed medium binding affinity whereas Fz57 showed weak binding affinity. Fz25 was slightly cytotoxic than sorafenib when dosed to MDA-MB-231 cells; Fz200 had similar IC_{50} value as sorafenib whereas the IC_{50} value of Fz57 was higher. Moreover, condensed nuclei with fragmented chromatin, phosphatidylserine flip, and changes in mitochondrial membrane potential clearly indicated the role of mitochondria in estrone analogs induced apoptosis. Also, an increase in the expression of proteins of the

intrinsic pathway (Apaf1, cytochrome c, cleaved PARP1, caspase-3, -9) confirms mitochondrial apoptosis and suggest estrone analogs induced apoptosis via caspase dependent pathways. Fz25 downregulated DyrK1B and cyclin D1 expression levels contributing to G_1 phase cell cycle arrest; Fz200 and Fz57 inhibited the expression of cyclin E impacting S-phase of the cell cycle. All the compounds inhibited the expression of EGFR and activated EGFR (Y1068); Activated proteins within ERK1/2 and AKT pathways were downregulated upon compound treatment. These results for the first time indicate that triazole derived estrone analogs may be an effective therapy for MDA-MB-231 cells and further studies are needed to develop these novel candidates as targeted agents for TNBC.

4.2   Introduction

Breast cancer continues to be the most common solid tumor affecting women and is the leading cause of cancer-associated mortality in females worldwide (Bray *et al*, 2018). Also, it is a heterogeneous disease with multiple subtypes including triple-negative breast cancer (TNBC). TNBC, which is clinically defined by the absence of estrogen receptor (ER), progesterone receptor (PR) and human epidermal growth factor receptor (HER2) expressions, forms about 20% of all breast cancer cases (Guerrab *et al*, 2016). According to molecular classification, about 75% of TNBC belong to the basal-like subtype and share a great similarity with infiltrating carcinomas carrying constitutional BRCA1 mutations (Santonja *et al*, 2018; Omarini *et al*, 2018). Its pattern of spread is distinct from that for non-TNBC; TNBC has a greater propensity for brain and lung metastases, and a lower prevalence of bone metastases (Lebert *et al*, 2018). Systemic chemotherapy including anthracyclines, taxanes and platinum compounds remains the most effective treatment for TNBC patients with advanced disease. Despite the effectiveness of these treatment modalities, patients who do not respond to chemotherapy develop resistance, and a more aggressive recurrent disease results which become virtually incurable (Székely *et al*, 2017; Wahba and El-Hadaad, 2015). In contrast to other cancers, no targeted therapy is currently approved for treating TNBC.

Previous studies report that the epidermal growth factor receptor (EGFR), a central regulator of tumor progression, is frequently overexpressed and aberrantly activated in TNBC (Yan *et al*, 2018; Nakai *et al*, 2016). This is associated with aggressiveness and poor prognosis of the disease. EGFR is a transmembrane tyrosine kinase receptor member of the HER family. Autophosphorylation of the intracellular EGFR domain activates multiple downstream signaling pathways including RAS/MAPK and PI3K/Akt cascades that lead to transcriptional regulation of genes involved in cell proliferation, motility and survival. As such, EGFR is considered a key clinical target for therapeutic intervention in TNBC. PI3K/Akt pathway regulates diverse cellular functions such as cell cycle progression and apoptosis whereas deregulation of its activity contributes to cell transformation (Ornelas *et al*, 2013). Cell cycle progression is initiated by the activity of phase-specific kinase complexes comprised of cyclins and cyclin-dependent kinases (CDKs) and the role of PI3K/Akt pathway in G1 to S phase transition was proposed. Also, during cell cycle progression, Akt prevents cyclin A, D and E degradation by regulating the activity of GSK3 and can negatively influence the expression of the CDK-inhibitors, p21 and p27 (Wang *et al*, 2015; Ornelas *et al*, 2013). In addition to the cell cycle, apoptosis induction of cancer cells is one of the most important and direct ways to contribute to the suppression of malignant transformation and eliminate tumors. Phosphorylated Akt inhibits apoptosis and promotes cell survival by phosphorylation and inactivation of several target proteins including the proapoptotic proteins, Bad, Bax, and the tumor suppressor p53, a regulator of Bcl-2 as well as initiator caspases-8 and -9 and effector caspase-3 (Hossini *et al*, 2016).

In cancers like non-small cell lung cancer and colorectal cancer, anti-EGFR agents, small molecule tyrosine kinase inhibitors and monoclonal antibodies, have been developed and currently been used to treat these diseases. Monoclonal antibodies (mAbs) target the extracellular domain whereas EGFR tyrosine kinase inhibitors (EGFR-TKIs) competitively block the binding of adenosine 5′ triphosphate (ATP) to the intracellular catalytic domain of EGFR. In both cases, mAbs and EGFR-TKIs are able to inhibit EGFR activation and thus suppress its downstream signal transduction (Imai, 2006). Cetuximab and panitumumab are two mAbs that are approved for the treatment of EGFR-expressing metastatic colorectal cancer with KRAS wild-type. Osimertinib, gefitinib, afatinib and erlotinib are few selective EGFR-TKIs used as therapy for patients with metastatic non-small-cell lung cancer who carry activating EGFR mutations (Rosa *et al*, 2015; Nakai *et al*, 2016; Bartholomew *et al*, 2017). Several clinical trials report the use of already discovered anti-EGFR inhibitors, either alone or in combination with chemotherapy or other therapies, as a treatment option for TNBC patients. In phase II clinical trial, gefitinib and erlotinib used as monotherapies in metastatic and recurrent breast cancer patients yielded only a partial response of 0-3% (Baselga *et al*, 2005; Dickler *et al*, 2009). Also, in another phase II clinical trial with second-generation irreversible EGFR TKI, afatinib, in patients with metastatic TNBC, no objective responses were observed (Nakai *et al*, 2016). In a different phase II clinical studies, the combination of cetuximab plus carboplatin showed an improved response rate than cetuximab or carboplatin alone (Carey *et al*, 2012). In light of this, only minimal success has been achieved and therefore the need to discover newer effective anti-EGFR agents is imperative.

Currently, natural endogenous metabolites of mammalian origin have become an alternate source for the discovery of anticancer agents for therapeutic intervention. In this regard, estradiol analogs have turned out to be the focus of research due to their ability to exert significant antimitotic effects against various cancers including breast cancer. In particular, Stander *et al*, 2011 report that 2-Methoxyestradiol (2ME), an endogenous metabolite of 17β-estradiol, possess both antiangiogenic and anti-breast cancer effects *in vitro* and *in vivo*. This compound exerts its cytotoxic effect independently of the cellular estrogen receptors and has no significant systemic hormonal effects (Leese *et al*, 2006). Estradiol, however, promotes the proliferation of various cancers (Verwey *et al*, 2016). The above studies also report on the limited bioavailability of the 2ME (Panzem®) drug due to its fast-metabolic breakdown during phase II clinical studies. Recently, a sulfamate derivative of 2ME has been found to possess potent antitumor activity against breast cancer cells due to its increased bioavailability by avoiding hepatic first-pass metabolism (Visagie *et al*, 2013; Verwey *et al*, 2016). This suggests that estradiol may be a privileged scaffold upon which modifications can be done to generate lead candidates with improved potency and pharmacokinetic properties as well as reduced toxicities. In our research group, estrone, an isomer of estradiol, is used as a starting material to synthesize novel estrone analogs. Many of our estrone derivatives, especially those bearing cucurbitacin side chains have been documented to exhibit potent cytotoxic effects against distinct cancers (Ahmed *et al*, 2017; Elshaier *et al*, 2017; Ahmed *et al*, 2014; Kopel *et al*, 2013). On the other hand, a set of novel compounds carrying 1,2,3-triazole scaffold has been reported as cytotoxic agents against different cancers (Prachayasittikul *et al*, 2015; El-Sherief *et al*, 2018). Recently,

our research group has synthesized a new series of estrone analogs (bearing modified triazole side chains) targeting EGFR dependent cancers using pharmacophore-docking-based virtual screening. In this study, we report on the synthesis and biological evaluation of novel estrone analogs bearing triazole side chains as potent compounds against EGFR dependent breast cancer cells. These compounds inhibited the MAP kinase and Akt signaling as a result of deregulating EGFR expression and induced apoptosis.

4.3   Materials and methods

4.3.1   Reagents and chemicals

Antibodies against EGF Receptor (D38B1) XP®, Phospho-p44/42 MAPK (Erk1/2) (Thr202/Tyr204) (197G2), Cyclin D1 (92G2), Phospho-Akt (Ser473) and anti-rabbit DyLight 680 conjugate (5366) secondary antibody were purchased from Cell Signaling Technology (Danvers, MA, USA); phospho-cyclin D1 (Thr286) (A537487), Phospho-A-Raf (Ser299) and anti-mouse DyLight 800 conjugate (W10815) from Thermo Fisher Scientific (Waltham, MA, USA); Phospho-EGF Receptor (Tyr1068), Phospho-p70S6 Kinase α, Dyrk1B, caspase 9, caspase 3, PARP1, cleaved PARP1, Bcl-2, APAF1, cytochrome C, Cyclin E and GAPDH were from Santa Cruz Biotechnology Inc. (Dallas, Texas, USA). Phosphate buffered saline (PBS) and trypan blue solution were from Thermo Fisher Scientific (Waltham, MA, USA). RealTime-Glo™ Annexin V apoptosis and

necrosis assay (JA1011) kit was from Promega (Madison, WI, USA). PI/RNase staining buffer was purchased from BD Biosciences (San Jose, CA, USA). Compound cytotoxicity was evaluated through measurement of mitochondrial dehydrogenase activities with 3-(4,5-dimethylthiazol-2-yl)-2,5-diphenyltetrazolium bromide (MTT) reagent (Sigma-Aldrich, St. Louis, MO, USA). Hoechst 33342 stain for evaluating chromatin condensation and nuclear fragmentation was purchase from Thermo Fisher Scientific (Waltham, MA, USA). Sorafenib (positive control) (Selleckchem, Houston, TX, USA) and novel triazole derived estrone analogs were dissolved in dimethyl sulfoxide (DMSO) (Fisher Chemical/Fisher Scientific). All other chemicals were of analytical grade.

4.3.2   Design and synthesis of estrone analogs

4.3.2.1   Molecular modeling

Molecular docking of novel estrone analogs into the EGFR binding domain (PDB code: 1M17) was carried out using the FRED application (version 2.2.5) as implemented through the graphical user interface of OpenEye® software. The 3D structure of the above protein was downloaded from Protein Data Bank. The three-dimensional structures of the aforementioned compounds were constructed using Chem. 3D ultra 12.0 software [Chemical Structure Drawing Standard; Cambridge Soft corporation, USA (2010)], then they were energetically minimized by using MMFF94 with 5000 iterations and minimum RMS gradient of 0.10. All bound water molecules and ligands were eliminated from the

proteins. Furthermore, multi-conformers were generated using OMEGA application (version 2.5.1.4) and VIDA application (version 4.1.2) was used as a visualization tool to show the potential binding affinity and binding interactions of the ligands to the receptor [24]. This software package generates consensus scoring which is a filtering process to obtain virtual binding affinity. The lower the consensus score, the better binding affinity of the ligands towards the receptor.

4.3.2.2   Synthesis of MMA307 and MMA320

Fz25, Fz57, and Fz200 were synthesized as previously described by Faez, 2017.

4.3.3   Cell culture

MCF-7 (a model for ER+, PR+, HER2- breast cancer) and MDA-MB-231 (a model for TNBC with amplified EGFR and KRAS mutant) were purchased from American Type Culture Collection (ATCC, Manassas, VA). The cells were cultured in Dulbecco's Modified Eagle Medium (DMEM) supplemented with 10% (v/v) fetal bovine serum (FBS), antibiotic-antimycotic (Gibco™, ThermoFisher Scientific) at 37°C equilibrated with 5% (v/v) CO_2 in humidified air. The cells for the assays were detached using a solution of trypsin with EDTA (ThermoFisher Scientific).

4.3.4   Cytotoxicity assay

4.3.4.1   3-(4,5-dimethylthiazol-2-yl)-2,5-diphenyltetrazolium bromide (MTT) Assay

The effect of novel synthetic estrone analogs on cell viability was tested with MTT reagent as described by Wang *et al*, 2010 with slight modifications. Briefly, to measure mitochondrial dehydrogenase activities, cells were seeded in 96-well plates at an initial density of 30,000 cells per well. After overnight incubation, cells were treated with different concentrations of compounds in a dose range of 0 - 100 μM. The final DMSO concentration was 0.05%. After 48 hrs of incubation, 20 μL of MTT reagent (5 mg/mL) was added to each well and the formed formazan crystals were dissolved in 250 μL of dimethyl sulfoxide (DMSO). Four independent experiments were completed to determine the mean optical density referred to as cell viability, using a Hidex Sense Beta Plus plate reader (Turku, Finland). Cell viability was expressed as a percentage of DMSO-treated controls.

4.3.5   Flow cytometry for cell cycle analysis

MDA-MB-231 and MCF-7 cells were seeded into six-well plates at a concentration of 300,000 cells/ well and allowed to attach in culture overnight, then treated with IC_{50} of

compounds or positive control (sorafenib) for 48 h. Afterward, cells were washed with PBS and harvested. Cell cycle analysis was investigated by adding propidium iodide (PI) stain (Thermo Fisher Scientific) to 1 mL of cell suspension. Briefly, harvested cells were fixed in 70% ethanol and incubated at 4ºC for 4hrs. Subsequently, the cells were cleaned of alcohol and stained with RNase free PI solution, the cell suspension was incubated in the dark for 45 minutes at room temperature. The samples were analyzed by flow cytometry and compared to DMSO-treated cells. All these experiments were performed on BD Accuri™ C6 flow cytometer (BD Biosciences, San Jose, CA, USA) using BD Accuri™ C6 software, version 1.0.

4.3.6   Apoptosis analysis

4.3.6.1   Annexin V assay

The annexin v assay was performed in accordance with the manufacturers' protocol with slight modifications. Briefly, MDA-MB-231 and MCF-7 cells were seeded in wells on a 96-white plate with clear bottom at an initial density of 30,000 cells for overnight attachment. Afterward, the cells were incubated with the IC$_{50}$ of compounds between 6 to 48 hrs. Subsequently, the RealTime-Glo™ Annexin V Apoptosis reagent (Promega, Madison, WI) was prepared (sequentially mix Annexin NanoBiT® Substrate, CaCl$_2$, Annexin V-SmBiT and Annexin V-LgBiT in a prewarmed media) and added to the reaction

set up before incubating for additional 1 hr. Luminescence was measured afterward using Hidex Sense Beta Plus plate reader (Turku, Finland). Apoptosis was expressed as a percentage relative to DMSO-treated controls.

4.3.6.2   Morphological analysis with fluorescence microscopy

To evaluate the apoptotic activity of the estrone analogs, nuclear staining with the DNA-binding dye Hoechst-33342 performed in accordance with manufacturers protocol. In brief, MDA-MB-231 and MCF-7 cells were plated into 6-well plates and treated with IC_{50} of compounds for 24 hrs. Cells were washed with PBS and incubated with Hoechst-33342 (10μg/mL) for 15 min in the dark, then observed under a fluorescence microscope (excitation 352 nm, emission 461 nm; NIKON TE2000-E). Apoptotic cells were identified by condensation of chromatin and fragmentation of nuclei. Pictures were obtained using a video camera Q-imaging (Burnaby, BC, Canada).

4.3.7   Protein expression analysis

4.3.7.1   In-Cell Western (ICW) Assay

Proteins involved in apoptosis, cell cycle progression, MAP kinase and Akt pathways were quantified by ICW. This technique was carried out in accordance with the manufacturer's

instruction with slight modifications. Briefly, about 50,000 cells per well were seeded into 96-well black walled plate with clear bottom for overnight attachment. Cells were then treated with IC_{50} of compounds for 24 hrs. Subsequently, cells were fixed with 3.7% formaldehyde solution, permeabilized with 0.1% Triton X-100 solution and blocked with fish gel buffer ($1\times$) prior to primary antibody addition. Wells were then incubated with the relevant antibodies EGF Receptor (D38B1) XP®, Phospho-p44/42 MAPK (Erk1/2) (Thr202/Tyr204) (197G2), Cyclin D1 (92G2), Phospho-Akt (Ser473), phospho-cyclin D1 (Thr286) (A537487), Phospho-A-Raf (Ser299), Phospho-EGF Receptor (Tyr1068), Phospho-p70S6 Kinase α, Dyrk1B, caspase 9, caspase 3, PARP1, cleaved PARP1, Bcl-2, APAF1, cytochrome C, Cyclin E and GAPDH, control, overnight followed by an hour incubation with anti-mouse or anti-rabbit DyLight conjugated (680 or 800 nm) secondary antibodies. Images were acquired using LICOR Odyssey® Fc Imaging System (Lincoln, Nebraska, United States) and image quantification done by Fiji software (Image J, Java 1.8.0).

4.3.8   Statistical Analysis

Microsoft® Excel® for Windows, version 16.0., was used for the calculation of mean and standard deviation values of different experiments and plotting of bar or line graphs. Mean IC_{50} values were compared by one-way analysis of variance (ANOVA) using GraphPad

Prism 5.01 (San Diego, USA) and values with p<0.05 were considered statistically significant.

4.4   Results

4.4.1   Docking simulations

To validate whether these designed estrone analogs can target EGFR dependent breast cancers, molecular docking was performed by fitting these designed compounds and reference compound (erlotinib) into the ATP binding site of the EGFR kinase domain (PDB codes: 1M17) crystallized from breast cancer cells. Then, the obtained results plotted as a line-scatter graph (Figure 4.1), which mainly displays the corresponding consensus scores of the molecular docking studies. Compared with the positive control drug, erlotinib, it was clearly observed that most estrone analogs showed lower consensus scores (a measure of better binding and potency) against EGFR kinase domain. Furthermore, Figure 4.3 – 4.5 show the binding mode of Fz25, Fz57 and Fz200 that exhibited potent cytotoxic activities compared to sorafenib and estrone *in vitro*. Directed addition of trimethylsilyl azide to compound 5 afforded Fz25 in 51% yield after column chromatography and the addition of phenylacetamide substituted triazole to compounds 4 and 5 yielded Fz200 (73%) and Fz57 (69%), respectively, after silica-gel column chromatography purification. These pure compounds were characterized by ^{1}H- and ^{13}C-NMR and mass spectrometry techniques.

The chemical shifts and accurate masses are documented in the method section. Fz25 was named as 3-Obenzyl Estra-17 (-1H-1,2,3-triazol), Fz57 as 3-Obenzyl Estra-17 (1H-1,2,3-triazol-1-yl)-N-phenylacetamide and Fz200 as 3-Oacetate estra-17 (1H-1,2,3-triazol-1-yl)-N-phenylacetamide.

4.4.2 Estrone analogs exhibit cytotoxic effects and affect the morphology of breast cancer cells

To evaluate the cytotoxic effects of the estrone analogs against MDA-MB-231 and MCF-7 cells, the cells were initially treated with different concentrations of the compounds, a dose range of 0-50 μM. Subsequently, effects on cell viability were determined by the MTT assay after 48 hrs. Overall, the compounds did show a significant cytotoxic effect toward the MDA-MB-231 and MCF-7 cells within the dose range tested after 48 h and therefore IC_{50} values were calculated. Most of the compounds were equally effective as the positive control-sorafenib but very potent than estrone in reducing the viability of MDA-MB-231 and MCF-7 cells. Particularly, we observed that Fz25, Fz57, Fz200, Fz300 and Fz400 recorded IC_{50} values of 8.12 ± 0.85, 21.18 ± 0.23, 10.86 ± 0.69, 14.95 ± 1.85 and 21.21 ± 0.76 μM, respectively (Table 4.1) against MDA-MB-231 cells. Also, Fz25, Fz57, Fz200, Fz300 and Fz400 recorded IC_{50} values of 8.13 ± 0.15, 11.94 ± 0.19, 20.86 ± 3.16, 18.38 ± 1.97 and 21.49 ± 0.95 μM, respectively towards the MCF-7 cells. Fz25 recorded which similar IC_{50} values in both cell lines was slightly better than the positive control, sorafenib-recorded an IC_{50} values of 10.62 ± 0.02 μM in MDA-MB-231 cells and 12.21 ± 0.96 μM

in MCF-7 cells. Because this research was focused on EGFR dependent breast cancer, further studies were conducted using the MDA-MB-231 cells. Morphological changes in MDA-MB-231 cells induced by Fz25, Fz57, Fz200 and sorafenib (positive control) were observed in Figure 4.6. Light microscope was used to evaluate the morphological response when the cells were treated with IC_{50} doses of compounds for 48 h. The cells exposed to 0.05% of DMSO showed no signs of cell stress and confluent cell growth was seen. Compared with DMSO control cells, the majority of the compound-treated MDA-MB-231 cells were stressed, and the confluency of the cells reduced. Particularly, the cells changed from regular spindle-shape to an increased proportion of either round-shaped (observed for Fz57) or rod-shaped (observed for Fz25, Fz200 and sorafenib) adding to the compound's cytotoxic effects.

4.4.3   Increased G_1- or S-phase cell cycle arrest in response to estrone analogs exposure

The quantification of cells at various stages within the cell cycle was determined with propidium iodide stain and analyzed by flow cytometry. Cell cycle distribution of MDA-MB-231 cells exposed to DMSO (Figure 4.11) showed an average of 40% in the G_0/G_1 phase, 2% in the S phase and 53% in the G_2/M phase. The exposure of cells to Fz25 resulted in significant accumulation of cells within G_0/G_1 phase, an average of 63%; there was decreased enrichment of cells in the G_2/M phase, an average of 29% was calculated. Fz57 and Fz200 treatments against MDA-MB-231 cells resulted in significant enrichment of

cells within the S-phase of the cell cycle. Fz57 recorded an average of 47% of cells in the S-phase and a lower number of cells (an average of 13%) in the G_2/M phase. Similarly, Fz200 recorded an average of 36% of cells within the S-phase and concomitant lesser number of cells in the G_2/M phase (an average of 22%).

4.4.3.1   Cell cycle activators and regulators are modulated post estrone analogs exposure

As a result of the significant ($p < 0.05$) cell cycle arrest induced by the estrone analogs, we analyzed the expression levels of known G_1- and S-phase cell cycle proteins. In-Cell Western approach was adopted to establish our findings. Cyclin D1 and Dyrk1B play important roles in regulating the progression of the cell cycle within the G_1 phase whereas cyclin E is associated with controlling the S-phase of the cell cycle. We observed that Fz25 administration to MDA-MB-231 cells resulted in the suppression of cyclin D1 and Dyrk1B in a concentration-dependent manner with 24hrs (Fig 4.12A). On the other hand, exposure of Fz57 and Fz200 to the TNBC cell model resulted in downregulation of cyclin E in a dose-dependent fashion (Fig 4.12B-C). These findings are in line with the significant cell cycle arrest recorded in Figure 7.

4.4.4   Estrone analogs induce apoptosis in breast cancer cells

4.4.4.1 RealTime-Glo™ Annexin V assay

The cell death inducing effect of the estrone analogs in MDA-MB-231 cells were evaluated by RealTime-Glo™ Annexin V apoptosis and necrosis luminescent assay. The detection reagent contains Annexin V-LgBiT and Annexin V-SmBiT (NanoBiT) fusion proteins and a profluorescent DNA dye. In healthy cells, most of the phosphatidylserine (PS) is confined to the inner leaflets of the cell membrane, fewer fusion proteins bind to PS and less luminescence is recorded. In apoptotic cells, PS is exposed to the outer leaflet of the cell membrane, more fusion proteins bind to PS and increased luminescence is measured. Increased luminescence corresponds to increased apoptosis. Treating MDA-MB-231 cells with the estrone analogs, increased apoptosis was observed in a dose-dependent manner (Figure 4.7). Notably, Fz25 and Fz57 induced apoptosis in MDA-MB-231 cells within 6 hrs (Fig 4.7A) whereas the apoptotic effect recorded by Fz200 was observed within 48 hrs of treatment (Figure 4.7B), all compared the positive control, camptothecin.

4.4.4.2 Morphological analysis with fluorescence microscopy

The morphological observation in the cell nuclei of MDA-MB-231 cells for 24 h after treatment with estrone analogs or sorafenib showed significant morphological alterations when compared to 0.05% DMSO control. As shown in Figure 4, the control or untreated cells appeared to be intact oval shape and the nuclei were stained with a less bright blue

fluorescence (due to the Hoechst 33342 dye). Cells treated with tested compounds exhibited typical features of apoptosis such as cell shrinkage, chromatin condensation, and fragmentation in multiple, segregated bodies, the formation of apoptotic bodies, and cell decrement. The apoptotic nuclei clearly showed highly condensed or fragmented chromatin that was uniformLy fluorescent. Fz25, Fz57, Fz200 and sorafenib treatments resulted in increased apoptotic cells (condensed chromatin, indicated by arrows) compared to the DMSO control (Figure 4.8).

4.4.4.3   Estrone analogs induce cell death via mitochondrial apoptosis pathway

In order to determine whether the compounds modulated proteins involved in cell death, ICW assay was performed to detect changes of protein expression in the mitochondrial apoptosis pathway. As shown in Figure 4.9, exposure of MDA-MB-231 cells to compounds resulted in increased expressions of cytochrome C and apoptotic protease activating factor 1 (APAF1), which are markers of mitochondrial apoptosis. Furthermore, we observed decreased expression of B Cell Lymphoma 2 (Bcl-2) protein when MDA-MB-231 cells were treated with Fz57 and Fz200 (Figure 4.10 B-C) but not Fz25 (data not shown). Also, all three compounds when administered to cells resulted in an increased expression of cleaved PARP1 but had no effect on PARP1 in a dose-dependent fashion. However, the expression levels of caspases-3 and -9 were decreased post-treatment with Fz57 and Fz200. No change in the expression levels of caspases-3 and -9 were noted when MDA-MB-231

cells were exposed to Fz25. In summary, these results reveal that the estrone analogs induced apoptosis in MDA-MB-231 cells via the mitochondrial pathway and in a caspase-dependent manner.

4.4.5 EGFR signaling pathways are inhibited after estrone analogs exposure

We evaluated the expression levels of total and activated (phosphorylated) forms of EGFR by ICW (Figure 4.13). Higher levels of EGFR were detected in the DMSO treated cells compared to compound treated cells, depicting EGFR downregulation. Similarly, levels of phosphorylated EGFR (Y1068) were also increased in the DMSO treated cells compared to compound-treated cells. EGFR and phosphorylated EGFR (Y1068) expression levels were downregulated in a concentration-dependent manner. The purpose of EGFR autophosphorylation is to activate signaling pathways, such as PI3K/AKT and RAS/MAPK pathways (Romano *et al*, 2011). We next investigated the activation of these pathways by quantifying activated (phosphorylated) forms of ERK1/2- and AKT-associated pathway proteins. Decreased amounts of phospho-ARaf (S299) and phospho-ERK1/2 (T202/Y204) were clearly detected in MDA-MB-231 cells when exposed to the estrone analogs in a dose-dependent manner (Figure 4.13). Also, phospho-AKT (S473), phospho-mTOR (S2448) and phospho-p70S6Kα (S411) expression levels were downregulated in concentration-dependent manner (Figure 4.14). Based on the levels of

ERK- and AKT-associated proteins phosphorylation, RAS/MAPK and PI3K/AKT signaling pathways were downregulated in MDA-MB-231 cell line.

4.5   Discussion

Estrone derivates, especially 2ME and its sulphamoylated analogs, have been proven to be cytotoxic against various cancers including TNBC (Verwey *et al*, 2016, Nolte *et al*, 2018). Mechanistically, the observed cytotoxicity has been attributed to inhibition of angiogenesis, actin depolymerization, autophagy induction, and the modulation of both intrinsic and extrinsic apoptosis. However, only a few studies have investigated estrone analogs inhibitory effects against EGFR and its downstream signaling pathways. EGFR is known to be overexpressed in TNBC. Previously, our research group has reported on estrone analogs EGFR inhibitory effects in different cancers *in vitro*. Notably, studies by Sara, 2018 documented that estrone analogs with cucurbitacin pharmacophores inhibit the proliferation of hepatocellular carcinoma via induction of apoptosis and suppression of EGFR and its downstream MAP kinase signaling. Also, Felix and colleagues (unpublished data) revealed that these compounds inhibit the proliferation of EGFR-wild-type NSCLC (NCIH226 cells) via inhibiting EGFR and MAP kinase signaling. Currently, we have synthesized a new series of estrone analogs (bearing triazole or substituted triazole at position 17 of the estrone scaffold-Fz series) using pharmacophore-docking-based virtual screening. In this study, we report for the first time that the triazole substituted estrone

analogs are potent cytotoxic agents against the MDA-MB-231 cell line. Also, these class of compounds mechanistically elicited mitochondrial apoptosis induction and suppressed EGFR expression as well as downregulate Akt and ERK1/2 pathways.

Previous co-crystallization studies by Stamos *et al*, 2002 revealed that hydrogen bonding between the amide nitrogen of MET769A within the EGFR kinase domain (1M17) and the pyrimidine N_2 of erlotinib (reference compound) was a key molecular interaction achieving drug potency (Figure 4.2). From our virtual screening studies *in silico*, we observed that most of our estrone analogs had a similar or lower consensus score (a measure of drug potency) compared to the reference compound, erlotinib (Figure 4.1). The lower the consensus score, the stronger the binding and the better the compound's potency. Fz25 and Fz200 had similar consensus score compared to erlotinib whereas Fz57 had a higher consensus score. These compounds showed interesting cytotoxic effects against MDA-MB-231 cells *in vitro*. In contrast to the findings published by Stamos *et al*, 2002, we report for the first time that Fz25, Fz57 and Fz200 showed hydrogen bonding towards different amino acid residues within EGFR kinase domain (Figure 4.3 and 4.5). Fz25 displayed hydrogen bonding from N_1, N_2 and N_3 of the triazole ring and hydroxy group towards ASP831A, GLU738A and THR766A amino acid residues, respectively, within the EGFR kinase domain. Also, Fz200 showed hydrogen bonding from N_2 and N_3 of the triazole ring towards the amide nitrogen of CYS773A. Similarly, Fz57 showed a single hydrogen bonding from N_3 of triazole towards the amide nitrogen of CYS773A. These different interactions may be key to these compounds eliciting their cytotoxic effects against MDA-

MB-231 cells. Next, the triazole substituent was installed onto the estrone scaffolded at position 17 to produce Fz25 whereas the addition of phenylacetamide substituted triazole onto the estrone nucleus afforded Fz200 and Fz 57 (Faez, 2017).

In the past our lab has designed several estrone analogs with enhanced cytotoxicity. These and other estrone analogs (Stander *et al*, 2012) have demonstrated cytotoxicity within nanomolar or micromolar concentrations against multiple cancer cell lines, including MDA-MB-231 cells. The cytotoxic effect of Fz25, Fz57 and Fz200 was confirmed in the current study revealing IC_{50} concentrations of 8.12 ± 0.85, 21.18 ± 0.23, 10.86 ± 0.69 μM, respectively, compared to sorafenib, IC_{50} value of 10.62 ± 0.02 μM (Table 4.1). All except Fz25 showed a different trend of cytotoxicity when MCF-7 cells were exposed to the estrone analogs. However, MDA-MB-231 cells were considered for further investigations because our hypothesis sought to test the estrone analogs cytotoxic effect against EGFR dependent breast cancers. MCF-7 is a model for estrogen receptor (ER) positive breast cancer and therefore does not fit into our hypothesis.

Cell cycle analysis suggested that the compounds inhibit cell growth via blocking cell division at the G_0/G_1 and S phases. In addition, treatment of MDA-MB-231 cells resulted in increased apoptosis (Figure 4.11). These results are in good agreement with previous findings demonstrating that different estrone analogs also induced a G_0/G_1 cell cycle arrest and apoptosis in human cancer cell lines *in vitro* (Verwey *et al*, 2016, Nolte *et al*, 2018;

Wolmarans *et al*, 2014; Boyd *et al*, 2018). To better understand the mechanism of triazole derived estrone analogs-induced cell cycle arrest and apoptosis, we firstly investigated the status of key proteins known to regulate G_0/G_1 and S phases transition and cell death. Dyrk1B, a checkpoint kinase important for G_1 to S phase cell cycle transition is aberrantly activated in many cancers, including breast cancer. In addition, Dyrk1B is responsible for modulating the expression of several cell cycle activators (eg. Cyclin D1) and regulators (eg. p27) (Chen *et al*, 2017). Our previous studies suggest that estrone analogs with modified cucurbitacin pharmacophores induce inhibitory effects against human EGFR-wild-type NSCLC cell lines via suppression of Dyrk1B expression (Unpublished Data). In the current study, it was clearly demonstrated that the levels of Dyrk1B and cyclin D1 proteins were decreased in MDA-MB-231 cells treated with Fz25 (Figure 4.12), suggesting that G_0/G_1 cell cycle arrest was at least partially mediated via suppression of cyclin D1 and Dyrk1B expressions. Similarly, the levels of cyclin E were decreased when TNBC cells were treated with Fz57 and Fz200 depicting that the S-phase cell cycle arrest was partially mediated by downregulating cyclin E expression.

The apoptotic nature of cell death in triazole-derived estrone analogs-treated cells was verified by different assays, including annexin V, chromatin condensation, and some markers involved in the mitochondrial apoptosis cascade. Viable cells contain phosphatidylserine (PS), located on the inside of the cell membrane. When apoptosis occurs, PS flip will occur. PS moves to the outside surface of cells to which annexin V binds. Analyzing MDA-MB-231 treated cells with real-time annexin V assay, it was

observed that Fz25 and Fz57 induced PS translocation within 6 hrs whereas Fz200 exhibited PS translocation after 48 hrs in a dose-dependent fashion when compared to camptothecin, positive control (Figure 4.7). Subsequently, morphological changes-chromatin condensation, induced by the estrone analogs were analyzed by fluorescence microscopy after staining cells with Hoechst 33342. Chromatin condensation paralleled by DNA fragmentation is one of the most important criteria used to identify apoptotic cells. All estrone analogs (Fz25, Fz57 and Fz200) and sorafenib, clearly induced chromatin condensation within 24 hrs of drug treatment (Figure 4.8). These results are in line with studies by (Verwey *et al*, 2016, Nolte *et al*, 2018) where different estrone analogs induced PS translocation and chromatin condensation in the estrogen negative and metastatic breast cancer cells, MDA-MB-231. Furthermore, the estrone analogs effect on markers involved in the mitochondrial apoptosis were investigated. The Bcl-2, an antiapoptotic protein, family consists of proapoptotic and antiapoptotic proteins. Bcl-2 binds to various proapoptotic family members and inhibits their insertion into the mitochondrial membrane. Upon receiving an apoptotic signal, Bcl-2 releases proapoptotic proteins, allowing them to form a complex on the mitochondrial membrane. Cytochrome c is consequently released into the cytoplasm, triggering increased caspase activity which leads to cell death. In apoptotic cells, cytochrome c binds to Apaf-1 to induce apoptosome formation. The Apaf-1 apoptosome catalyzes the autocatalytic activation of the caspase-9 zymogen (initiator caspase), which subsequently cleaves and activates caspase 3 (Hu *et al*, 2014). Finally, caspase 3 cleaves and inactivates PARP-poly (ADP-ribose) polymerase, which is important for damaged DNA repair (Soldani and Scovassi, 2002). Estrone analogs

administration to MDA-MB-231 cells resulted in mitochondrial apoptosis induction where increased expressions of cytochrome c and Apaf-1 were observed whereas the expression of Bcl-2 was decreased (Figure 4.9 and 4.10). Also, dosing Fz25 to MDA-MB-231 cells resulted in stable expression of PARP 1 whereas the expression levels of caspase 9, caspase 3 and cleaved PARP 1 were increased. However, the levels of caspases-3 and -9 decreased upon Fz57 and Fz200 treatment, but the levels of cleaved PARP1 increased (Figure 4.10). These findings partially concur with studies by Nolte *et al*, 2018 where different estrone analogs addition to MCF-7 cells decreased the expression of Bcl-2. This study is the first to report on triazole derived estrone analogs mitochondrial-induced apoptosis in a TNBC model.

Furthermore, we demonstrated that triazole derived estrone analogs can target directly the epidermal growth factor receptor (EGFR), suppressing its phosphorylation at the docking site Y1068 in a concentration-dependent manner in EGFR-expressing MDA-MB-231 cells, followed by inhibition of its secondary PI3K/AKT and RAS/ERK signaling pathways. Phosphorylation of EGFR on Y1068 creates binding sites for the adaptor protein, Grb2, leading to activation of the MAPK/ERK cascade, and a binding site for Gab1, which recruits the p85 subunit of phosphatidylinositol 3-kinase (PI 3-kinase), leading to AKT activation (Yamaoka *et al*, 2011). EGFR is overexpressed and genetically amplified in one-third of metastatic or recurrent breast cancers, and this has been inversely correlated with relapse-free survival (Nagaria *et al*, 2017). EGFR has been implicated in numerous processes including promoting tumor cell development and proliferation, and survival by

activating the MAPK/ERK and AKT pathways, respectively (Nagaria *et al*, 2017). MAPK/ERK activation leads to the induction of target proteins, including Bcl-2, caspase-9, and cyclin D1, regulating growth and proliferation of cells (Nagaria *et al*, 2017). Similarly, activated AKT exerts its survival and protein synthesis activities by directly activating mammalian target of rapamycin (mTOR) and ribosomal protein S6 kinase (p70S6K) (Manning and Toker, 2017). Therefore, considerable attention has been given to targeting the EGFR pathway for anticancer therapy. It must be noted that currently no anti-EGFR agent has been approved for treating TNBC clinically. Treating MDA-MB-231 cells with estrone analogs resulted in decreased expression of EGFR in a dose dependent manner within 24 hrs. Similarly, activated EGFR (Y1068) expression levels were downregulated after estrone analogs administration (Figure 4.13). Furthermore, MAPK/ERK pathway was inactivated as the compounds downregulated the expression levels of phospho-ARaf (Ser299) and phospho-ERK1/2 (T202/Y204) (Figure 4.13) in a dose-dependent fashion. The AKT pathway was also inactivated as the expression levels of activated proteins, phospho-AKT (Ser473), phospho-mTOR (Ser2448) and phospho-p70S6Kα (Ser411) (Figure 4.14) were decreased when the TNBC model was treated with triazole derived estrone analogs.

It must be mentioned that while the status of selected cell cycle activators (cyclin D1, cyclin E and Dyrk1B), apoptosis initiator and effector proteins and EGFR dependent proteins were analyzed in this study, the functions of other proteins associated with these

pathways were likely modulated as well, and therefore, the cytotoxic effects of the estrone analogs reported here may not be solely due to these proteins.

4.6   Conclusion

We report for the first time on the synthesis of a new series of estrone analogs (a hybrid of estrone scaffold and triazole or modified triazole pharmacophores). Fz25, Fz57 and Fz200 showed good binding affinity towards EGFR kinase domain *in silico* and were cytotoxic against MDA-MB-231 cells *in vitro*. Fz25 arrested the TNBC model within the G_1 phase whereas Fz57 and Fz200 induced cell cycle arrest within the S phase. Dyrk1B, cyclin D1 (G_1 phase) and cyclin E (S phase) expression levels were downregulated by the estrone analogs accounting for the observed G_1- and S-phase cell cycle arrest. Furthermore, morphological studies showed that the compounds induced apoptosis and modulated key apoptotic proteins. BCl2 expression level was decreased whereas cytochrome c and Apaf1 expression levels were increased indicating mitochondrial apoptosis induction. Also, cleaved PARP1 levels were elevated along with caspase 3 and 9 activations. EGFR and its downstream ERK1/2 and AKT pathways were downregulated suggesting that the estrone analogs inhibit proliferation and induce cell death. Taken together, the present study offers initial evidence that triazole derived-estrone analogs are effective agents that can be developed as novel therapies for TNBC.

4.7 References

Ahmed, M. S., El-Senduny, F., Taylor, J., and Halaweish, F. T. (2017). Biological screening of cucurbitacin inspired estrone analogs targeting mitogen-activated protein kinase (MAPK) pathway. *Chemical Biology and Drug Design*, *90*(3), 478-484.

Ahmed, M. S., Kopel, L. C., and Halaweish, F. T. (2014). Structural optimization and biological screening of a steroidal scaffold possessing cucurbitacin-like functionalities as B-raf inhibitors. *ChemMedChem*, *9*(7), 1361-1367.

Alotaibi, F. (2017). Design, Synthesis and Biological Evaluation of Novel Estradiol-Triazole Analogs Targeting Epidermal Growth Factor Receptors in Colorectal Cancer.

Bartholomew, C., Eastlake, L., Dunn, P., and Yiannakis, D. (2017). EGFR targeted therapy in lung cancer; an evolving story. *Respiratory Medicine Case Reports*, 20, 137-140.

Baselga, J., Albanell, J., Ruiz, A., Lluch, A., Gascón, P., Guillém, V., ... and Koehler, M. T. (2005). Phase II and tumor pharmacodynamic study of gefitinib in patients with advanced breast cancer. *Journal of Clinical Oncology*, 23(23), 5323-5333.

Boyd, L. S., Gozuacik, D., and Joubert, A. M. (2018). The in vitro effects of a novel estradiol analog on cell proliferation and morphology in human epithelial cervical carcinoma. *Cellular and Molecular Biology Letters*, 23(1), 10.

Bray, F., Ferlay, J., Soerjomataram, I., Siegel, R. L., Torre, L. A., and Jemal, A. (2018). Global cancer statistics 2018: GLOBOCAN estimates of incidence and mortality worldwide for 36 cancers in 185 countries. CA: a cancer journal for clinicians.

Chen, Y., Wang, S., He, Z., Sun, F., Huang, Y., Ni, Q., and Cheng, C. (2017). Dyrk1B overexpression is associated with breast cancer growth and a poor prognosis. *Human Pathology*, 66, 48-58.

Dickler, M. N., Cobleigh, M. A., Miller, K. D., Klein, P. M., and Winer, E. P. (2009). Efficacy and safety of erlotinib in patients with locally advanced or metastatic breast cancer. *Breast Cancer Research and Treatment*, 115(1), 115-121.

El Guerrab, A., Bamdad, M., Kwiatkowski, F., Bignon, Y. J., Penault-Llorca, F., and Aubel, C. (2016). Anti-EGFR monoclonal antibodies and EGFR tyrosine kinase inhibitors as combination therapy for triple-negative breast cancer. *Oncotarget*, 7(45), 73618.

Elgazwi, S. (2018). Study of Anti-proliferative Activity of Cucurbitacins Inspired Estrone Analogs on Hepatocellular Carcinoma. *Electronic Theses and Dissertations*. 2640. https://openprairie.sdstate.edu/etd/2640

Elshaier, Y. A., Shaaban, M. A., El Hamid, M. K. A., Abdelrahman, M. H., Abou-Salim, M. A., Elgazwi, S. M., and Halaweish, F. (2017). Design and synthesis of pyrazolo [3, 4-d] pyrimidines: Nitric oxide releasing compounds targeting hepatocellular carcinoma. *Bioorganic and Medicinal Chemistry*, 25(12), 2956-2970.

El-Sherief, H. A., Youssif, B. G., Bukhari, S. N. A., Abdel-Aziz, M., and Abdel-Rahman, H. M. (2018). Novel 1, 2, 4-triazole derivatives as potential anticancer agents: Design, synthesis, molecular docking and mechanistic studies. *Bioorganic Chemistry*, 76, 314-325.

Hossini, A. M., Quast, A. S., Plötz, M., Grauel, K., Exner, T., Küchler, J., and Zouboulis, C. C. (2016). PI3K/AKT signaling pathway is essential for survival of induced pluripotent stem cells. *PloS One*, 11(5), e0154770.

Hu, Q., Wu, D., Chen, W., Yan, Z., Yan, C., He, T., and Shi, Y. (2014). Molecular determinants of caspase-9 activation by the Apaf-1 apoptosome. *Proceedings of the National Academy of Sciences*, 111(46), 16254-16261.

Imai, K., and Takaoka, A. (2006). Comparing antibody and small-molecule therapies for cancer. *Nature Reviews Cancer*, 6(9), 714.

Kopel, L. C., Ahmed, M. S., and Halaweish, F. T. (2013). Synthesis of novel estrone analogs by incorporation of thiophenols via conjugate addition to an enone side chain. *Steroids*, *78*(11), 1119-1125.

Lebert, J. M., Lester, R., Powell, E., Seal, M., and McCarthy, J. (2018). Advances in the systemic treatment of triple-negative breast cancer. *Current Oncology*, 25(Suppl 1), S142.

Leese, M. P., Leblond, B., Smith, A., Newman, S. P., Di Fiore, A., De Simone, G., and Potter, B. V. (2006). 2-substituted estradiol bis-sulfamates, multitargeted antitumor

agents: synthesis, in vitro SAR, protein crystallography, and in vivo activity. *Journal of Medicinal Chemistry*, 49(26), 7683-7696.

Manning, B. D., and Toker, A. (2017). AKT/PKB signaling: navigating the network. *Cell*, 169(3), 381-405.

Nagaria, T. S., Shi, C., Leduc, C., Hoskin, V., Sikdar, S., Sangrar, W., and Greer, P. A. (2017). Combined targeting of Raf and Mek synergistically inhibits tumorigenesis in triple negative breast cancer model systems. *Oncotarget*, 8(46), 80804.

Nakai, K., Hung, M. C., and Yamaguchi, H. (2016). A perspective on anti-EGFR therapies targeting triple-negative breast cancer. *American Journal of Cancer Research*, 6(8), 1609.

Nakai, K., Hung, M. C., and Yamaguchi, H. (2016). A perspective on anti-EGFR therapies targeting triple-negative breast cancer. *American Journal of Cancer Research*, 6(8), 1609.

Nolte, E., Joubert, A., Lakier, R., Van Rensburg, A., and Mercier, A. (2018). Exposure of Breast and Lung Cancer Cells to a Novel Estrone Analog Prior to Radiation Enhances Bcl-2-Mediated Cell Death. *International Journal of Molecular Sciences*, 19(10), 2887.

Omarini, C., Guaitoli, G., Pipitone, S., Moscetti, L., Cortesi, L., Cascinu, S., and Piacentini, F. (2018). Neoadjuvant treatments in triple-negative breast cancer patients: where we are now and where we are going. *Cancer Management and Research*, 10, 91.

Ornelas, I. M., Silva, T. M., Fragel-Madeira, L., and Ventura, A. L. M. (2013). Inhibition of PI3K/Akt pathway impairs G2/M transition of cell cycle in late developing progenitors of the avian embryo retina. *PloS One*, 8(1), e53517.

Prachayasittikul, V., Pingaew, R., Anuwongcharoen, N., Worachartcheewan, A., Nantasenamat, C., Prachayasittikul, S., and Prachayasittikul, V. (2015). Discovery of novel 1, 2, 3-triazole derivatives as anticancer agents using QSAR and in silico structural modification. *SpringerPlus*, 4(1), 571.

Romano, E., Schwartz, G. K., Chapman, P. B., Wolchock, J. D., and Carvajal, R. D. (2011). Treatment implications of the emerging molecular classification system for melanoma. *The Lancet Oncology*, 12(9), 913-922.

Rosa, B., de Jesus, J. P., de Mello, E. L., Cesar, D., and Correia, M. M. (2015). Effectiveness and safety of monoclonal antibodies for metastatic colorectal cancer treatment: systematic review and meta-analysis. *Ecancermedicalscience*, 9.

Santonja, A., Sánchez-Muñoz, A., Lluch, A., Chica-Parrado, M. R., Albanell, J., Chacón, J. I., and Fernández-De Sousa, C. E. (2018). Triple negative breast cancer subtypes and pathologic complete response rate to neoadjuvant chemotherapy. *Oncotarget*, 9(41), 26406.

Soldani, C., and Scovassi, A. I. (2002). Poly (ADP-ribose) polymerase-1 cleavage during apoptosis: an update. *Apoptosis*, 7(4), 321-328.

Stamos, J., Sliwkowski, M. X., and Eigenbrot, C. (2002). Structure of the epidermal growth factor receptor kinase domain alone and in complex with a 4-anilinoquinazoline inhibitor. *Journal of Biological Chemistry*, 277(48), 46265-46272.

Stander, A., Joubert, F., and Joubert, A. (2011). Docking, synthesis, and in vitro evaluation of antimitotic estrone analogs. *Chemical Biology and Drug Design*, 77(3), 173-181.

Székely, B., Silber, A. L., and Pusztai, L. (2017). New Therapeutic Strategies for Triple-Negative Breast Cancer: Page 2 of 2. *Oncology*, 31(2).

Verwey, M., Nolte, E. M., Joubert, A. M., and Theron, A. E. (2016). Autophagy induced by a sulphamoylated estrone analogue contributes to its cytotoxic effect on breast cancer cells. *Cancer Cell International*, 16(1), 91.

Visagie, M., Theron, A., Mqoco, T., Vieira, W., Prudent, R., Martinez, A., ... and Joubert, A. (2013). Sulphamoylated 2-methoxyestradiol analogues induce apoptosis in adenocarcinoma cell lines. *PLoS One*, 8(9), e71935.

Wahba, H. A., and El-Hadaad, H. A. (2015). Current approaches in treatment of triple-negative breast cancer. *Cancer Biology and Medicine*, 12(2), 106.

Wang, L., Wu, J., Lu, J., Ma, R., Sun, D., and Tang, J. (2015). Regulation of the cell cycle and PI3K/Akt/mTOR signaling pathway by tanshinone I in human breast cancer cell lines. *Molecular Medicine Reports*, 11(2), 931-939.

Wang, P., Henning, S. M., and Heber, D. (2010). Limitations of MTT and MTS-based assays for measurement of antiproliferative activity of green tea polyphenols. *PloS One*, 5(4), e10202.

Wolmarans, E., Mqoco, T. V., Stander, A., Nkandeu, S. D., Sippel, K., McKenna, R., and Joubert, A. (2014). Novel estradiol analogue induces apoptosis and autophagy in esophageal carcinoma cells. *Cellular and Molecular Biology Letters*, 19(1), 98.

Yamaoka, T., Frey, M. R., Dise, R. S., Bernard, J. K., and Polk, D. B. (2011). Specific epidermal growth factor receptor autophosphorylation sites promote mouse colon epithelial cell chemotaxis and restitution. *American Journal of Physiology-Gastrointestinal and Liver Physiology*, *301*(2), G368-G376.

Tables and Figures
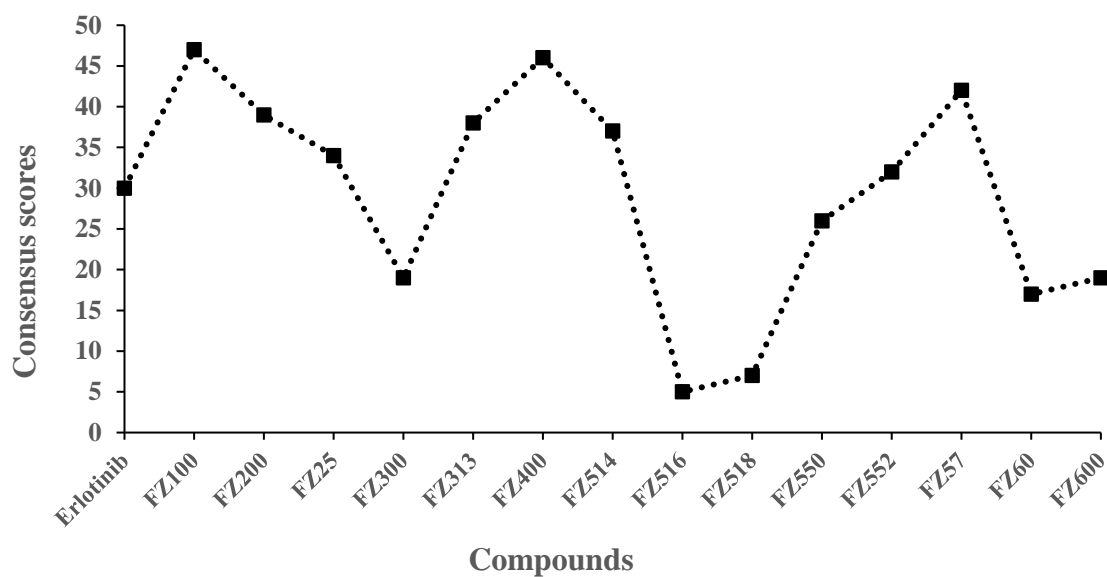
Figure 4.1 Molecular docking study of designed estrone analogs against EGFR binding site (Pdb: 1M17). Scatter plot of compounds consensus scores generated by VIDA application.
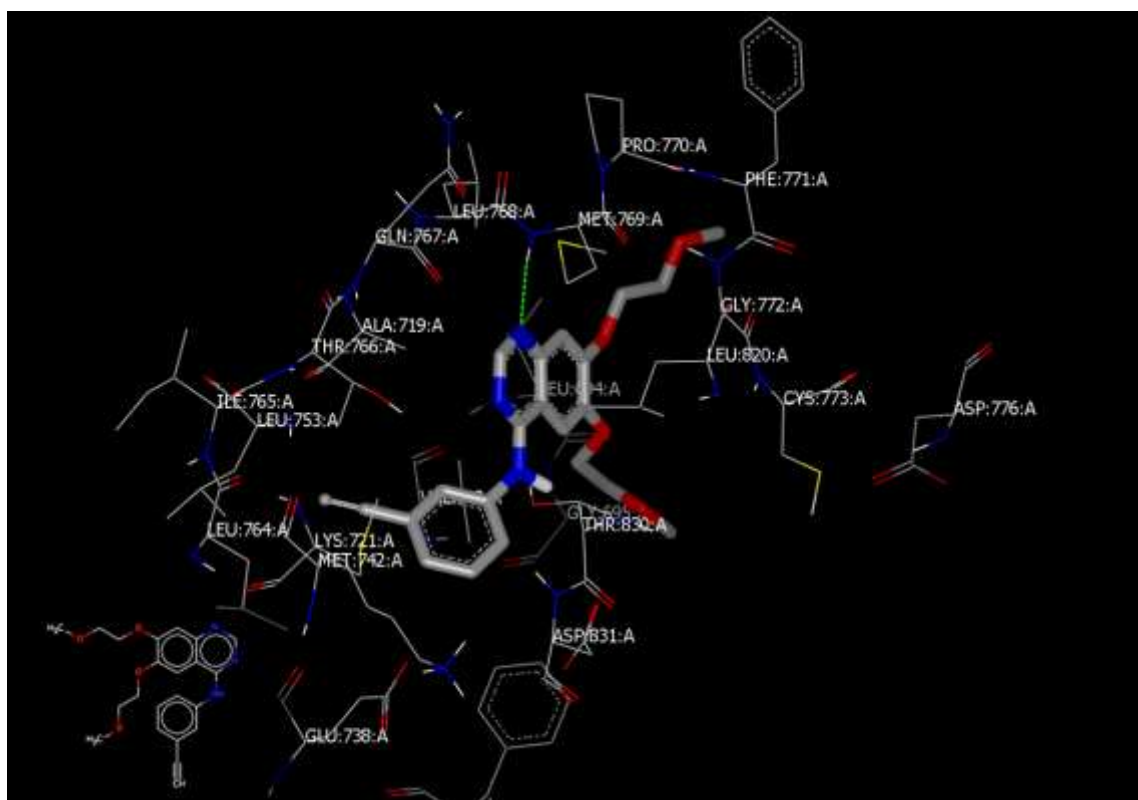
Figure 4.2. 3D visual representation of reference drug, erlotinib, docked against EGFR binding site. There is hydrogen bonding from the pyrimidine-N_2 of erlotinib towards MET769A of 1M17 binding site.
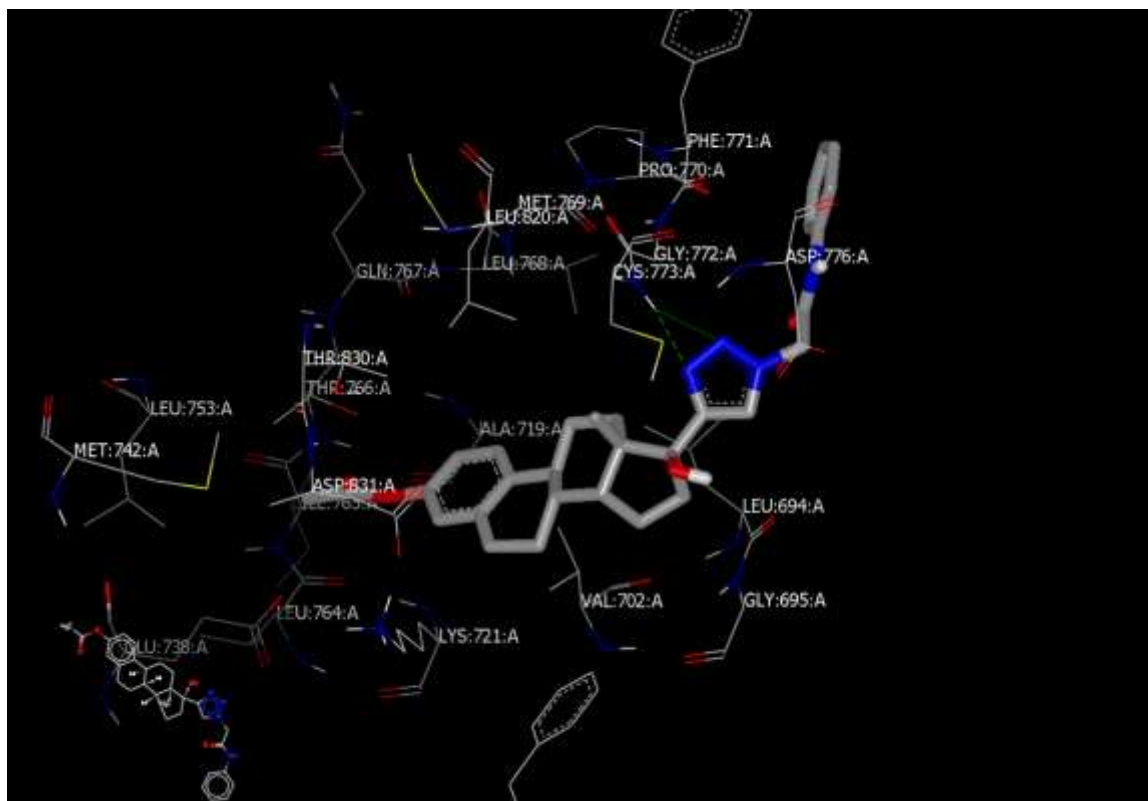
Figure 4.3 3D visual representation of Fz25 docked against EGFR binding site. The dashed green lines show hydrogen bonding from the triazole, N_1, N_2 and N_3, and hydroxy group towards ASP831A, GLU738A and THR766A, respectively of 1M17.

Figure 4.4. 3D visual representation of Fz200 docked against EGFR binding site. The dashed green lines show hydrogen bonding from the triazole-N_1 and N_2 of Fz200 towards CYS773A of 1M17 binding site.
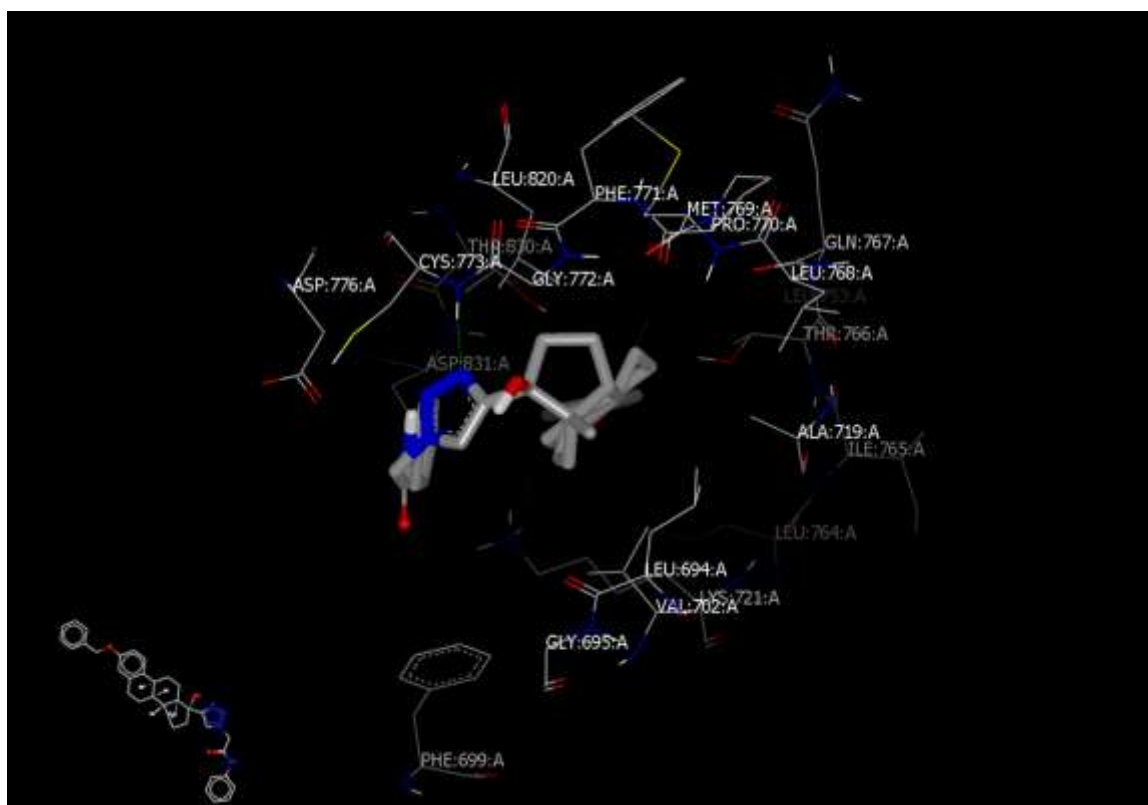
Figure 4.5 3D visual representation of Fz57 docked against EGFR binding site. Fz57 shows hydrogen bonding from the triazole-N_1 towards CYS773A of 1M17 binding site.

Table 4.1 Cytotoxic effects of estrone analogs against breast cancer cells.

	IC$_{50}$ (µM)	
Compound	**MDA-MB-231 cells**	**MCF-7 cells**
Sorafenib	10.62 ± 0.02	12.21 ± 0.96
Fz 25	8.12 ± 0.85	8.13 ± 0.15
Fz 200	10.86 ± 0.69	20.86 ± 3.16
Fz 57	21.18 ± 0.23	11.94 ± 0.19
Fz 60	28.88 ± 0.86	25.21 ± 0.87
Fz 300	14.95 ± 1.85	18.38 ± 1.97
Fz 400	21.21 ± 0.76	21.49 ± 0.95
Fz 100	>100	>100
Fz 516	>100	>100
Fz 313	>100	>100
Fz 600	>100	>100
Fz 518	>100	>100
Fz 60	>100	>100
Fz 552	> 100	> 100
Fz 550	50.00 ± 0.20	100.00 ± 0.00
Fz 514	$> 100 \pm 0$	$> 100 \pm 0$
Estrone	80.07 ± 0.85	>100

In vitro cytotoxic activities (IC$_{50}$, µM) of estrone analogs against breast cancer cells. IC$_{50}$ values were calculated by non-linear regression analysis. Values represent Mean $\pm$ SD of the quadruplicate experiment (n = 4).
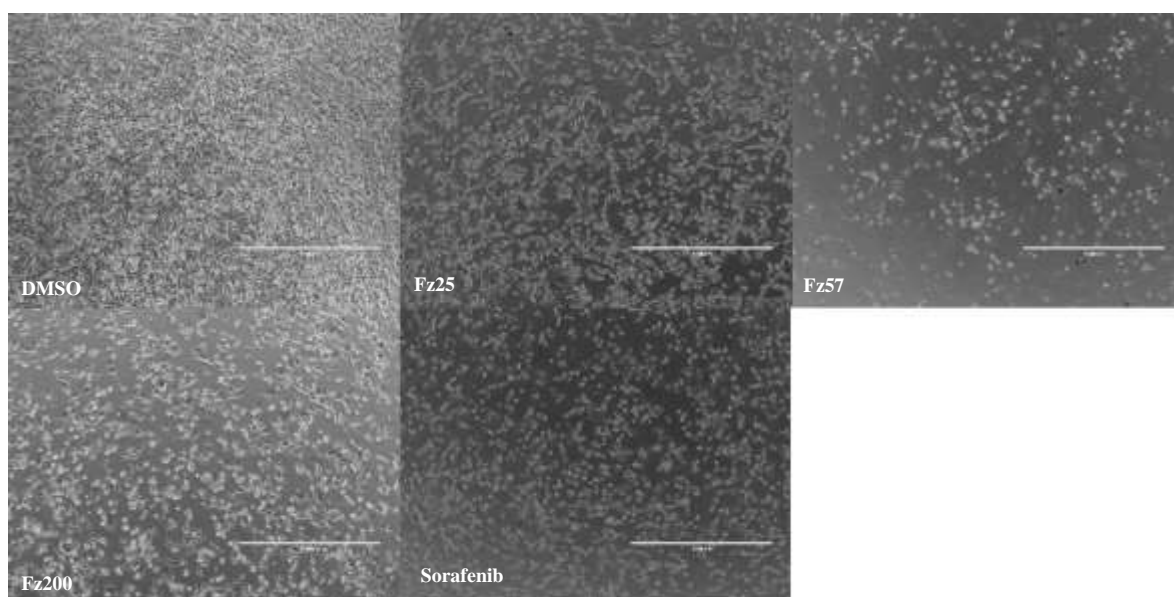
Figure 4.6 Morphological changes in of MDA-MB-231 cells after treatment with 0.05% DMSO, Fz25, Fz57, Fz200 and sorafenib. Images were acquired with ×4 objective lens of Evos XL cell imaging system (ThermoFisher Scientific), scale bar = 1000 µm.
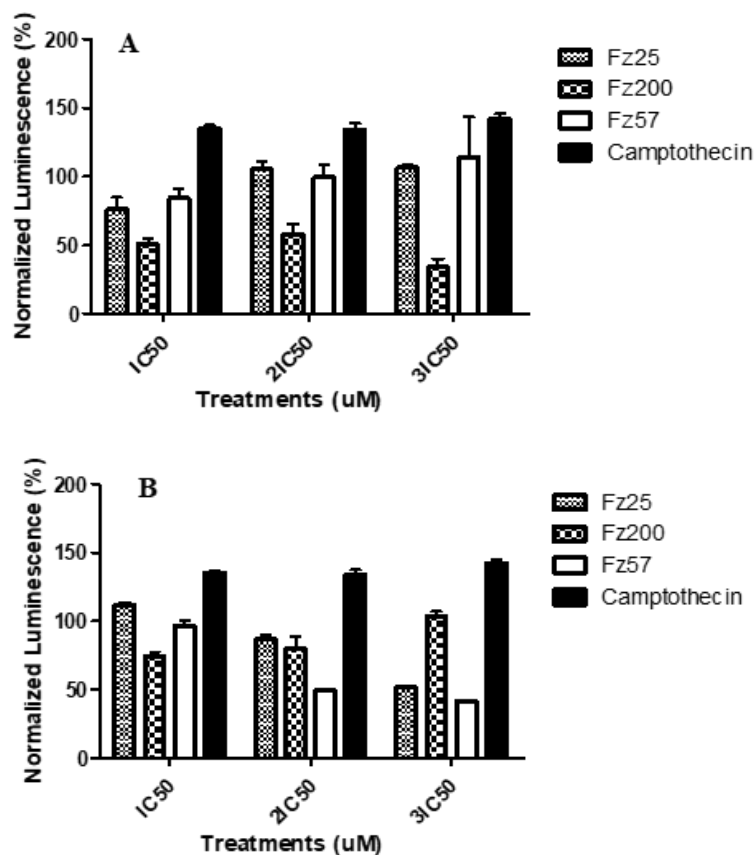
Figure 4.7 Initial apoptosis induction in MDA-MB-231 cells assayed by Annexin V. Cells were treated with IC_{50}, $2IC_{50}$ and $3IC_{50}$ of estrone analogs or positive control, camptothecin. The cells were then incubated with Annexin V reagent and luminescence measured by a luminometer. At least two independent experiments were performed in triplicate. (**A**) Quantification of apoptotic cells after 6 hrs of incubation of drug treatments (**B**). Quantification of apoptotic cells after 48 hrs of incubation with the compounds.
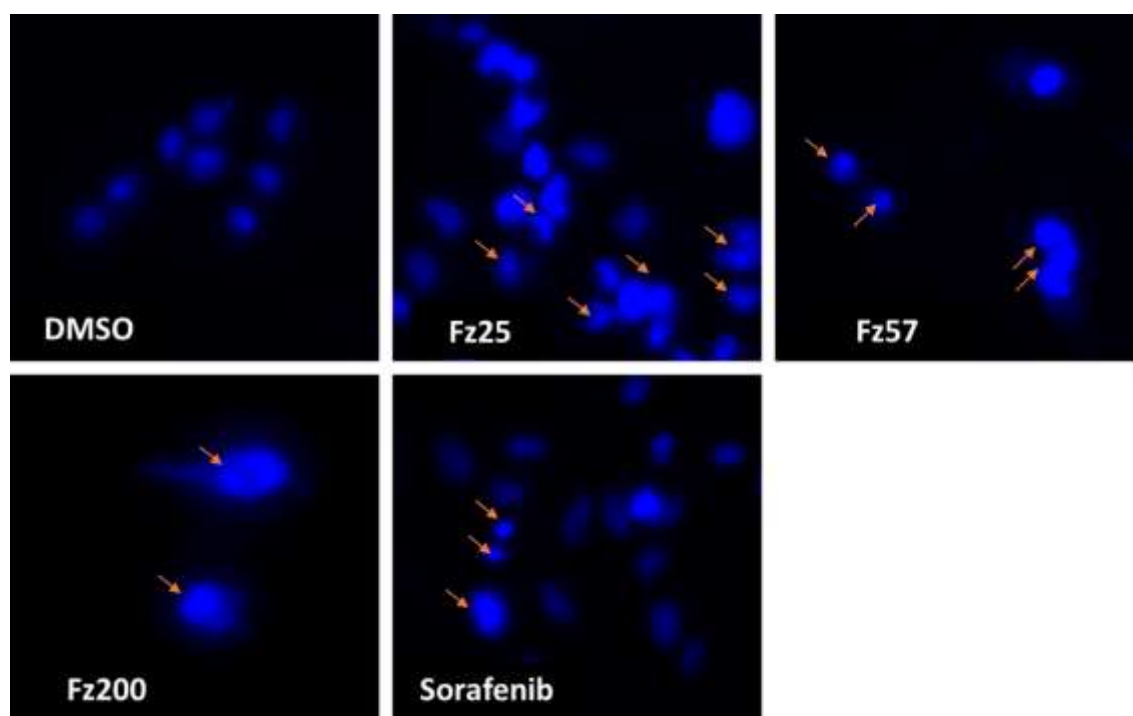
Figure 4.8 Apoptotic cells observed by Hoechst 33342 staining. MDA-MB-231 cells were treated with 0.05% DMSO (**A**), IC_{50} of estrone analogs (**B**-Fz25, **C**-Fz57 and **D**-Fz200) or positive control, sorafenib (**E**). Apoptotic cells exhibited chromatin condensation and nuclear fragmentation.
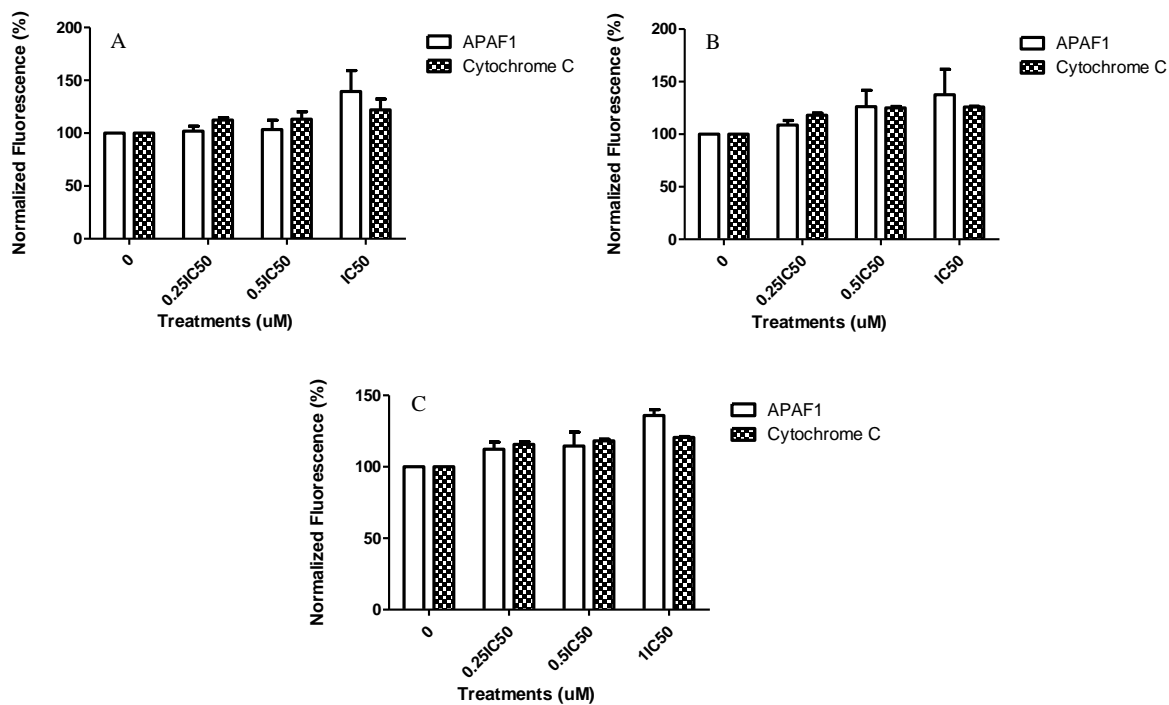
Figure 4.9 Expression levels of cytosolic cytochrome C and APAF1 in MDA-MB-231 cells assayed by In-Cell Western (ICW). After treatment with estrone analogs in a dose-dependent manner, fixed cells were incubated with specific antibodies for each protein. The cells were washed and incubated with DyLight conjugated (680 nm) detection antibodies, and plates scanned with LICOR Odyssey® Fc imaging system to measure the levels of APAF1, cytochrome C and GAPDH. Quantitation of proteins was completed using scanned images from Fiji software, and expression levels of APAF1 and cytochrome C normalized to GAPDH. At least two independent experiments were performed. (**A**) Fz25 (**B**) Fz57 and (**C**) Fz200.
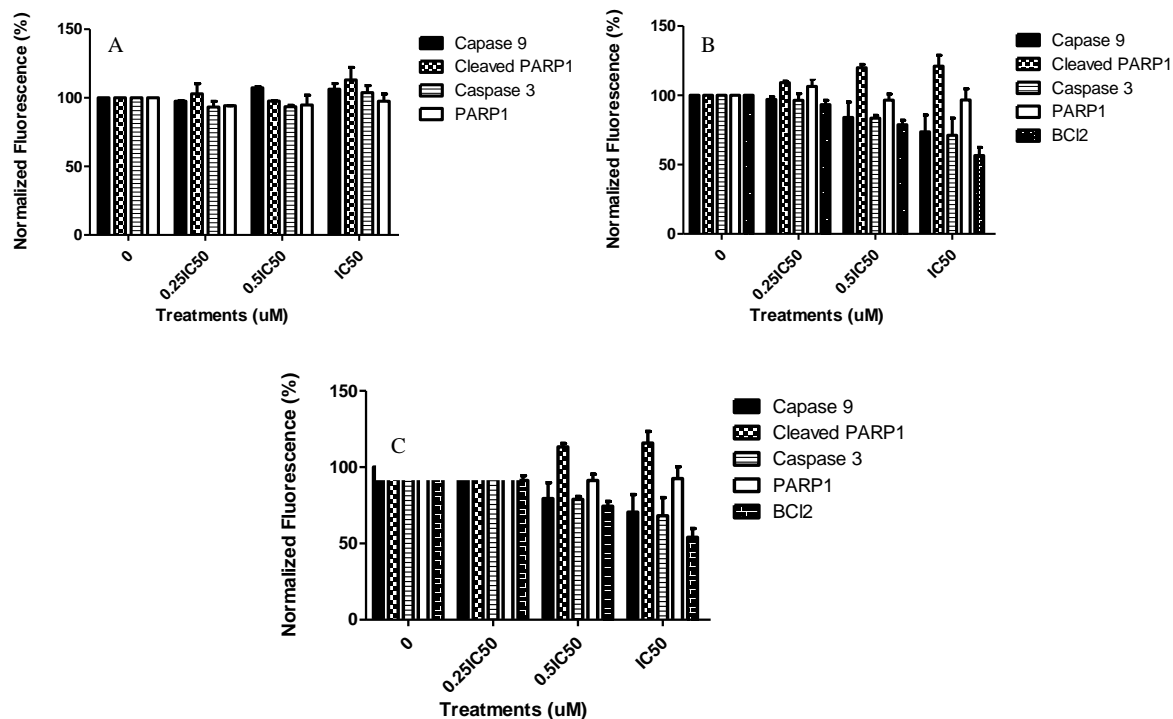
Figure 4.10 In-Cell Western quantification of apoptosis-associated proteins. After treatment with estrone analogs in a dose-dependent manner, fixed cells were incubated with specific antibodies for each protein. The cells were washed and incubated with DyLight conjugated (680 nm) detection antibodies, and plates scanned with LICOR Odyssey® Fc imaging system to measure the levels of each protein. Quantitation of proteins was completed using scanned images from Fiji software, and expression levels of the proteins normalized to GAPDH. At least two independent experiments were performed. (**A**) Fz25 (**B**) Fz57 and (**C**) Fz200
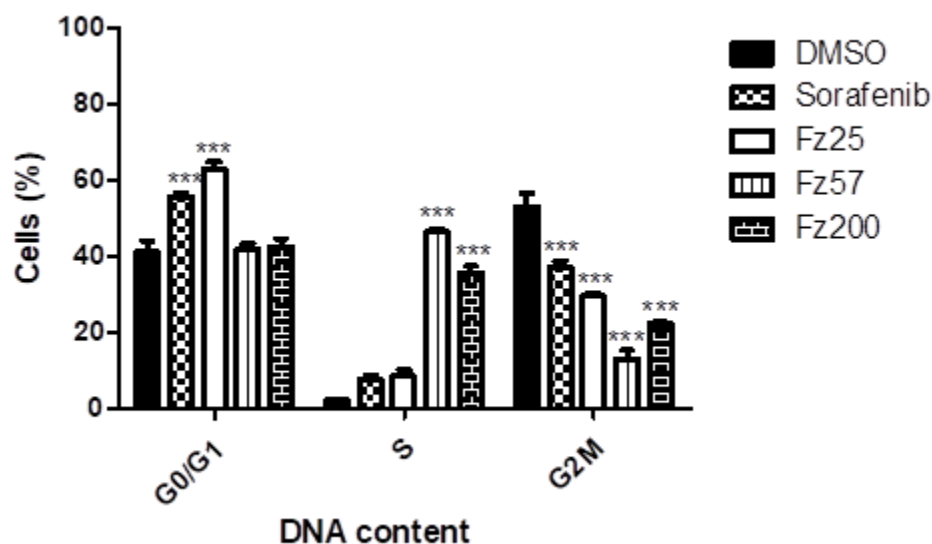
Figure 4.11 Estrone analogs exposure resulted in G_1- or S-phase cell cycle arrest. MDA-MB-231 cells were treated with IC_{50} values of estrone analogs and analyzed after 48 hrs by flow cytometry. Distribution of cells in distinct phases of the cell cycle. Fz25 and sorafenib, positive control, showed G_0/G_1 phase cell cycle arrest compared to the negative control, DMSO. Fz57 and Fz200, on the other hand, showed an S-phase cell cycle arrest. The bar graphs show Mean ± SD of the percentages of MDA-MB-231 cells in the indicated phases of the cell cycle (G_0/G_1, S and $G_2/$ M). At least three independent experiments were performed. $^*p < 0.05$, $^{**}p < 0.01$, $^{***}p < 0.001$ significant differences in cell cycle arrest compared to DMSO control.
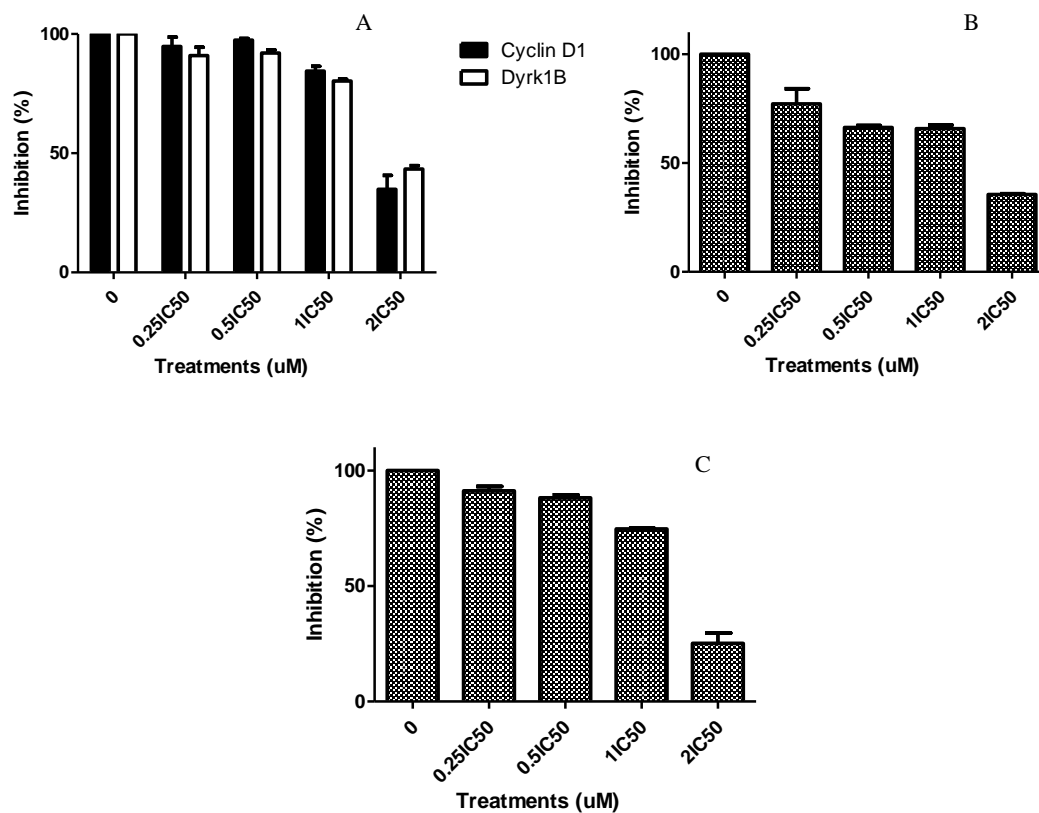
Figure 4.12 Effects on G_1- or S-phase cell cycle regulators after treatment of MDA-MB-231 cells with estrone analogs. Cells were treated for indicated concentrations, fixed and analyzed by ICW. Wells were incubated with appropriate primary antibodies and subsequently incubated with appropriate DyLight conjugated (680 or 800 nm) detection antibodies. LICOR Odyssey® Fc imaging system was used to scan wells. Protein quantification was completed using scanned images from Fiji software, and expression levels of the proteins normalized to GAPDH. Bar graphs are means ± SD from at least two independent experiments. (**A**) Fz25 (**B**) Fz57 and (**C**) Fz200.
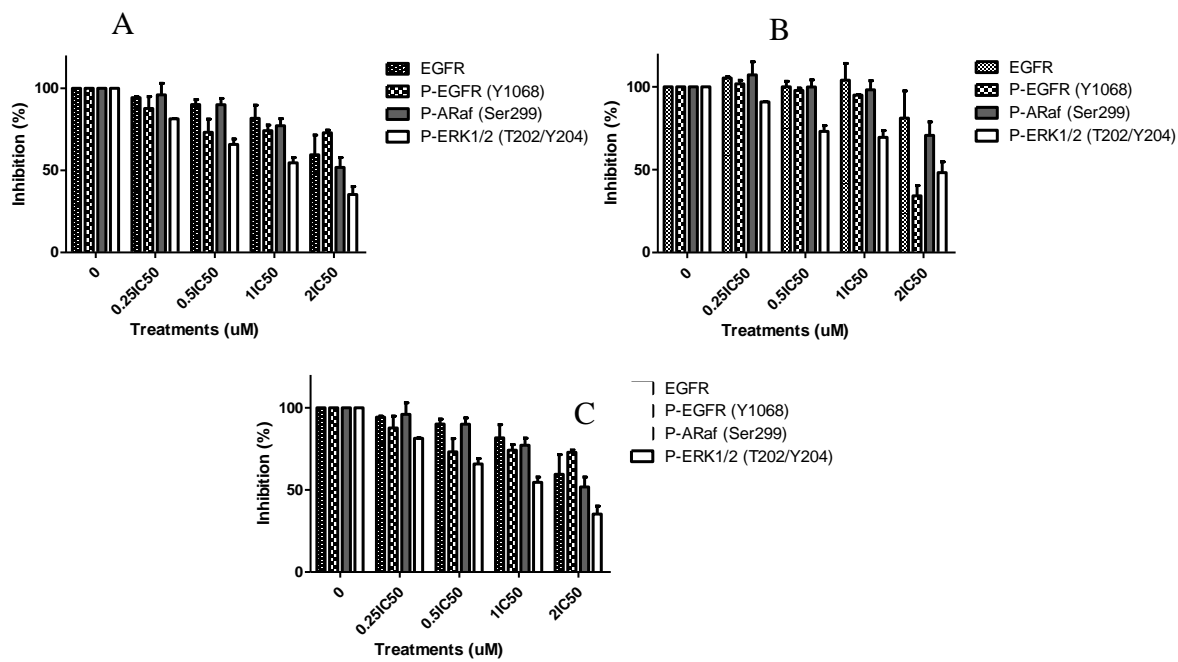
Figure 4.13 Effect of estrone analogs treatment on EGFR and downstream ERK1/2 effector molecules in MDA-MB-231 cells. Cells were treated for indicated concentrations, fixed and analyzed by ICW. Wells were incubated with appropriate primary antibodies and subsequently incubated with appropriate DyLight conjugated (680 or 800 nm) detection antibodies. LICOR Odyssey® Fc imaging system was used to scan wells. Protein quantification was completed using scanned images from Fiji software, and expression levels of the proteins normalized to GAPDH. Bar graphs are means ± SD from at least two independent experiments. (**A**) Fz25 (**B**) Fz57 and (**C**) Fz200.
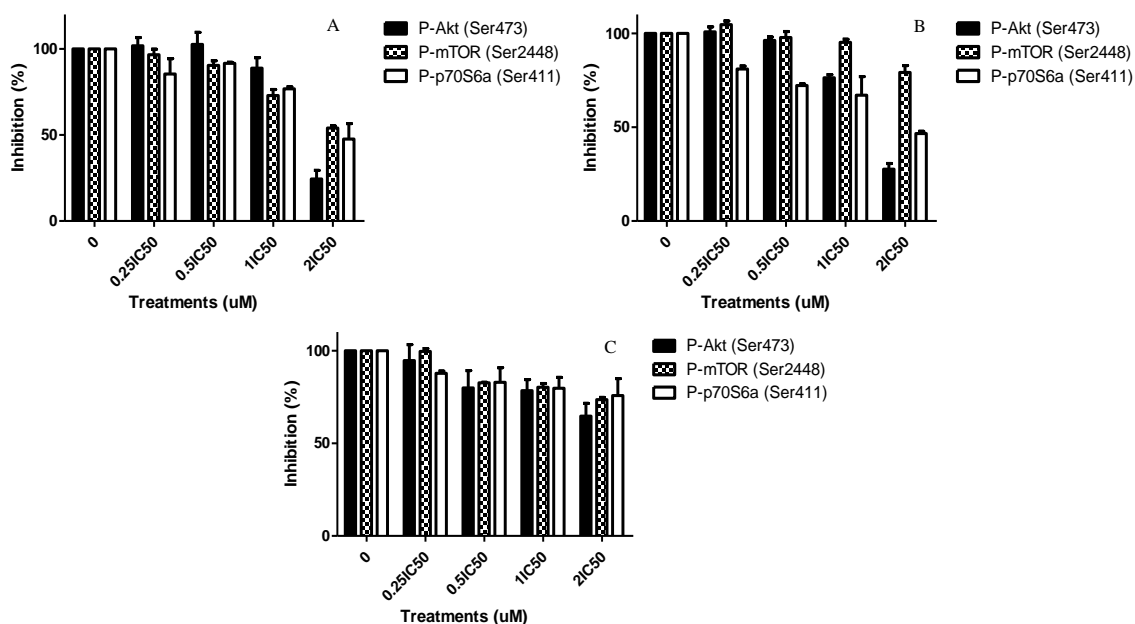
Figure 4.14 Effect of estrone analogs treatment on Akt pathway proteins in MDA-MB-231 cells. Cells were treated for indicated concentrations, fixed and analyzed by ICW. Wells were incubated with appropriate primary antibodies and subsequently incubated with appropriate DyLight conjugated (680 or 800 nm) detection antibodies. LICOR Odyssey® Fc imaging system was used to scan wells. Protein quantification was completed using scanned images from Fiji software, and expression levels of the proteins normalized to GAPDH. Bar graphs are means ± SD from at least two independent experiments. (**A**) Fz25 (**B**) Fz57 and (**C**) Fz200.

Chapter 5

5.1   General Conclusions and Recommendation

In conclusion, we have demonstrated that a new series of estrone analogs have been synthesized and have been investigated against EGFR-dependent cancers. Using molecular docking studies, these analogs were first designed, the receptor of interest, the EGFR kinase domain was prepared, and the docking simulations carried out to identify hits. The hit compounds showed key interactions like hydrogen bonding, cation-π interaction, and other hydrophobic interactions towards amino acid residues within the EGFR kinase domain. These compounds were synthesized, and their biological activity evaluated. The cytotoxic effects of the novel analogs were established and the mechanisms of action underlying the cytotoxic effect were elucidated (inhibition of cell proliferation and /or induction of cell death). Cell cycle arrest, modulation of EGFR, and its downstream MAPK and AKT signaling were investigated as the mechanisms underlying inhibition of cell proliferation. The mitochondrial apoptosis pathway was investigated as the mechanism responsible for cell death.

In our first study where estrone hybrids with modified cucurbitacin size chains (MMA series) were tested against NCIH226 (model for EGFR wild-type NSCLC), we came to the conclusions that novel estrone analogs (a hybrid of modified cucs pharmacophore and

estrone-base scaffold) were potent and bind better to wild-type EGFR ATP binding site *in silico*. Among these, MMA307 and MMA320 significantly inhibited the proliferation of NCIH226 cells *in vitro*. This effect could be ascribed in part to the suppression of EGFR and its downstream ERK1/2 signaling pathway and to the arrest of G_1 phase the cell cycle.

In our second study, we demonstrated that some MMA series of compounds were very effective against the TNBC model MDA-MB-468. Molecular docking studies revealed that MMA307 and MMA321 were very potent against EGFR kinase domain (pdb code: 1M17) *in silico*. Moreover, this study revealed that MMA307 and MMA321 induced mitochondrial apoptosis, arrested G_1 phase of the cell cycle, suppressed activated EGFR and its downstream MAPK and AKT signaling.

Finally, we showed that the estrone analogs with modified triazole pharmacophores (Fz series) were potent against the TNBC model MDA-MB-231. Fz25 showed better binding and potency *in silico* towards EGFR kinase domain. This compound induced mitochondrial apoptosis, arrested G_1 phase of the cell cycle, and suppressed activated EGFR and its downstream MAPK and AKT signaling.

To the best of our knowledge, there was no report about estrone analogs with modified cucurbitacin or triazole pharmacophores having potential therapeutic applications in treating NSCLC and TNBC cancers which possess a high risk of brain metastasis. The results presented herein provide novel information on such lead compounds. Taken

together, the present results suggest that estrone analogs may be the next generation of small molecules anti-EGFR targeting multiple types of EGFR-dependent cancers.

Further studies are needed to progress these compounds into clinical trials. Monolayer cell culture screens are often the initially applied methods for cytotoxic studies. Even though these procedures represent a fast and convenient approach to determine drug bioactivity, they do not mimic the heterogeneity of three-dimensional growth *in vivo*. As such, the toxicity and predictions of off-target effects of small molecules cannot be properly evaluated by 2D monolayer cellular screens. On the contrary, *in vivo* and primary *in vitro* 3D tumor models used in preclinical drug development are more closely related to the three-dimensional growth of a patients tumor in clinical settings. Moreover, these tumor models are better at predicting clinical effects when compared with *in vitro* 2D tumor models because several parameters including pharmacokinetics, efficacy and safety of lead candidates are monitored in parallel. We propose that these compounds should first be tested in 3D models of NSCLC and TNBC primary tumors to establish their dosing and toxicity. Secondly, the compounds physicochemical profiles should be predicted *in vitro*. Finally, these compounds should be tested in appropriate preclinical settings. Based on the compound's toxicity profiles and pharmacokinetics, a lead optimization step may be conducted to improve their efficacy and safety be performing clinical trial studies.
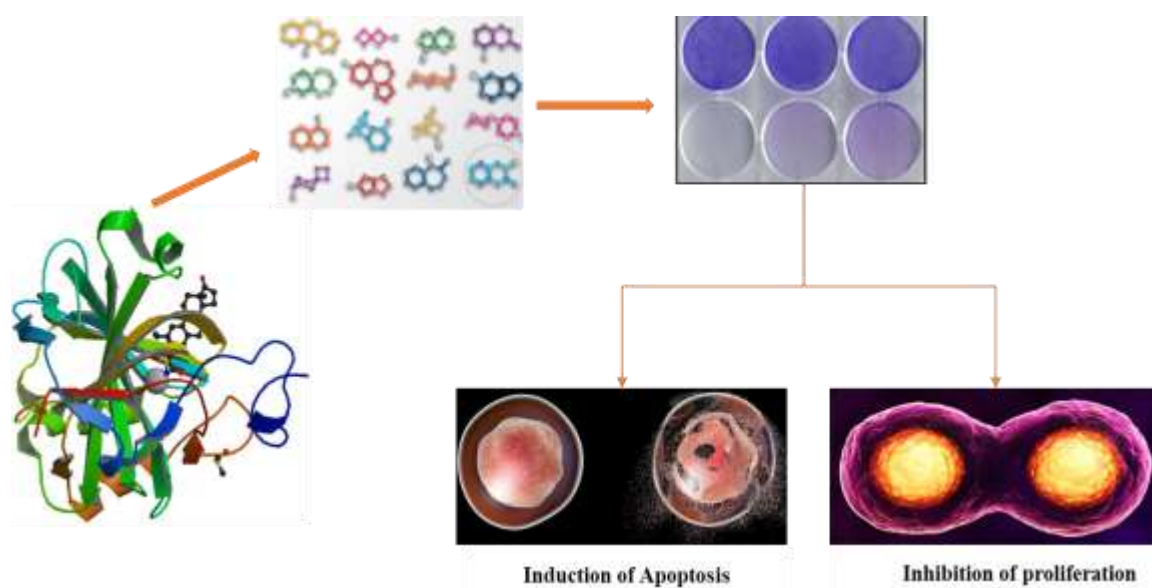
Figure 5.1 Graphical summary of design, synthesis and biological evaluation of estrone analogs. Estrone analogs were designed and screened with CAMM to identify hits. The hits were synthesized using estrone as a starting material to obtain MMA or Fz series of compounds. The cytotoxic effects of the compounds were tested and mechanisms of induction of apoptosis and/or inhibition of cell proliferation elucidated.